The Key Laboratory of Advanced Technique and Fabrication for Weak-Light Nonlinear Photonics Materials, Ministry of Education

Annual Report

2005

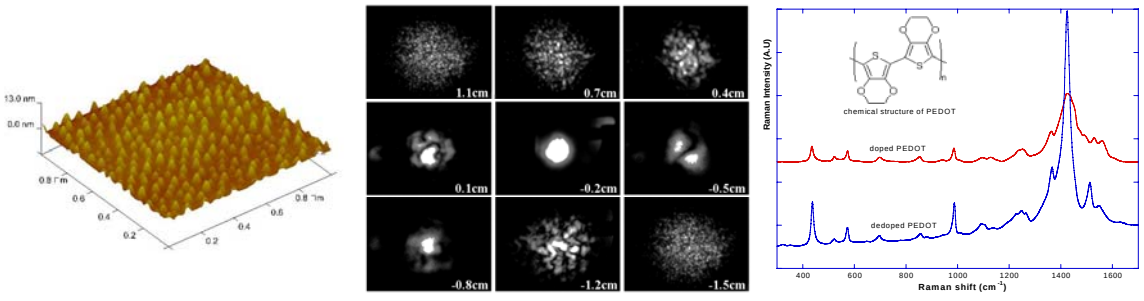

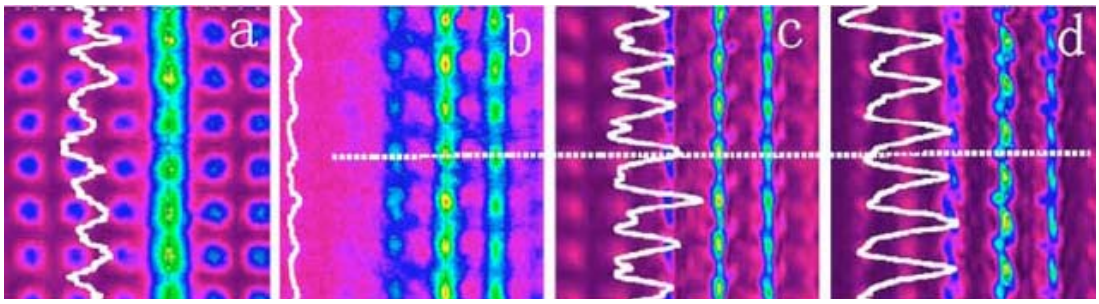

Nonlinear Optics at Weak Light and Quantum Coherent Optics

This section summarizes the main research activities in 2005, performed within the division of "Nonlinear Optics at Weak Light and Quantum Coherent Optics". In 2005 our division made a great progress in the following respects:

1. The research in slow-light and the giant nonlinear optics which led by Prof. Guoquan Zhang, has attracted the interest from the colleagues, especially from Thales R&T Center. And Dr. Fang BO in this group won the OSA student traveling award due to his contribution to this achievement;
2. Study of photonic lattice and the optical discrete behavior led by Prof. Chen, have been going well. And Chen's group has been keeping one of the top research teams in this area. Meanwhile Dr Lou has finished the first work on this topic which was totally carried out in TEDA lab.
3. The new research topic on the optical-magnetic-optic effect has been started up, led by Prof. Qian Sun. And they have got some marvelous results to make this topic become one of the main-stream directions in our division.
4. The research in the photorefractive nonlinear optics is going along well. And our reputation in this area has been greatly promoted this year. We successfully organized the 11^{th} international photorefractive nonlinear optics conference. In this topic, the study of ultraviolet PR effect has been under a deep investigation, especially in PMMA materials.
5. Besides, we also make a progress in the ultra-fast nonlinear optics by Dr. Qiang Wu, who has build up several experimental measurements, especially two-dimensionally spectral imaging, which pay a solid path for our future research. And the lab for light transmission in quantum coherent ensembles has almost be finished by Prof. Zhang and Dr. Gao, and the photonics detection system, low-temperature system, micro-scanning system have been under constructions. In addition, the topic about weak-light nonlinear optical effect in micro-fluid systems was under discussion, mainly investigated by Dr. Xuanyi Yu.

In summary, even though we have progressed a lot this year, our division is also at the beginning stage. We hope that our group will grow up next year and become the world-leading group in the near future.

Prof. Jingjun Xu
2006-1-20

Transition between super- and subluminal light propagation in room-temperature $Bi_{12}SiO_{20}$ crystals

Fang Bo, Guoquan Zhang, and Jingjun Xu

We have achieved superluminal light propagation with a negative group velocity V_g = -5.7 m/s in a room-temperature photorefractive $Bi_{12}SiO_{20}$ crystal by using the dispersive phase coupling effect in a nondegenerate two-wave mixing process. To the best of our knowledge, this is the first experimental demonstration of superluminal light propagation at room temperature in solids by using a classical wave mixing technique. We have realized the tunability of the group velocity of light even between the negative (superluminal light) and the positive (subluminal light) by simply tuning the experimental conditions such as the frequency of the coupling beam Ω, the incident intensity I_p, and the externally applied electric fields E. As an example, Fig. 1 shows the dependences of V_g on I_p and E. This technique can be used as controllable optical delay/advance lines.

References

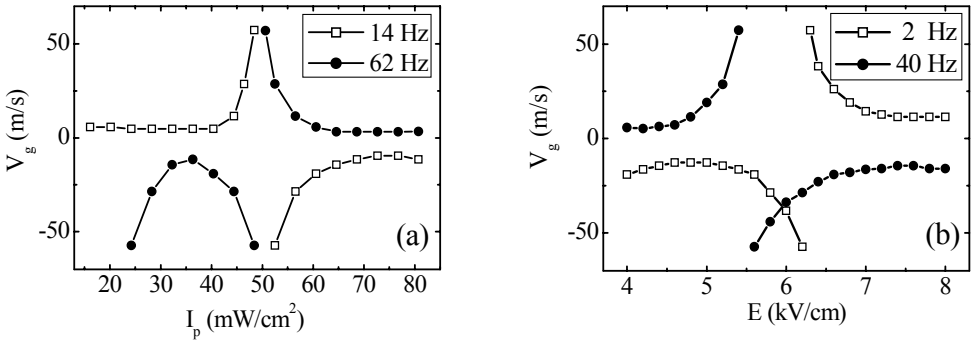

Fig. 1 The tunable properties of V_g. (a) dependences of V_g on I_p with E = 8 kV/cm at Ω = 14 Hz and 62 Hz, respectively. (b) E-dependence of V_g with I_p = 19.5 mW/cm^2 at Ω = 2 Hz and 40 Hz, respectively. Other parameters for both cases: the peak intensity of the signal beam I_{peak} = 0.1 mW/cm^2, the grating spacing Λ = 21.3 μm, and the period time of the sinusoidal signal beam T = 30 ms.

[1] G. Zhang, R. Dong, and J. Xu, Chin. Phys. Lett. **20**, 1725 (2003).
[2] G. Zhang, R. Dong, F. Bo, and J. Xu, Appl. Opt. **43**, 1167 (2004).
[3] G. Zhang, F. Bo, R. Dong, and J. Xu, Phys. Rev. Lett. **93**, 133903 (2004).
[4] F. Bo, G. Zhang, and J. Xu, Opt. Exp. **13**, 8198 (2005).
[5] F. Bo, G. Zhang, and J. Xu, TOPS, **99**, 386 (2005).

Supported by the Key Project of Chinese Ministry of Education (No. 104054), the National Natural Science Foundation of China (No. 60308005 and 10334010), the Program for New Century Excellent Talents in University, the Program for Changjiang Scholars and Innovative Research Team in University, and the Cultivation Fund of the Key Scientific and Technical Innovation Project, Ministry of Education of China (No. 704012).

Published on Opt. Exp. **13**, 8198 (2005) and TOPS, **99**, 386 (2005)
To be published on Opt. Com. (2006)

Nonvolatile two-step, two-color holographic recording sensitivity with continuous-wave lights in $LiNbO_3$:Fe

Yan Shen, Guoquan Zhang, Bo Fu, Qingjun Xu and Jingjun Xu

We have studied theoretically the nonvolatile two-step, two-color holographic recording sensitivity based on the two-center model (the deep-trap and the shallow-trap centers are Fe^{2+}/Fe^{3+} and $Nb_{Li}^{4+}/Nb_{Li}^{5+}$, respectively). We find that, under the same recording conditions, the sensitivity of the near-stoichiometric $LiNbO_3$:Fe is much higher than that of the congruent $LiNbO_3$:Fe. We show that the recording sensitivity is proportional to the concentration of Nb_{Li}^{4+} in the crystal and the intensity of the gating light. Moreover, using short-wavelength gating lights and high-concentration Fe dopant are other two possible ways to improve the sensitivity.

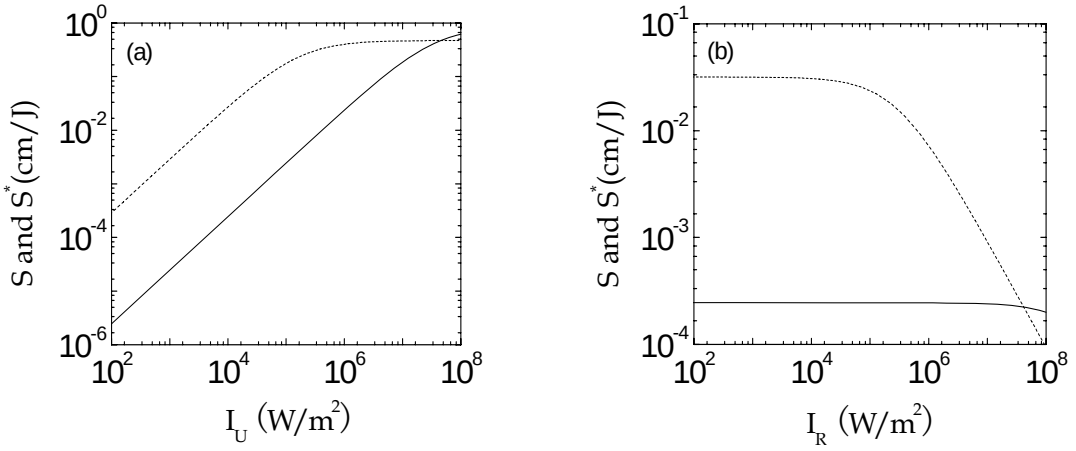

Fig. 1 Two-step, two-color holographic recording sensitivities at various experimental conditions for the near-stoichiometric $LiNbO_3$:Fe with a Li molar concentration of 49.5% (S^s: the dashed curves) and the congruent one with a Li molar concentration of 48.6% (S: the solid curves). (a) depicts the dependences of the recording sensitivity on I_{U0} with I_{R0} set to be 5×10^4 W/m^2; (b) is the I_{R0}-dependences of the recording sensitivity with a gating intensity of 1.0×10^4 W/m^2.

References

[1] Y. S. Bai and R. Kachru, Phys. Rev. Lett. **78**, 2944 (1997).
[2] L. Hesselink, S. S. Orlov,et.al, Science **282**, 1089 (1998).

Supported by the EYTP (No. 2002-350) and SRF for ROCS, SEM (No. 2003-406), the NSFC (Nos. 60308005 and 60108001) and the Key Project of NSFC (No. 10334010). It is also partially sponsored by the Key Project of Chinese Ministry of Education (No. 104054) and the Cultivation Fund of the Key Scientific and Technical Innovation Project, Ministry of Education of China (No. 704012).
Published on Optics Communications.**256/1-3**: 24 (2005).

Influence of thermal treatment on two-color holography in near-stoichiometric lithium niobate

Bo Fu, Guoquan Zhang, Xiangming Liu, Yan Shen, Jingjun Xu

We studied the influence of oxidization and reduction on the two-color holographic storage properties of near-stoichiometric lithium niobate (SLN). Three SLN crystals were used in our experiment: an as-grown one, an oxidized one that was annealed in the air for 6 hours at 745 ºC and denoted as SLN1, a reduced one that was reduced in argon gas of high purity for 3 hours at 745 ºC and denoted as SLN2. In the experiments, an incoherent ultraviolet light at 365 nm was employed as a gating beam. Two extraordinarily polarized recording beams at 780nm from a Diode Laser were set to be of equal intensity of 1.78 W/cm^2 with an external crossing angle of 32.8º at the incident crystal surface. We measured the parameters of interest for holographic storage such as diffraction efficiency, sensitivity and dynamic range. The results show that the diffraction efficiency, the sensitivity and the dynamics range of SLN increase after reduction, while they decrease after oxidation, as shown in Fig. 1 and Fig. 2. We attributed the observed increase in the diffraction efficiency, the sensitivity and the dynamic range to the increase in the concentration of the bipolarons after the reduction, which increase the absorption at the gating wavelength and therefore the gating is more effective in the reduced SLN than the oxidized SLN.

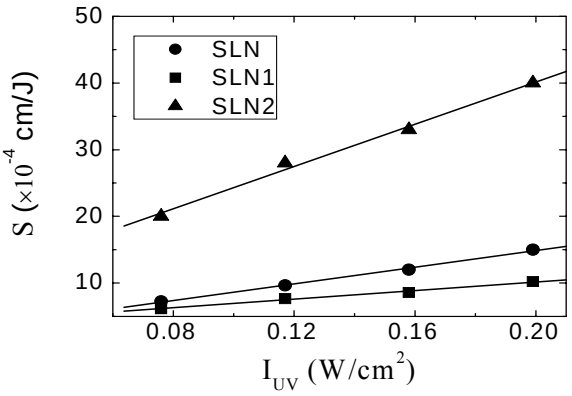

Fig. 1: Dependence of the Sensitivity on the gating intensity for three samples.

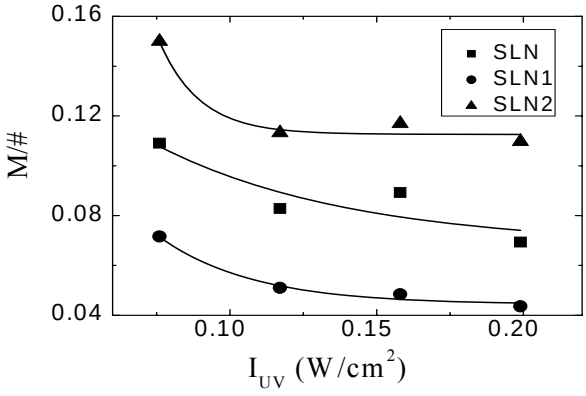

Fig. 2: Dependence of the dynamic range on the gating intensity for three samples.

References:

[1] H. Guenther, R. Macfarlane, Y. Furukawa, et al., Appl.Opt. **37**, 7611-7623 (1998).
[2] K. Buse, A. Adibi, D. Psaltis, Nature **393,** 665-668 (1998).

A recursion formula for reflectance of stratified holographic grating layers intervened with homogeneous buffer layers

Weiyue Che, Guoquan Zhang, Bin Han, and Jingjun Xu

We derived a recursion formula for the reflectance of stratified holographic grating layers intervened with homogeneous buffer layers. The reflection spectrum of such a stratified optical element was studied. It is shown that transparencies appear within the stop-band of the reflection spectrum of the volume holographic gratings due to the existence of the intervening homogeneous buffer layers. The influences of the buffer layer thickness on the reflection spectrum were studied. We found that the number of pass bands increased and the band-width became narrower when the number of the grating and buffer layers increased. The number of the transparencies within the stop-band was found to be equal to the number of the buffer layers. Because of the pectinate profile of the reflectance spectrum for the above stratified structures, multi-channel narrow pass band filtering can be achieved in such a structure under proper operating parameters. We also found that the reflection spectrum of such a stratified optical element is highly dispersive which can be used to generate subluminal and superluminal light propagation.

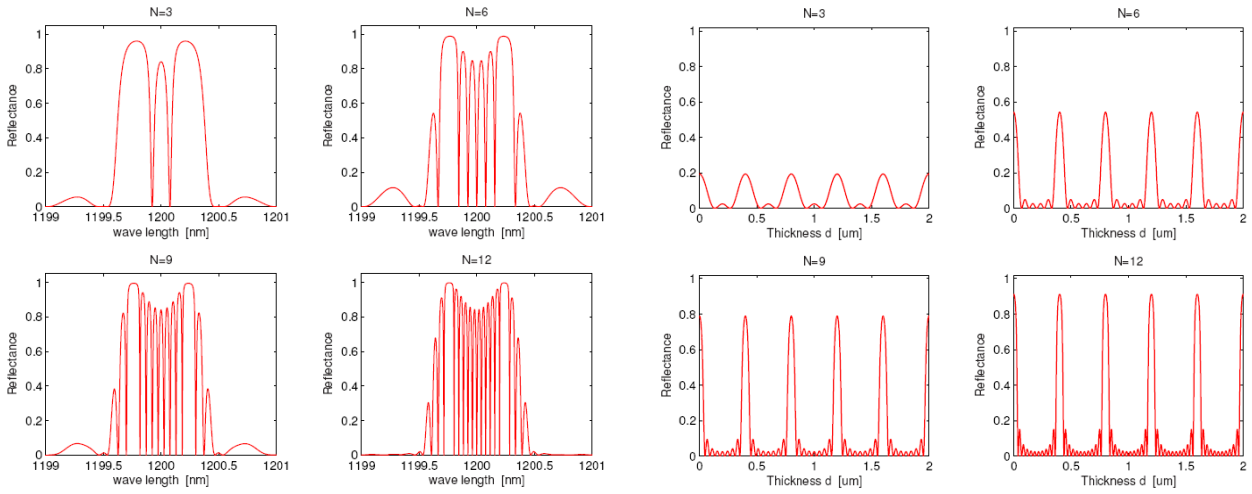

Fig.1. Reflectance spectra for different layer number *N* and for different thickness of holographic gratings *d*.

References

[1] J. D. Joannopoulos, R. D. Meade, J. N. Winn, *Photonic Crystals* (Princeton University Press, Princeton , N. J ,1995)

[2] V. M. Petrov, C. Caraboue, J. Petter, T. Tschudi, V. V. Bryksin, M. P. Petrov, "A dynamic narrow-band tunable optical fliter ," Appl. Phys. B **76,** 41–44 (2003)

[3] J. J. Monz´on, T. Yonte, L. L. S´anchez-Soto, "Characterizing the reflectance of periodic layered media," Opt. Commun. **218,** 43–47 (2003)

[4] Pochi Yeh, *Optical Waves in Layered Media*, (Wiley-Interscience Publication,Canada ,1988)

White-light photorefractive phase mask

Yuanmei Gao, SiminLiu, Ru Guo, Xiaohua Zhang, Yi Lu

Volume photorefractive phase mask has been fabricated with incoherent white light from an incandescent source in $LiNbO_3$: Fe self-defocusing photorefractive crystal for the first time to our knowledge. It can guide and modulate a probe white light or a laser beam and can be used to transmit an incoherent dark image as the guided modes of the waveguides induced by white-light dark spatial solitons. This also proves the existence of photorefractive nonlinearity of white light.

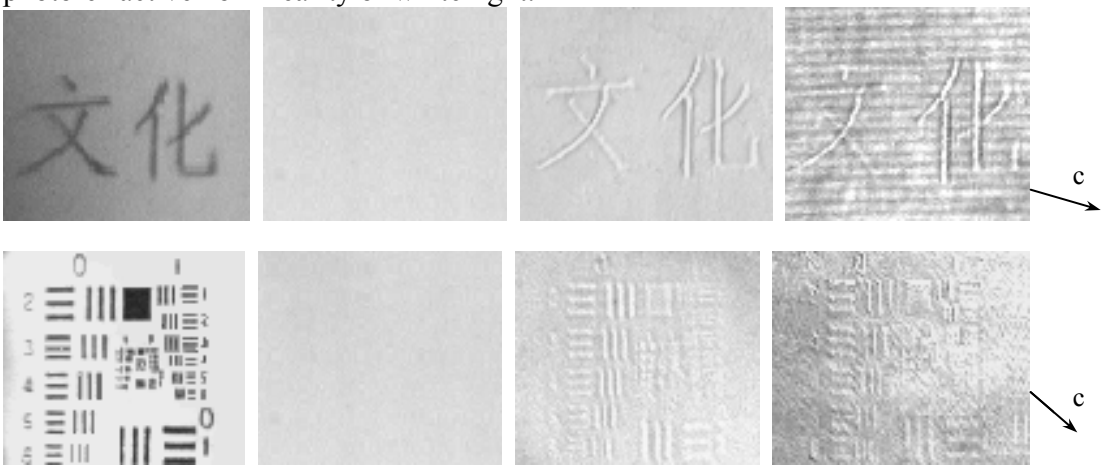

Fig1. White light phase masks in $LiNbO_3$: Fe crystal fabricated amplitude masks

References:

[1] A.Yariv, "Three-dimensional pictorial transmission in optical fibers," Appl. Phys. Lett. 28, 88-89 (1976).

[2] E. M. Dianov, P. V. Mamyshev, A. M. Prokhorov, and S. V. Chernikov, "Fiber-optic wavelength-division multiplexing and demultiplexing using volume holographic gratings," Opt. Lett. 14, 1088-1090 (1989).

[3] G. Stegeman and M. Segev, "Optical Spatial Solitons and Their Interactions: University and Diversity," Science 286, 1518-1523 (1999).

[4] A. Kasapi, M. Jain, G. Y. Yin, and S. E. Harris, "Electromagnetically Induced Transparency: Propagation Dynamics," Phys. Rev. Lett. 74, 2447-2451 (1995).

[5] B. Fischer, M. Cronin-Golomb, J. O. White, and A. Yariv, "Real-time phase conjugate window for one-way optical field imaging through a distortion," Appl. Phys. Lett. 41, 141-143 (1982).

Supported by National Natural Science Foundation of China (No. 60378013, 60278006 and 10474047).

Published on App. Opt, 44（9），1533-1537

Spatiotemporal coherence of white light beams trapped within dark spatial solitons

Chun-Fu Huang, Ru Guo, Si-min Liu, Nan Zhu Da-Yun Wang, Yuan-Mei Gao, LuYi

We study experimentally and theoretically temporal and spatial coherence of white light beam through its interaction with a coherent dark spatial soliton in $LiNbO_3$: Fe noninstantaneous nonlinear self-defocusing crystal. Experimental observations show that during this process a portion of the white light beam is trapped within the dark notch of the dark spatial soliton, thus forming a sharp intensity spike. Moreover, numerical simulations show that in this region the coherence length of white light beam increases from ~11 μm to 1200 μm after 6 mm of propagation for almost all frequencies. We find that the intensity spike of each frequency of white light increases with the increase of frequency. While the spatial coherence length of each frequency of white light decreases with the increase of frequency.

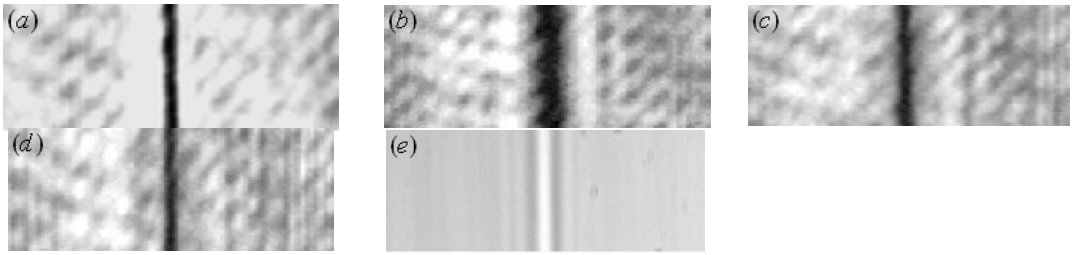

Fig.1. Photographs and intensity profiles of the coherent dark soliton and the incoherent white light beam guided in the dark notch

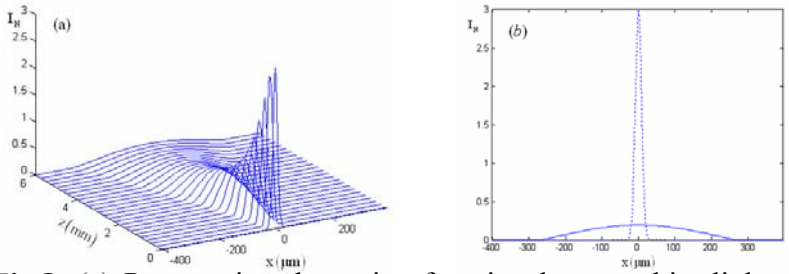

Fig.2. (a) Propagation dynamic of an incoherent white light along a 6 mm $LiNbO_3$:Fe self-defocusing crystal.(b) input (dashed curved) and output (solid curved) intensities of the incoherent white light at $z \approx 6$ mm.

Reference:

[1] L. Mandel and E. Wolf, Optical Coherence and Quantum Optics, Cambridge University Press, New York, 1995.

[2] N.V. Bogodaev, L.I. Ivleva, A.S. Korshunov, N.M. Polozkov, and V.V. Shkunov, J. Opt. Soc. Am. B 10 (1993) 2287.

Supported by National Natural Science Foundation of China (No. 60378013, 60278006 and 10474047).

Published on Opt. Commun.248（2005）449-457

Interaction between a dark stripe and a two-dimensional photonic lattice with fully incoherent white light

Xiaohua Zhang, Simin Liu, Ru Guo, Dayun Wang, Zhaohong Liu, Yi Lu

Two-dimensional nonlinear photonic lattices are created with fully incoherent white light emitted from an incandescent lamp in the self-defocusing photovoltaic media. We study experimentally the interaction of a dark stripe with such a nonlinear photonic lattice and observe a novel type of composite state. The composite state is generated by coupling of localized stripe and the periodic pixles nearest neighboring to the stripe.

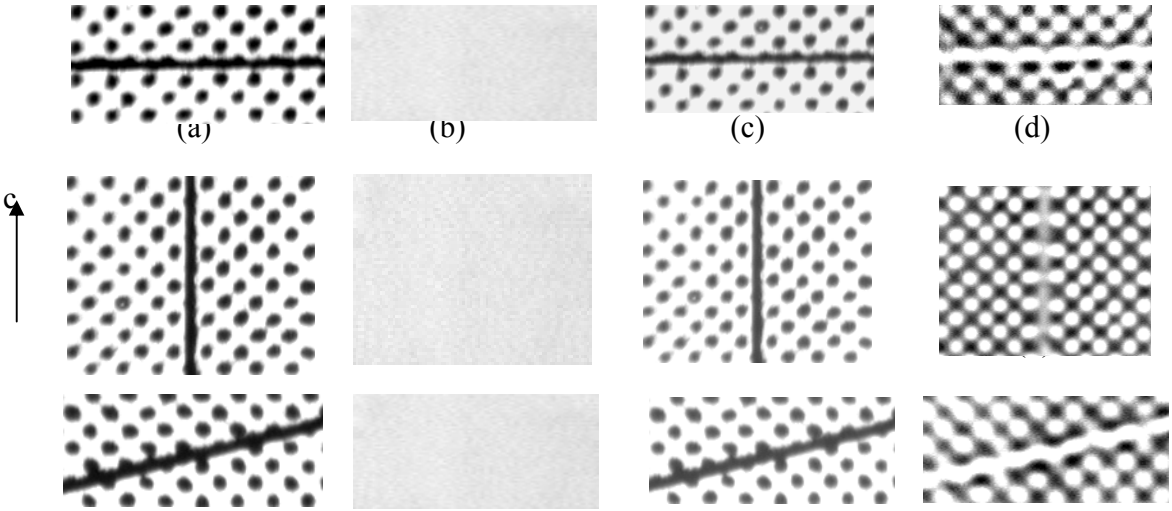

Fig1. Interaction of a lattice with a dark stripe beam.

References

[1] A.B.Aceves, and J.V.Moloney, Opt.Lett 17(1992)1488.
[2] C.D.Angelis and G.F.Nalesso, JOSA B 10 (1993)55.
[3] J. S. Aitchison, A. M. Weiner, Y. Silberberg, D. E. Leaird, M. K. Oliver, J. L. Jackel, and P. W. E. Smith, Opt. Lett. 16 (1991) 15.

Supported by National Natural Science Foundation of China (No. 60378013, 60278006 and 10474047).
Published on Opt. Commun. 252 (2005) 84-90

Photovoltic Gray Spatial Solitons in Photorefractive crystal

Zhu Nan, Guo Ru, Liu Si-Min, Huang Chun-Fu, Wang Da-Yun, Gao Yuan-Mei

Plane waves are absolutely stable against small modulations in self-defocusing media, the dark spatial soliton exist only in the form localized dark hole on the plane wave background. Base on such modulation stability we present the evolution equations for one-dimensional gray spatial solitons supported by the photovoltaic self-defocusing nonlinearity and its stationary solution in photovoltaic photorefractive crystal $LiNbO_3$:Fe. We investigate numerically the properties associated with these gray solitons, such as soliton profile and its phase distribution for different values of soliton grayness, and the normalized transverse velocity and the normalized FWHM of photovoltaic gray soliton as functions of normalized intensity and degree of grayness. These properties can be steered by adjusting the relative phase difference on either side of the soliton wave. Both similarities and differences between photovoltaic gray solitons and screening gray solitons are emphasized, such as in a certain range of parameters their total phase shift can exceed π i.e., they become "darker than black".

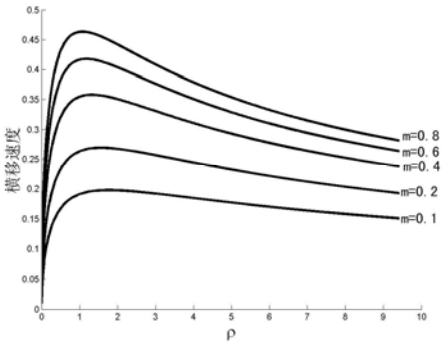

Fig.1. transverse velocity v of a photovoltaic gray soliton as a function of ρ and m

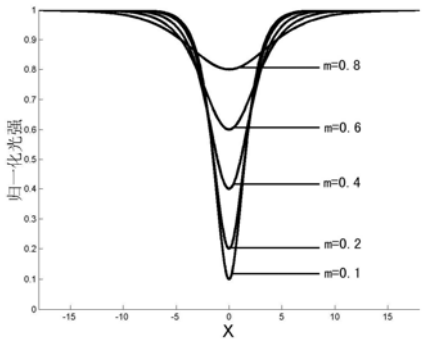

Fig.2. Normalized intensity profile of a photovoltaic gray soliton at $\rho = 1$ and for various of the grayness factor m

Reference:

[1] Kivshar Y S, Luther-Davies B. Dark Optical Solitons: Physics And Applications [J]. *Physics Reports*, 1998, **298**(2): 81~198

[2] A. G.. Grandpierre, D. N. Christodoulides, T. H. Coskun. Gray spatial solitons in biased photorefractive media [J]. *Journal of the Optical Society of America B*, 2001, **18**(1): 55~63

[3] Agrawal G P. *Nonlinear Fiber Optics* [M]. Academic Peer, Boston Mass, 2001;
Trillo S, Torruellas W. *Spatial solution* [M]. Springer-Verlag Berlin, 2001

Supported by National Natural Science Foundation of China (No. 60378013, 60278006 and 10474047).
Published on Chinese journal of lasers 32(2005) 903-907

Transmission of digital images consisting of white-light dark solitons

Yuanmei Gao, Simin Liu, Ru Guo, Zhaohong Liu, Tao Song

The distortion-free digital image is transmitted through parallel propagation of white-light photovoltaic dark solitons. The waveguide channels induced by white-light dark solitons can guide both the laser beam and the white-light beam well. We determine experimentally the critical separations of the dark solitons in the directions parallel and perpendicular to the crystalline c axis, respectively, for the given crystal thickness.

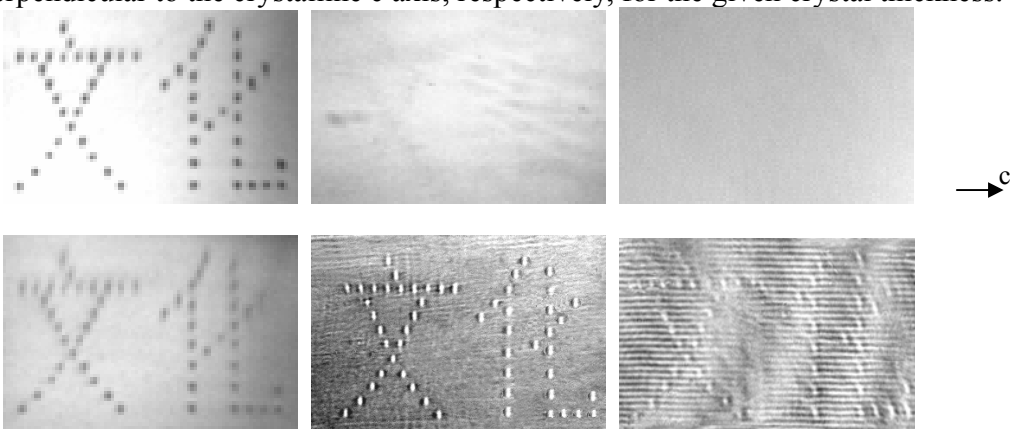

Fig.1. Digits-images transmitting with white-light photorefractive solitons

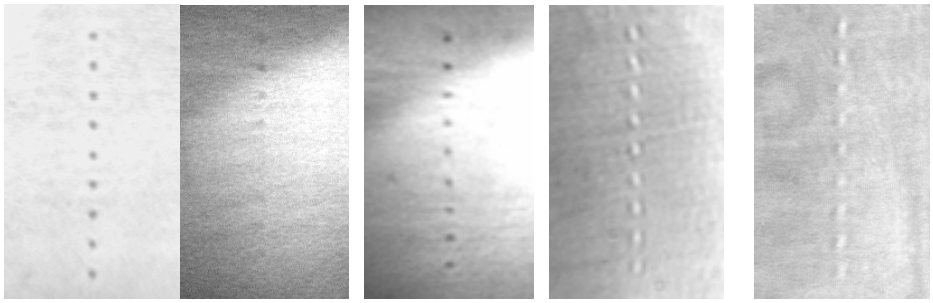

Fig.2. Experimental solitons rows of white light

Reference:

[1] G. Stegeman and M. Segev, "Optical Spatial Solitons and Their Interactions: University and Diversity," Science 286, 1518-1523 (1999).

[2] A. Kasapi, M. Jain, G. Y. Yin, and S. E. Harris, "Electromagnetically Induced Transparency: Propagation Dynamics," Phys. Rev. Lett. 74, 2447-2451 (1995).

Supported by National Natural Science Foundation of China (No. 60378013, 60278006 and 10474047).

Published on APP. Opt, 44(32), (2005)

The circular and elliptic white-light dark spatial solitons in a photovoltaic self-defocusing nonlinear medium

Yuanmei Gao, Simin Liu, Ru Guo, Zhaohong Liu, Tao Song, Nan Zhu

We observed circular white-light dark spatial solitons in photovoltaic self-defocusing $LiNbO_3$: Fe crystal using an ordinary incandescent lamp as light source (a line source) with the filament of the bulb parallel to the crystalline c axis. Besides the above condition, the formation of the elliptic soliton needs an additive condition that the crystalline c axis is parallel to the minor axis of dark elliptic spot.

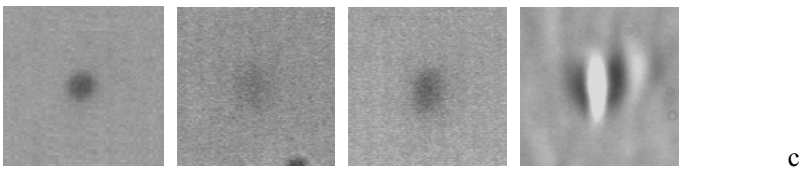

Fig.1. Profiles of dark-spot-bearing beam at input-output faces of the crystal and the probe beam at the output face of the crystal with tungsten-halogen lamp as light source

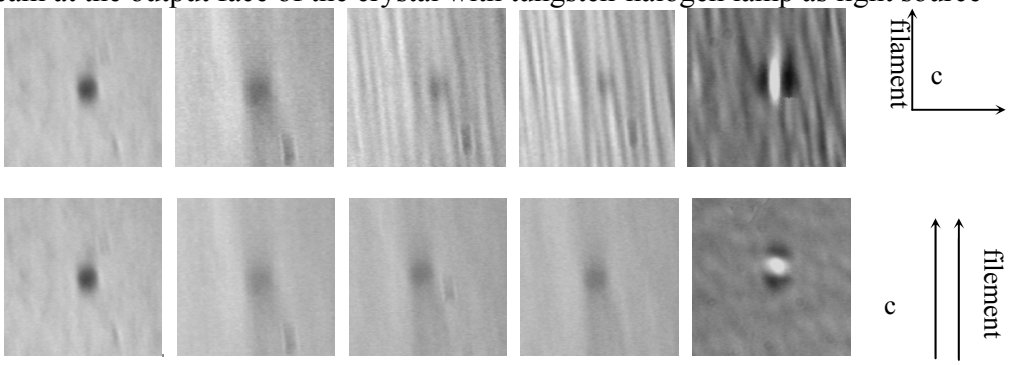

Fig.2. Profiles of an dark-spot-bearing beam at input-output faces of the crystal and the probe beam at the output face of the crystal with incandescent lamp as light source: the images in the top row with c axis of the crystal perpendicular to the filament of the incandescent lamp; the images in the bottom row with c axis parallel to the filament.

Reference:

[1] M. Segev, B. Crosignani, A. Yariv, and B. Fischer, Phys. Rev. Lett. 68 (1992) 923.
[2] M. Segev, B. Crosignani, P. Diporto, G. C. Valley, and A. Yariv, Phys. Rev. Lett. 73 (1994) 3211.
[3] G. C. Valley, M. Segev, B. Crosignani, A. Yariv, M. Fejev, and M. Bashaw, Phys. Rev. A 50 (1994) R4457.

Supported by National Natural Science Foundation of China (No. 60378013, 60278006 and 10474047).
To be published on Opt. Commun.

Coherence enhancement of spatially incoherent light beams through soliton interaction in logarithmically saturable nonlinear media

Huang Chun-Fu, Guo Ru, Liu Si-Min

We investigate numerically the interaction between incoherent spatial solitons in a nonlinear medium with logarithmic saturable nonlinearity base on the coherent density approach. Numerical simulations show that both the intensity and the spatial coherence can be greatly enhanced through soliton interaction. At the same time, we show that the soliton interaction can be controlled by the total partial incoherence, which can not only suppress the coherent soliton interaction such as attractive, repulsive or exchange energy, but also induce weak attractive due to incoherent superimposition of two incoherent solitons.

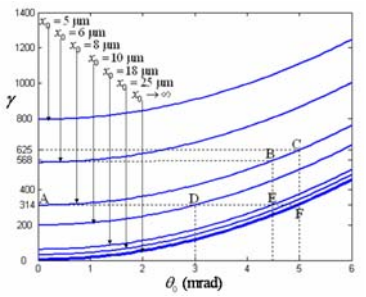

Fig.1.the existent curve of incoherent solitons in logarithmically saturable nonlinear media

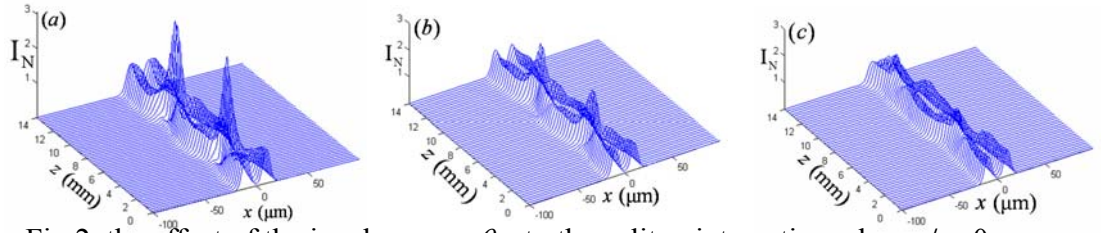

Fig.2. the effect of the incoherence θ_0 to the soliton interaction when $\phi = 0$

(a) $\theta_0 = 0$； (b) $\theta_0 = 3$ mrad； (c) $\theta_0 = 6$ mrad

References:

[1] Mandel L and Wolf E 1995 *Optical Coherence and Quantum Optics* (New York: Cambridge University Press)

Supported by National Natural Science Foundation of China (No. 60378013, 60278006 and 10474047).

To be published on Chinese Physics 55（3），2006

Modulation instability of broad beam in self-defocusing photorefractive crystal $LiNbO_3$: Fe

Nan Zhu, Ru Guo, Simin Liu, Zhaohong Liu, Tao Song

We report on the experimental observation of the modulation instability of quasi-plane-wave beams in the self-defocusing photorefractive crystal $LiNbO_3$:Fe. Theoretical analysis shows that this modulation instability is ascribed as the nonlocal respond of refractive index to the optical illumination. Our analysis also indicates that the perturbation periods depend on the ratio of the optical beam's intensity to that of the dark irradiance. The agreement between experiment and theory for the perturbation period is good.

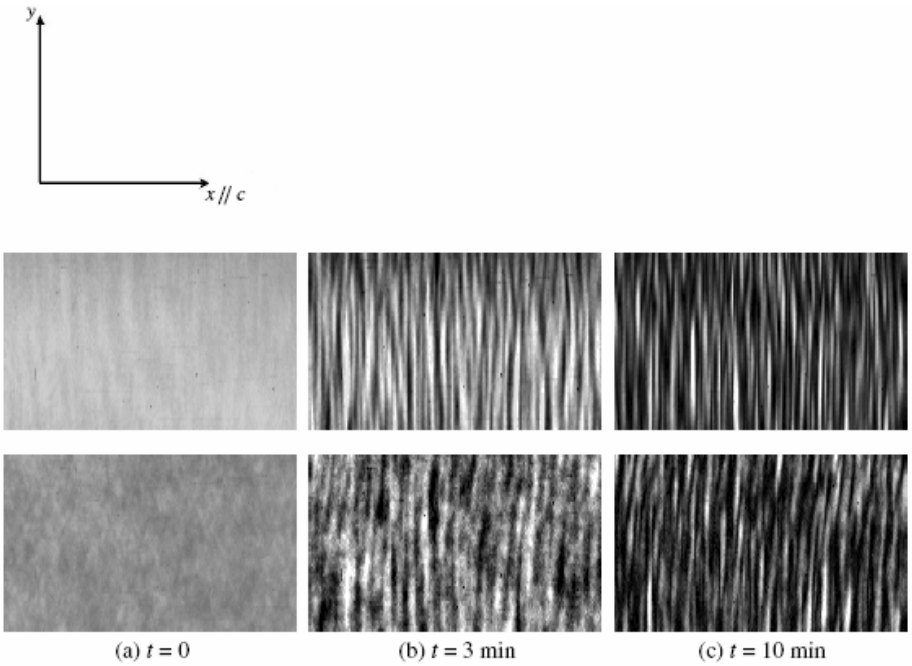

Fi
int
an expanded and collimated laser, respectively (bottom)

References

[1]A. Hasegawa 1975 *Plasma instabilities and nonlinear effects* (Heidelberg: Springer-Verlag)

[2]Bilbaut J M, Marquite P and Michaux B 1995 Modulational instability of two counterpropagating waves in an experimental transmission line *Phys. Rev.* E **51** 817-20

Supported by National Natural Science Foundation of China (No. 60378013, 60278006 and 10474047).

To be published on Journal of Optics A

Time-Resolved Femtosecond Degenerate Four-Wave Mixing in $LiNbO_3$:Fe,Mg Crystal

Wang Zhenhua, Zhang Xinzheng, and Xu Jingjun

Forward degenerate four-wave mixing (DFWM) processes are investigated with a femtosecond pulse laser in lithium niobate crystal doubly-doped with magnesium and iron. The laser is operated at 520 nm with pulse duration of 200 fs. The pulse energy dependence reveals a pure third-order nonlinear response, and the third-order nonlinear susceptibility $\chi^{(3)}$ in the material is evaluated to be 4.96×10^{-13} esu. The time-resolved DFWM process shows a response time of $\chi^{(3)}$ shorter than 100 fs, which is due to the nonresonant electronic nonlinearities. Our results indicate that LiNbO3 crystals have potentials for ultrafast real-time optical processing systems, which require a large and fast $\chi^{(3)}$ optical nonlinearity.

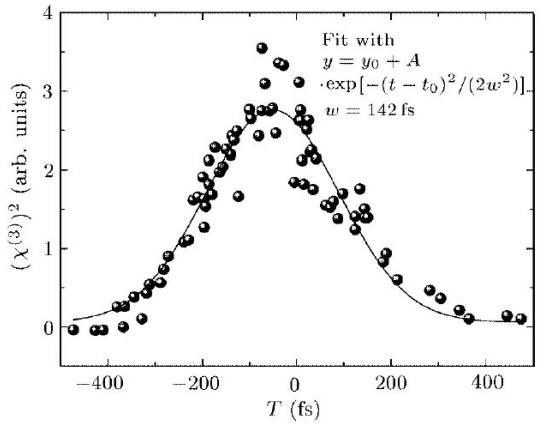

Fig. 1: Time-resolved third-order nonlinear susceptibility in LN:Fe, Mg by DFWM.

References

[1] Adibi A, Buse K and Psaltis D, Opt. Lett. **24**, 652 (1999).
[2] Liu Y W et. al., Opt. Lett. **25**, 908 (2000).
[3] Xu J J et. al., Chin. Phys. Lett. **16**, 29 (1999).

Supported by the National Natural Science Foundation of China (60208003)
Published on Chin. Phys. Lett. **22**, 2831 (2005)

Improvement of precision and SNR in time-resolved fluorescent spectroscopy

Wang Kun, Zhang Xinzheng, and Wang Zhenhua

When the gating time is far larger than the response time of the electronic gate, the sampling gate can be assumed rectangular. Under this approximation, we simulated the time-resolved fluorescent decay influenced by the random noise. We found that the longer the gate width the higher the signal to noise ratio, and the precision is determined mainly by the sample interval. The relative intensity between two components in multi-exponential fluorescent decay has been deduced. The theoretical analysis is coincident with the experimental results in GaP sample. By increasing the gating time and keeping small sample interval, we measured the fluorescent lifetime in LN:Er crystal at nanosecond time scale.

References

[1] Larsen OFA et. al. Biophys. J. **81**, 1115 (2001).
[2] I. V. Rubtsov et. al. J. Phys. Chem. A **106**, 2795 (2002).
[3] M. Straub et. al. Appl . Phys . Lett. **73**, 1769 (1998).

Supported by the National Natural Science Foundation of China (60208003)
Published on Laser Technology **29**, 126 (2005) (in Chinese)

Observation of strong stimulated photorefractive scattering and self-pumped phase conjugation in $LiNbO_3$:Mg in the ultraviolet

Haijun Qiao, Yasuo Tomita, Jingjun Xu, Qiang Wu, Guoquan Zhang and Guangyin Zhang

Since the first demonstration of self-pumped phase conjugation (SPPC) in $BaTiO_3$ the physical mechanism and applications of SPPC have been studied extensively. Although stimulated photorefractive backscattering was found to generate SPPC, reported experiments were performed in the visible. With the development of ultraviolet lasers and the increasing demands for high-resolution photolithography and laser-beam control in the ultraviolet, it would be necessary to use SPPC in the ultraviolet as well. In this work, we report on what we believe to be the first demonstration of ultraviolet SPPC by stimulated photorefractive backscattering that results from large two-wave coupling gains in highly Mg-doped $LiNbO_3$.

In the experiment we used a congruent $LiNbO_3$ crystal doped with 5 mol% Mg that was above the optical damage threshold. An Ar^+ laser operating at 351 nm was employed as a light source. We found that the crystal had the coupling gain coefficient as large as 16.1 cm^{-1} with the gain direction from the +c to -c crystal axis. Stimulated photorefractive backscattering was observed by simply passing the focused laser beam through the sample along the +c axis. We found that the morphology of backscattering patterns was strongly dependent on the distance between the crystal and the focal point, as shown in Fig.1 (where a minus value corresponds to the focal point inside the crystal). It can be seen that backscattering patterns mostly consist of a group of tiny speckles. Yet, the tiny speckles merged into a single spot at the distance of ~0.2 mm. This single spot beam was found to be a phase-conjugate replica of an incident beam. We proved it by intentionally inserting a phase distorter in the beam path between the lens and the crystal. The self-pumped phase-conjugate reflectivity of approximately 10% was obtained when the input beam intensity was 483 kW/cm^2.

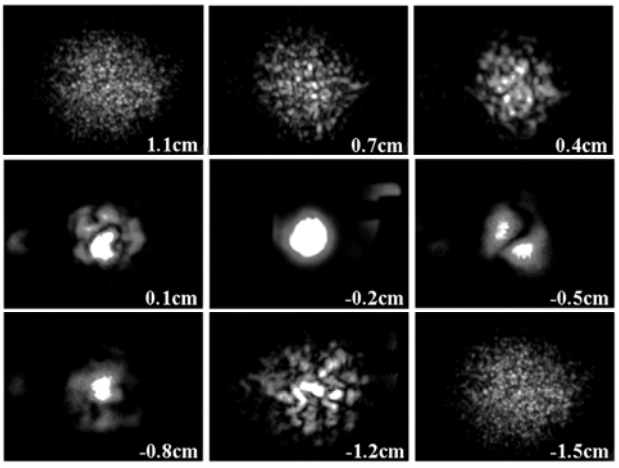

Fig. 1: Backscattering patterns at different distances.

References

[1] J. Feinberg, Opt. Lett. 7, 486 (1982).
[2] W. She and W. Lee, Opt. Commun. 146, 249 (1998).
[3] J. Xu, G. Zhang, F. Li, X. Zhang, et al., Opt. Lett. 25, 129 (2000).

Supported by the Key Project of Chinese Ministry of Education
Published on Optics Express **13**, 7666 (2005)

On the dark-decay behaviors of photorefractive gratings in Mg-doped near stoichiometric lithium niobate crystals at 351 nm

Haijun Qiao, Jingjun Xu, Guoquan Zhang, Dengsong Zhu, Wei Li, Xuanyi Yu, Guangyin Zhang and Yasuo Tomita

We studied the photorefractive properties of magnesium doped near stoichiometric lithium niobate crystals in the near-ultraviolet at 351 nm. Dark-decay behaviors of the photorefractive gratings were particularly investigated in detail. It was found that the photorefraction was increased with increasing magnesium concentrations, and with increasing the [Li]/[Nb] ratio as well. We also noticed that the dark-decay dynamics was strongly dependent on magnesium concentrations.

In particular, a dark build-up behavior after short recording, as similar to that seen in $BaTiO_3$, was observed in heavily magnesium doped crystals. A decay dark behavior, as similar to two-color nonvolatile recording during readout, was also found in heavily magnesium doped crystals. Yet the latter trend was much prominent in lightly magnesium doped crystals. The two typical dark-decay behaviors observed in one sample seemed self-contradictory to each other. Such unusual phenomena can be partly explained within the framework of multi-center model, but the underlaying grating-formation mechanism needs more investigations.

Table 1. Materials and photoprefreactive parameters of the five samples at 351 nm.

Samples	CLN	SLN	SMg02	SMg1	SMg2
Thickness along the b axis (mm)	0.494	0.860	0.703	0.703	0.746
Mg concentration (mol. %)	0	0	0.2	1.0	2.0
[Li]/([Li]+[Nb]) ratio in the crystal (%)	48.6	49.8	50.2	49.88	49.34
Maximum index change Δn_{max} ($\times 10^{-5}$)	2.73	4.94	2.27	3.03	4.59
Two-beam coupling gain Γ (cm^{-1})	7.2	NM	4.4	9.9	11.8
Photorefractive time constant τ (s)	8.1	6.3	3.5	1.4	0.12
Photoconductivity σ_p ($\times 10^{-12}$ cm/Ω·W)	0.27	0.35	0.46	1.6	18.6

References

[1] K. Buse, J. Frejlich, G. Kuper and E. Kraetzig, Appl. Phys. A 57, 437 (1993).
[2] J. Otten, A. Ozois, M. Reinfelde, K. H. Ringhofer, Opt. Commun. 72, 175 (1989).
[3] H. Qiao, J. Xu, G. Zhang, G. Zhang, Phys. Rev. B 70, 094101(2004)

Supported by the Key Project of Chinese Ministry of Education
Published on OSA Trends in Optics and Photonics (TOPS) **99**, 91 (2005)

The photo-assisted wet-etching effect in lithium niobate crystals by laser irradiation at different wavelengths

Xuanyi Yu, Jingjun Xu, Haijun Qiao, Baiquan Tang, Hua Yu

With the development of photonic micro-structure devices, the research on fabricating three-dimensional photonic structure in lithium niobate (LiNbO3) crystals is in the ascendant. Several techniques such as plasma etching, ion beam etching, electron beam etching and ablation are developed so far. Besides them, the wet-etching technique has been widely used in various materials, and has been used to detect the domain and defect structure in LiNbO3 crystals. The photo-assisted wet-etching has also been the subject of many research interests, in which the material is immersed in a cell filled with the etchant and exposed to light illumination of several mW/cm^2 to a few W/cm^2. Till now, many aspects remain unclear such as etching anisotropy and dopant-selective etching which add further versatility to this technique.

The photo-assisted wet-etching effects were investigated in z-cut lithium niobate wafers. Through the investigation on the etching behavior in the LiNbO3 crystals with different dopants and under illumination of different wavelengths, it is found that both of them influence the photo-assisted wet-etching process. In the crystals of LN:Mg,Fe, the photo-assisted etching process was suppressed under all the wavelengths of 532nm, 488nm and 351nm, while totally different phenomena were observed in the undoped one. The involved mechanism is tentatively explained by the passivating action of the fluorine ion that is accelerated or inhibited due to the illuminating light. The results are of interest to the fabrication of photonic surface-microstructure and to the clarification on the mechanism of the photo-assisted wet-etching effect in LiNbO3 crystals.

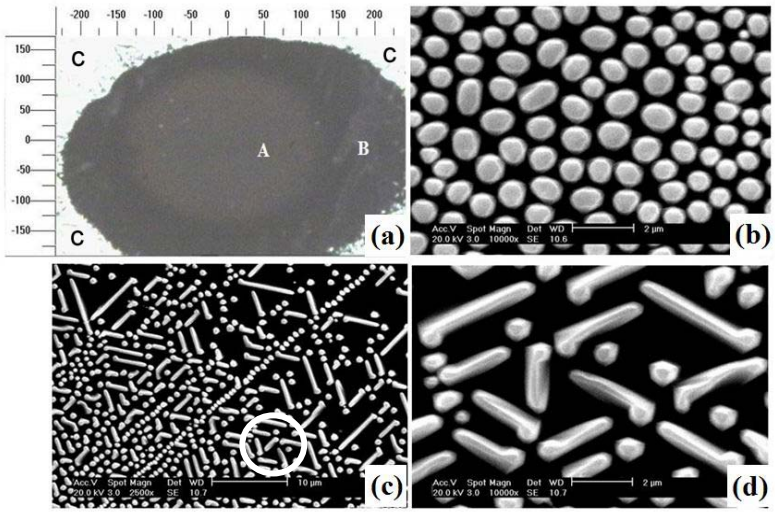

Fig. 1: (a) The illuminated region under the optical microscope in LN:Mg,Fe.(μm), (b) (c) (d)The SEM view of region A and B after etching.

References

[1] V. Bermúdez, F. Caccavale, et al., J. Cryst. Gr. **191** 589-593 (1998).
[2] Ian E. Barry, Robert W. Eason, Gary Cook, App. Surf. Sci. **143** 328-331 (1999).

Supported by the Cultivation Fund of the Key Scientific and Technical Innovation Project, Ministry of Education of China (No.704012) and the Start-up research foundation of Nankai University
Published on OSA Trends in Optics and Photonics (TOPS) **99**, 807 (2005)

Coherent backscattering, phase conjugation, and waveguide in photovoltaic media

Qiang Wu, Zhenhua Wang, Tiezheng Wang, Jingjun Xu, Romano Rupp, and Sveta Bugaychuk

We studied the coherent backscattering for a converging beam in typical photovoltaic media, $LiNbO_3$:Fe crystals and paid special attention to the complicated interaction among the incident light, changed scattering centers, and nonlinearity of the crystal. By controlling the interaction, we changed the temporally fluctuant backscattering speckles with random phases to be one phase conjugate wave of the incident light; meanwhile the random scattering centers could be self-arranged into order. And at the same time, a waveguide was formed in the sample. These results not only are interesting for the study of coherent backscattering, but also give a good reference for phase conjugation and waveguide in the photovoltaic crystals. And our experimental results also point to a new type of phase conjugation.

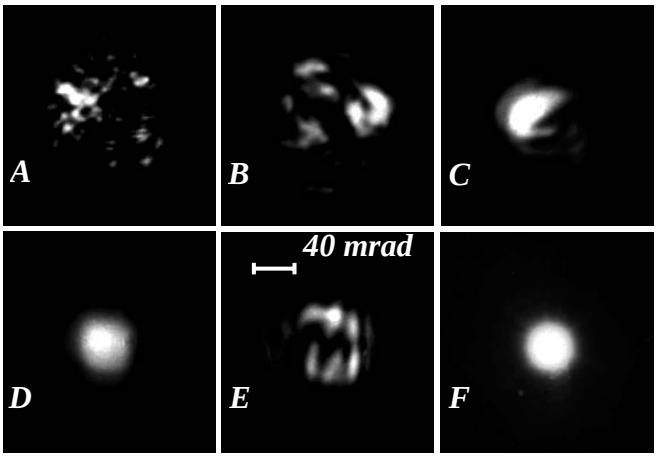

Fig. 1. The transition from backward scattering to phase conjugation

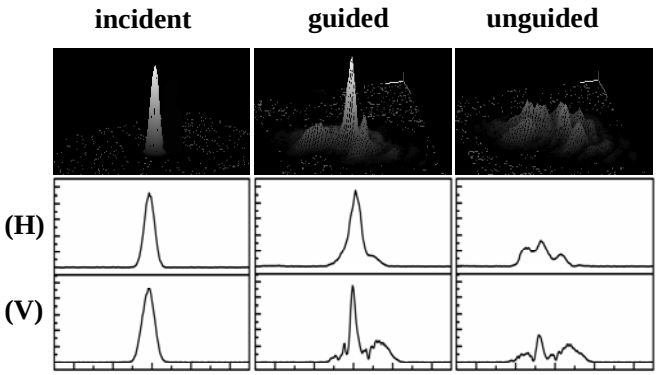

Fig.2. Guided and un unguided beams

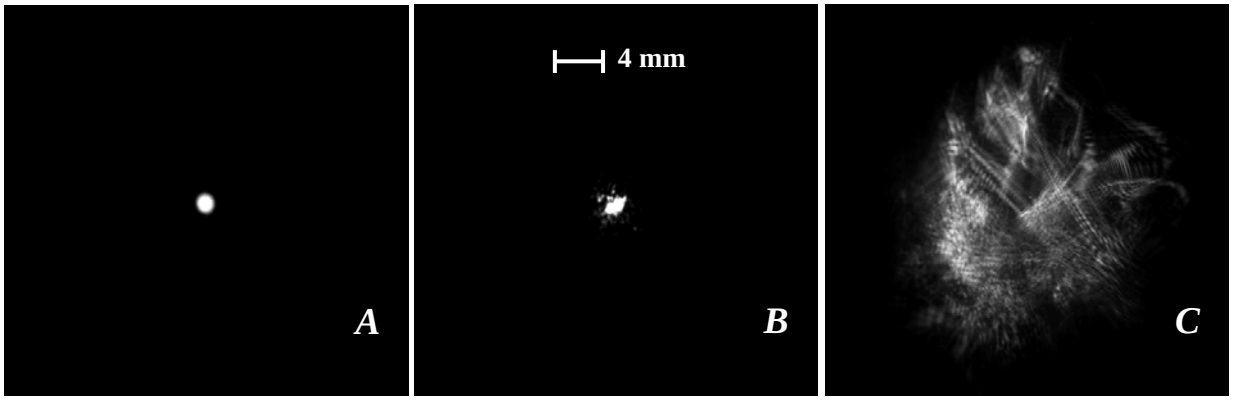

Fig.3. Distortion recovery by phase conjugation

Supported by "973" Project (G1999033004), National Science Foundation (60208003), the Key Project of the National Natural Science Foundation of China (10334010), and the Cultivation Fund of the Key Scientific and Technical Innovation Project, Ministry of Education of China(NO. 704012)We would like to thank Prof. Simin Liu for her helpful discussions.
Published on OSA Trends in Optics and Photonics(TOPS) , vol. 99, 391 (2005)

Refractive index changes by electrically induced domain reversal in a *c*-cut slab of LiNbO3

Feng Gao, Jingjun Xu,a_ Boxia Yan, Jianghong Yao, Bo Fu, Zhenhua Wang, Jiwei Qi, Baiquan Tang and Romano A. Rupp

Refractive index changes caused by electrically induced domain reversal are investigated by light diffraction from domains in periodically poled LiNbO3. Light diffraction from this type of refractive index modulation is calculated theoretically thus providing an effective and damage-free technique to characterize periodically poled materials. Examplarily, the refractive index modulation and the duty cycle are determined. The refractive index modulation obtained by electrically induced domain reversal is in the order of magnitude of 10^{-5}.

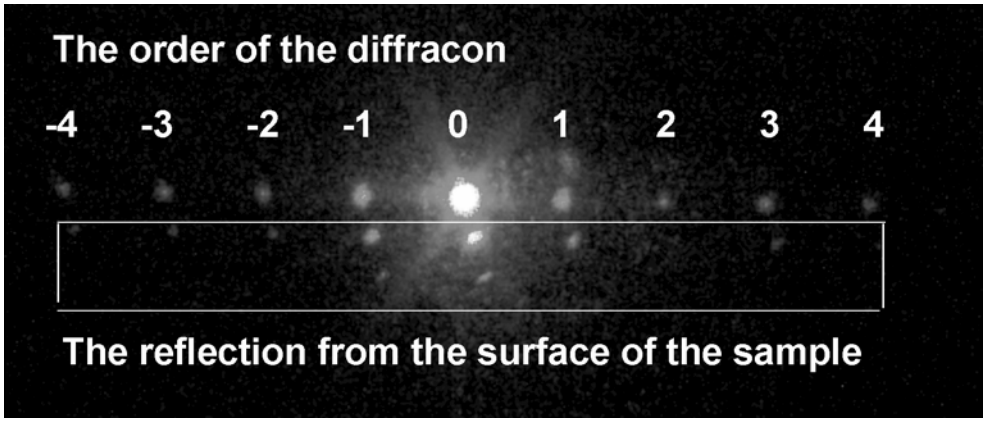

Fig. 1: Diffraction pattern of a PPLN sample with a period of 25 _m. The beams below the diffracted beams are reflections from the surface of the sample.

References

[1] T. Khayim, A. Maruko, K. Shibuya, A. Morimoto, and T. Kobayashi, IEEE J. Quantum Electron. 37, 964(2001)
[2] D. A. Bryan, R. Gerson, and H. E.Tomaschke, Appl. Phys. Lett. 44, 847(1984)
[3] A. Harada and Y. Nihei, Appl. Phys. Lett. 69, 2629(1996)
[4] A. Harada, Y. Nihei, Y. Okazaki and H. Hyuga, Opt. Lett. 22, 805(1997)
[5] Michael Bass, Handbook of Optics, 2nd ed. Vol. I, Part 2
[6] G. Rosenman, P. Urenski, A. Agronin, Y. Rosenwaks, and M. Molotskii, Appl. Phys. Lett. 82, 103(2003)
[7] G. D. Miller, Periodically Poled Lithium Niobate: Modeling, Fabrication and Nonlinear-Optical Performance (Stanford University Doctoral Dissertation), Chap.2.1.2, p. 16
[8] U. Schlarb and K. Betzler, Phys. Rev. B 50, 751(1994)
[9] Bo Fu, Nankai University, Fubo@eyou.com _private communication

supported by the Natural Science Foundation of Tianjin (Grant No. 033600911), the Cultivation Fund of the Key Scientific and Technical Innovation Project, Ministry of Education of China (Grant No. 704012), National Science Foundation of China (Grant No. 60208003), the Key National Natural Science Foundation of China (Grant Nos. 033800111 and 10334010), and the National Advanced Materials Committee of China (Grant No. 2001AA313030).
Published on Appl. Phys. Lett. 87, 252905(2005)

Observation of superluminal and slowdown light3 propagation in doped lithium niobate crystals

Feng Gao, Jingjun Xu , Haijun Qiao, Qiang Wu, Yin Xu, Guoquan Zhang

We investigate the group velocity of light in a one-dimensional volume grating inside lithium niobate crystals doped with different impurities. The superluminal and slowdown light propagations are both observed in the crystals. The relationships between the group refractive index and the grating amplitude and phase shift are presented and discussed.

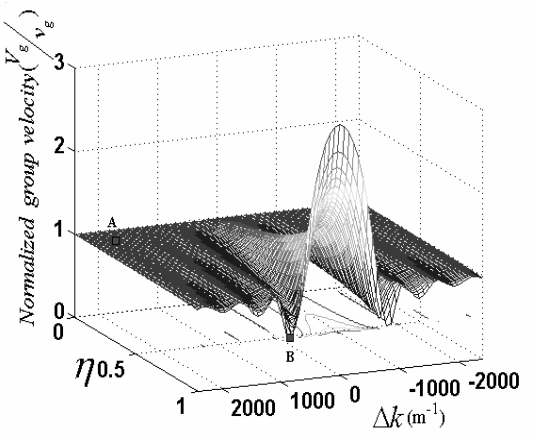

Fig. 1: The dependence of the normalized group velocity on the diffraction efficiency and the phase mismatch.

References

[1] C. Kittel, Quantum Theory of Solids (Wiley, New York, 1968).
[2] M. Scalora, R. J. Flynn, S. B. Reinhardt, and R. L. Fork, Phys. Rev. E ,54, 1078 -1081(1996)
[3] B. J. Eggleton, C. M. de Sterke, and R. E. Slusher, J. Opt. Soc. Am. B 16, 587-599(1998)
[4] Shiuan Huei Lin, Ken Y.Hsu, and Pochi Yeh, Opt. Lett. 25, 1582-1584(2000)
[5] H.Kogelnik, Bell Syst. Tech. J. 48 2909-2947(1969)
[6] P. Yeh, Optics of Layered Media (Wiley, New York, 1993).
[7] A.Kasapi, Maneesh Jain, G.Y.Yin and S.E.Harris, Phys. Rev. Lett. 74, 2447-2449(1995)
[8] Lene Vestergaard Hau, S.E.Harris, Zachary Dutton, Cyrus H.Behroozi et al., Nature 397, 594-598(1999)
[9] Zhang Guoquan, Dong Rong, Xu Jingjun, Chin.Phys.Lett. 20(10), 1725-1728(2003)
[10] K. Buse, A. Adibi, and D. Psaltis, Nature 393, 665-668(1998)

Supported by National Advanced Materials Committee of China (grant 2001AA313020), the National Natural Science Foundation of China (grants 60308005 and 0378013 and 60278006) and the Key Project of the National Natural Science Foundation of China (grants 1999033004)
To be published on Optic Communications 257/1, 185-190 (2006)

Observation of higher-band defect modes in two-dimensional photonic lattices

Igor Makasyuk, Zhigang Chen* and Jianke Yang

Here we report the first experimental demonstration of BG guidance of a light beam in optically-induced 2D photonic lattices with a single-site negative defect. In such a defect, the refractive index has its minimum as compared to that in the surrounding "rods" (akin to an "air defect" in photonic crystals or hollow-core PCF [1, 2], and much alike all-solid low-index-core PCF [5]). We observe that a probe beam at different wavelengths is spatially confined in the defect during its linear propagation, although the defect is repulsive and the beam itself has no nonlinear self-action. The observed "guidance" of light in the negative defect arises from linear propagation of the DM formed in the spatial BG of the photonic lattice, which is fundamentally different from linear guidance by TIR or nonlinear self-guidance as in a spatial soliton. In particular, we show that the "guided" patterns by the defect display fine spatial structures such as dipole and vortex cells which arise from the DM excited at higher BGs. Our theoretical analysis finds good agreement with experimental observations.

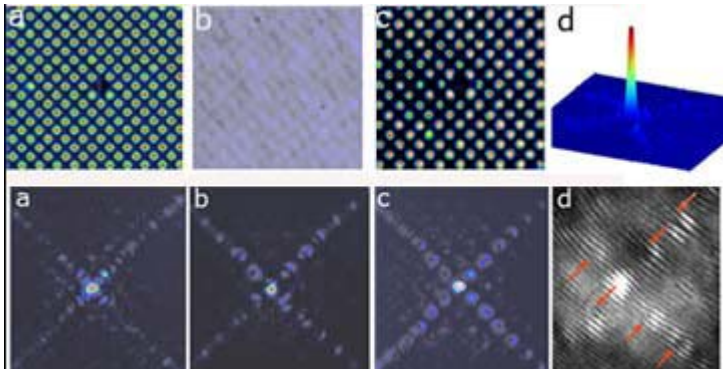

Fig. 1: Top panel: Intensity pattern of a 2D induced lattice with a single-site negative defect at crystal input (a) and output (b, c). The defective lattice can disappear (b) or survive (c) after propagating through the 20-mm long crystal. (d) 3D plots of a guided pattern by the defect. Bottom panel: Intensity patterns of DM under different lattice conditions. (a) lattice spacing Λ=27 μm, bias field E= 2.6 kV/cm; (b) Λ=42 μm, E= 2.4 kV/cm; (c) Λ=42 μm, E= 3.0 kV/cm. (d) zoom-in interferogram of (c) with a plane wave where arrows indicate location of vortices.

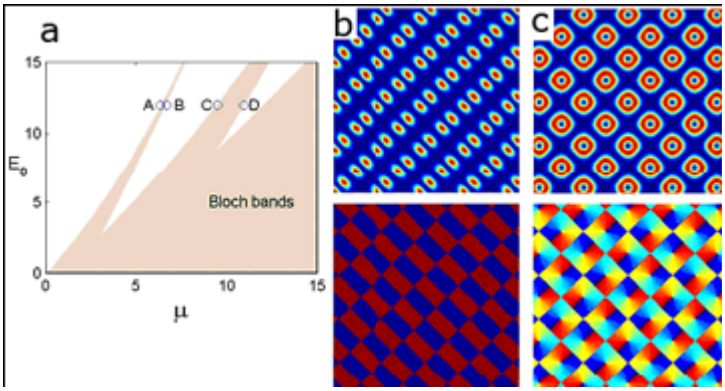

Fig. 2. (a): Bandgap structure of a 2D uniform lattice (circles indicate points where Bloch modes are analyised). (b): a Bloch wavefunction ψ(x, y) at point D; (c): a linear superposition of Bloch functions ψ(x, y) and ψ(x, y) with a -phase delay. Upper panel shows intensity patterns and lower panel the phase plots.

References

[1] P. Russell, "Photonic Crystal Fibers." Science, 299, 358 (2003).
[2] J.D. Joannopoulos et al., Photonic Crystals: Molding the Flow of Light (Princeton Univ. Press, 1995).
[3] F. Luan wt al., Opt. Lett. 29, 2369 (2004); A. Argyros et al., Opt. Express 13, 309 (2005).

Supported by the National Natural Science Foundation of China
Published on OPTICS LETTERS 30 (12), 1506-1508(2005)

Self-trapping of charge-2 vortices in optically induced photonic lattices

Anna Bezryadina, Eugenia Eugenieva, Anita Fors, Jingjun Xu and Zhigang Chen*

Optically-induced lattices have served as a test bench for studying many fascinating light behaviors due to their novel physics as well as potential applications in light-routing and navigation [1, 2]. One of the interesting phenomena is vortex propagation in such photonic lattices. Fundamental vortex (charge-1) solitons in lattices have been predicted [3] and successfully observed in experiment [4]. However, the existence and stability of higher-order discrete vortex solitons remains to be a topic of only theoretical interest. Here we report the experimental demonstration of charge-2 vortex solitons in 2D lattices of partially coherent light. In linear lattices, both on-site and off-site excitations lead to stable quasi-vortex solitons, somewhat different from quadrupole or cross-dipole structures. In nonlinear lattices, the vortex-induced lattice deformation depends on the lattice potential as controlled by nonlinearity as well as coherence. Our experimental observations are corroborated by numerical simulations.

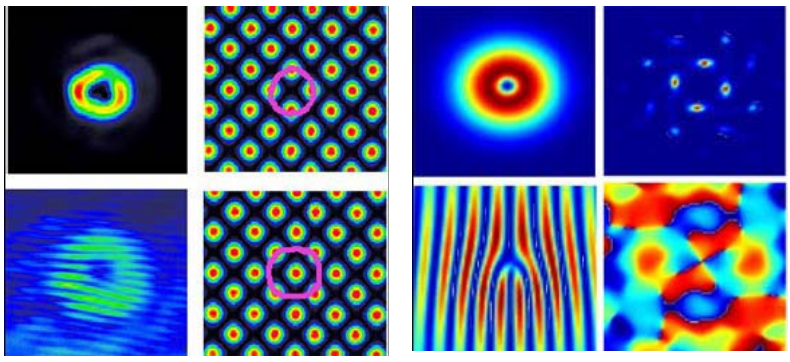

Fig. 1. Left panels: A vortex beam of topological charge m=2 (left) propagating in an optically-induced waveguide lattice (right). Shown are the input intensity pattern and interferogram of the vortex (left) and off-site (top) and on-site (bottom) vortex orientations in the square lattice (right). Right panels: Numerical simulation of the charge-2 vortex for off-site excitation. Shown are the input intensity and interferogram of the vortex at input (left), and the intensity and phase patterns of the self-trapped vortex after 8-mm of propagation.

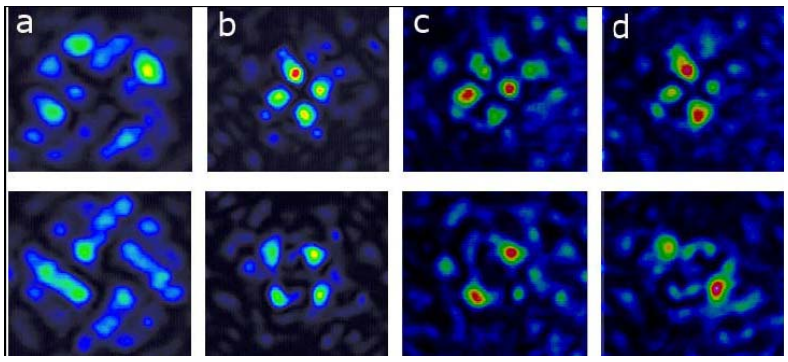

Fig. 2. Experimental demonstration of charge-2 (m=+2) quasi-vortex solitons for both off-site (top) and on-site (bottom) excitations. (a) Diffraction of the vortex at low bias field of 1.2 kV/cm. (b) Self-trapping of the vortex at high bias field of 3.4 kV/cm. The vortex breaks up into major 4 spots as in a charge-1 discrete vortex soliton but with different phase structure. (c, d) Interference of the vortex beam with a broad coherent beam (quasi-plane wave), showing the two spots in one diagonal are in phase but are out-of-phase with the two spots in the other diagonal. (The background noise is mainly from the plane wave).

References

[1] D.N. Christodoulides, F. Lederer and Y. Siberberg, Nature **424**, 817 (2003).
[2] D. Campbell, S. Flach and Yu.S. Kivshar, Phys. Today, **57**, 43 (2004).
[3] J. Yang and Z.H. Musslimani, Opt. Lett. **28**, 2094 (2003).
[4] D.N. Neshev, T.J. Alexander, E.A. Ostrovskaya, Yu.S. Kivshar, H. Martin, I. Makasyuk, Z. Chen, Phys. Rev. Lett. **92**, 123903 (2004).

Supported by the National Natural Science Foundation of China

Defect Solitons in Photonic Lattices

Jianke Yang and Zhigang Chen*

Light propagation in periodic optical structures is drastically different from that in homogeneous media [1]. For instance, the periodic potential in the uniform waveguide arrays and photonic lattices gives rise to lattice solitons that would have been impossible in a homogeneous medium [2]. Light propagation in non-uniform waveguide arrays or photonic lattices is also of particular interest. In the linear regime, light may be locally trapped by a repulsive defect in the form of defect modes due to repeated Bragg reflections. At higher power, light tends to spread rather than focus in a Kerr medium. Recently, we have predicted and observed linear defect modes in optically-induced photonic lattices [3]. Here, we present our theoretical and experimental results on nonlinear defect-modes (defect-solitons) in optically-induced 1D photonic lattices with a single-site repulsive defect in a photorefractive crystal. We show that such defect solitons bifurcate from linear defect-modes as nonlinearity is increased. In addition, these defect solitons are fully stable.

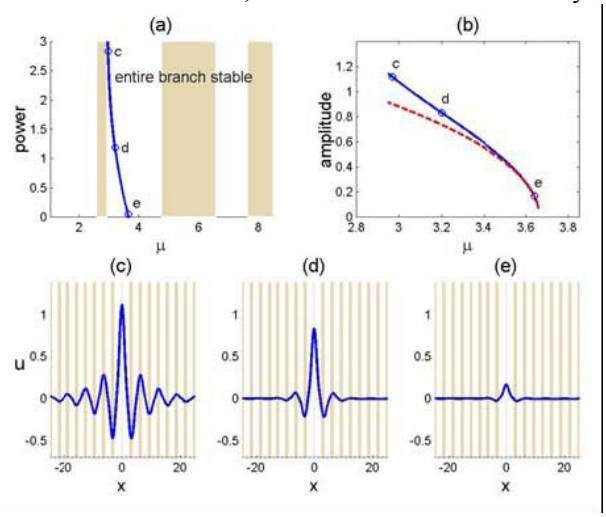

Fig . 1 Defect solitons in a repulsive defect. (a) the power diagram; (b) the amplitude diagram (solid: numerical; dashed: analytical); (c, d, e) profiles of three defect solitons at μ= 2.95, 3.2 and 3.64 [marked by circles in (a, b)] respectively.

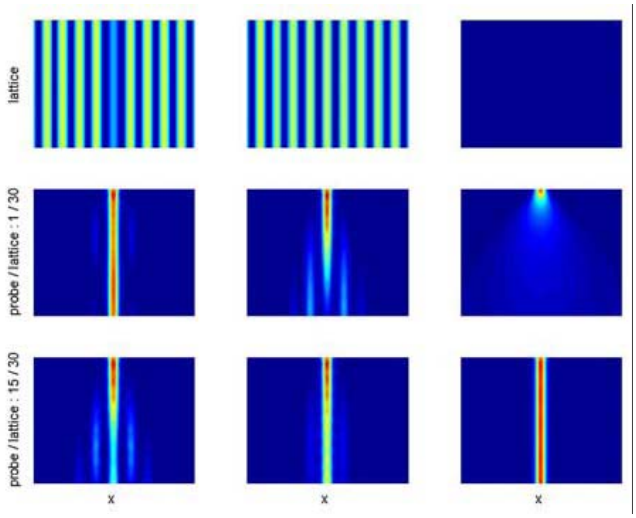

Fig. 2 Propagation of a Gaussian beam in the repulsive defected lattice (left col.), uniform lattice (middle col.), without lattice (right col.), at low (middle row) and high (bottom row) powers. Top row: lattice intensity.

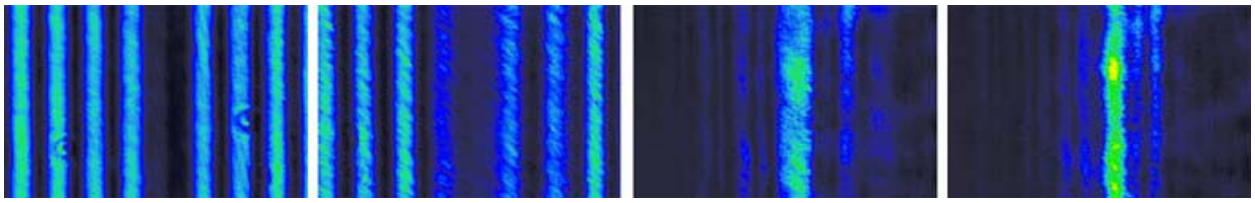

Fig.3 Experimental demonstration of a 1D lattice with a repulsive defect and observation of nonlinear defect modes. From left to right: lattice input and output, and probe beam (cylindrically focused into defect at input) output at low and high nonlinearity after 20-mm propagation **.**

References

[1] D.N. Christodoulides, et al., Nature 424, 817 (2003); D.K. Campbell, et al., Physics Today 57, 43 (2004).
[2] H.S. Eisenberg, et al., Phys. Rev. Lett. 81, 3383 (1998); J.W. Fleischer, Nature 422, 147 (2003).
[3] F. Fedele, et al., Opt. Lett. 30, 1506 (2005); Stud. Appl. Math. 115, 279-301 (2005);

Supported by the National Natural Science Foundation of China
Published on STUDIES IN APPLIED MATHEMATICS, 115(2), 279-301(2005)

Optically-induced "photonic bandgap fiber" with a low refractive index core

Xiaosheng Wang, Zhigang Chen* and Jianke Yang

One of the most intriguing properties of photonic bandgap (PBG) structures is a fundamentally different way of guiding light, as in a hollow-core photonic crystal fiber (PCF) [1]. Using the band gap properties in frequency domain, a beam with selected wavelengths can be guided in the low-index region, as has been proposed and demonstrated in air-core PCF, "Bragg fiber" or "Omniguide fiber", and recently in all-solid PCF with a lower-index core. Such PBG materials or fibers typically require sophisticated fabrication technology, as the period in photonic crystals is usually in the range of wavelength and the desired refractive index contrast is typically very high. On the other hand, in waveguide lattices often the analyses of how a light field distributes itself focuses on the PBG of spatial frequency modes (propagation constant vs. transverse wave vector) [6]. Although recent work has revealed the possibility of PBG guidance in optically-induced 1D waveguide lattices, it remains to be a challenge to induce a PCF-like lattice structure and to spatially confine a light beam around its low-index core. Here we demonstrate the formation of Bessel-like photonic lattices by optical induction in a *self-defocusing* nonlinear crystal. Such ring-shaped lattices induce a ring-shaped periodic index change with a low index core in a 10-mm long photorefractive crystal. Such index structure is similar to those of Bragg fiber and Omniguide fiber, but it is reconfigurable with the index contrast on the order of 10^{-3} to 10^{-4} and the lattice period ("pitch") on the order of tens of microns. The transition from discrete diffraction to bandgap guidance of a probe beam input at the low-index core is clearly observed by fine-tuning the lattice potential (as controlled by the lattice-beam intensity and/or the applied external voltage).

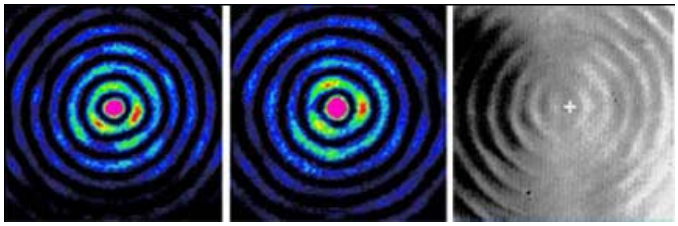

Fig. 1: Intensity pattern of a ring lattice at input (a) and output (b) of a 10-mm long crystal. With a *self-defocusing* nonlinearity, the pattern induces a waveguide lattice akin to a PBG fiber with a low-index core. A higher intensity corresponds to a lower index. A broad white-light beam probing through thelattice shows a reversed contrast in intensity pattern (c). The lattice has a spacing of about 20 μm and is induced by a 532-nm laser beam.

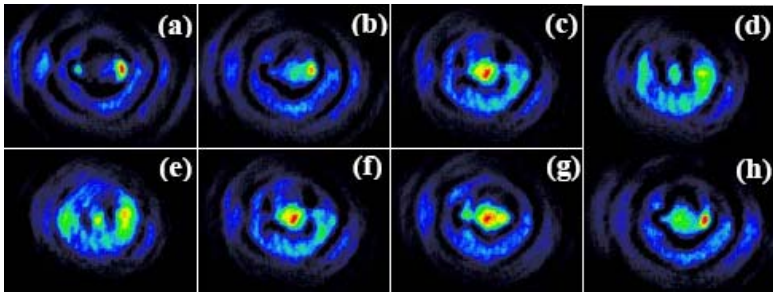

Fig. 2: Propagation of a probe beam (633 nm, no nonlinear self-action) through the optically-induced low-index core. Top: Output intensity patterns at a fixed negative bias field of 1.4 kV/cm with increasing lattice intensity. Bottom: Output intensity patterns at fixed lattice intensity with increasing bias field (0.6, 1.4, 1.7, and 2.0 kV/cm). Bandgap guidance is clearly visible in (c) and (g).

References

[1] S. D. Hart et al. , Science, **296**, 510(2002); P. Russell, Science **299**, 358 (2003).

Supported by the National Natural Science Foundation of China

Discrete diffraction and solitons in light-induced Bessel-like photonic lattices

Xiaosheng Wang, Zhigang Chen* and P.G. Kevrekidis

Optical waveguide lattices provide a test bench for studying many intriguing phenomena of light propagation including discrete solitons (DS) [1-4]. Thus far, all experimental work on DS has been performed either in one-dimensional (1D) lattices or in two-dimensional (2D) lattices with no rotational symmetry (e.g., square lattices). Here we demonstrate for the first time the formation of Bessel-like photonic lattices by optical induction. Such ring-shaped lattices remain nearly invariant in a 10-mm long photorefractive nonlinear crystal. Discrete diffraction and discrete solitons are observed when a probe beam is launched both into the lattice center and into different lattice rings. In the former case (center excitation), we demonstrate a clear transition from discrete diffraction to linear single-channel guidance by fine-tuning the lattice potential and to nonlinear self-trapping of the probe beam by fine-tuning the self-focusing nonlinearity. In the latter case (off-center excitation), we also demonstrate controlled soliton rotation in different lattice rings by imposing an initial transverse momentum to the soliton. Our experimental results are in good agreement with the theoretical/numerical analysis of these effects. These rotary solitons are expected to play new roles in soliton-driven photonics [8], and their experimental realization might provide insights for studying similar phenomena in other nonlinear systems of periodic ring structures.

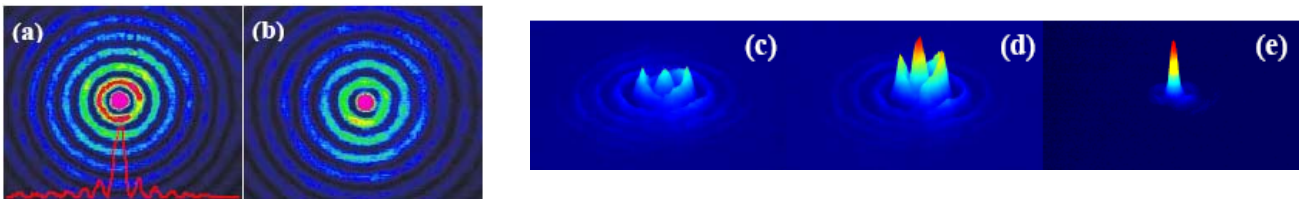

Fig. 1: Top: Intensity patterns of ring lattice at crystal input (a)and output (b) with a 4.0 kV/cm bias field. The intensity profile cross the ring lattice was inserted at the bottom of (a). Bottom: Transition from discrete diffraction to central channel guidance of a probe beam in ring lattice as the background illumination is enhanced gradually.

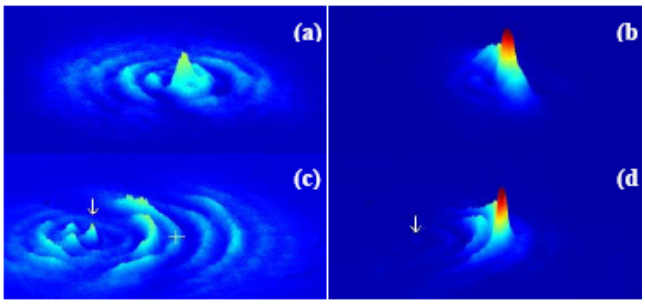

Fig. 2: Transition from discrete diffraction (a, c) to nonlinear self-trapping (b, d) of a probe beam launched in the center (a, b) and the third ring (c, d) of the lattice. Patterns in (a, c) were taken instantaneously (<0.1 s) while those in (b, d) were taken in steady state. The arrow indicates the center of the ring lattice, and the cross indicates the input position of the probe beam.

References

[1] D. N. Christodoulides et al., Nature **424**, 817 (2003).
[2] J. W. Fleischer et al., Nature (London) **422**, 147 (2003).
[3] H. Martin et al., Phys. Rev. Lett. **92**, 123902 (2004).
[4] Z. Chen et al., Phys. Rev. Lett. 92, 143902 (2004); J. Yang et al., Phys. Rev. Lett. 94, 113902 (2005).

Supported by the National Natural Science Foundation of China

Symmetric and anti-symmetric solitons and Bloch states in two-dimensional photonic lattices

Cibo Lou, Liqin Tang, Jingjun Xu, Zhigang Chen* and P.G. Kevrekidis

The dynamics of soliton propagation in coupled optical waveguides, from two coupled waveguides such as dual-core fiber couplers and directional couplers to three coupled waveguides and multiwaveguide arrays, has been studied extensively during the past decades.[1,2] Much of the earlier theoretical work focused on energy switching and stability of solitons in coupled waveguide structures. For instance, it has been shown that, in a dual-core coupler, symmetry breaking typically occurs such that a symmetric soliton becomes unstable when its energy exceeds a threshold value. We study the dynamics of off-site excitations in a two-dimensional weakly-coupled waveguide lattice. A single beam centered between two waveguides leads to an asymmetric beam profile as the nonlinearity reaches a threshold. When two probe beams are launched in parallel into two nearby off-site locations, they form symmetric or anti-symmetric (twisted)(Fig.1) soliton states depending on their relative phase. We also observe a transition from symmetric to anti-symmetric Bloch states(Fig.2) by launching a quasi-one-dimensional plane wave into the lattice.

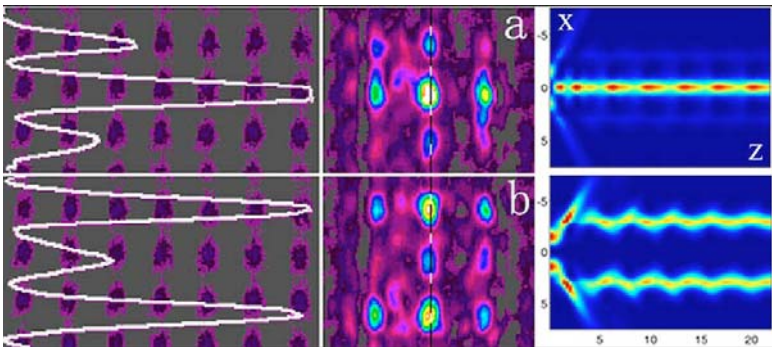

Fig. 1. (Color online) Interbeam site probing with two mutually coherent beams. Shown are the combined output beam profile (left) and the intensity pattern (middle) for (a) in-phase and (b) out-of-phase excitation. Right, simulation of dynamic evolution of two in-phase and out-of-phase beams launched at two interbeam site locations (x=−1.5 and x=1.5).

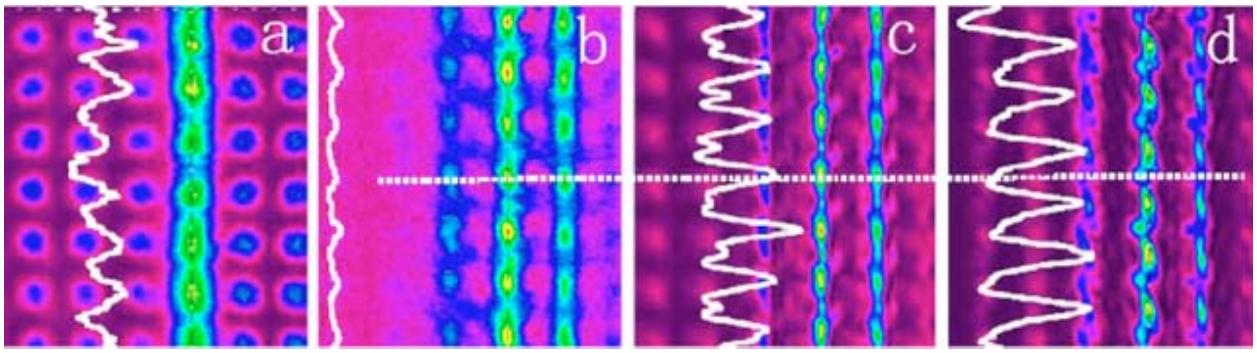

Fig. 2. (Color online) Probing with a stripe beam: (a) combined input of lattice and stripe beams; (b)–(d) output of the stripe beam at normalized intensities of (b) 0.2 and 0.8 after (c) 1 s and (d) 30 s.

References

[1] D. N. Christodoulides and R. I. Joseph, Opt. Lett. **13**, 794 (1988).
[2] A. B. Aceves, M. Santagiustina, and C. Angelis, J. Opt. Soc. Am. B **14**, 1807 (1997).

Supported by the National Natural Science Foundation of China
To be Published on OPTICS LETTERS

Publication

1. 张国权, 薄方, 许京军, “位相耦合色散效应与光速调控”, 激光与光电子进展 42(12), 36(2005)
2. 付博, 张国权, 赵璐冰, 乔海军, 徐庆君, 申岩, 许京军, 孔勇发, 孙军, 陈绍林, “同成分掺镁铌酸锂晶体紫外光致吸收阈值效应的研究”, 光学学报 25(11), 1531-1534(2005)
3. Fang Bo, Guoquan Zhang, and Jingjun Xu, “Dispersive phase coupling induced superluminal gaussian light pulses in BSO crystals at room temperature”, OSA Trends in Optics and Photonics (TOPS) Vol.99, 386 (2005)
4. Bo Fu, Guoquan Zhang, Lubing Zhao, Haijun Qiao, Qingjun Xu, Yan Shen, Jingjun Xu, Yongfa Kong, Jun Sun and Shaolin Chen, “Studies on the ultraviolet-light-induced ansorption changes in congruent $LiNbO_3$:Mg”, OSA Trends in Optics and Photonics (TOPS) Vol.99, 138 (2005)
5. Qingjun Xu, Guoquan Zhang, Haijun Qiao, Bo Fu, Yan Shen, Jingjun Xu, Yongfa Kong, Jun Sun, and Shaolin Chen, “Studies on thermal activation energy of ultraviolet-induced small polarons O^- in damadge-resistant lithium niobate crystals”, OSA Trends in Optics and Photonics (TOPS) Vol.99, 121 (2005)
6. Yan Shen, Guoquan Zhang, Bo Fu, Qingjun Xu and Jingjun Xu, “Theoretical studies on nonvolatile two-step, two-color holographic recording sensitivity for $LiNbO_3$:Fe”, Optics Communications 256(1-3), 24-34(2005)
7. 申岩, 张国权, 付博, 徐庆君, 许京军, “对不同组份 LiNbO3:Fe 非挥发全息存储的研究” , 红外与毫米波学报 24(4), 269(2005)
8. Fang Bo, Guoquan Zhang, and Jingjun Xu, “Transition between superluminal and subluminal light propagation in photorefractive Bi12SiO20 crystals”, Optics Express 13(20), 8198-8203 (2005)
9. Cibo Lou, Liqin Tang, Jingjun Xu, Zhigang Chen and P.G.Kevrekides “Observation nonlinearity-induced symmetry breaking in a photorefractive waveguide lattice”, OSA Trends in Optics and Photonics (TOPS) Vol.99, 535 (2005)
10. 陈志刚, 许京军, 楼慈波, “光诱导光子晶体结构中新型的离散空间孤子”, 物理 34(1), 12(2005)
11. Chen ZG, Martin H, Bezryadina A, et al., “Experiments on Gaussian beams and vortices in optically induced photonic lattices”, JOURNAL OF THE OPTICAL SOCIETY OF AMERICA B, 22(7), 1395-1405(2005)
12. Fedele F, Yang JK, Chen ZG, “Properties of defect modes in one-dimensional optically induced photonic lattices”, STUDIES IN APPLIED MATHEMATICS, 115(2), 279-301(2005)
13. Kevrekidis PC, Chen ZG, Malomed BA, et al., “Spontaneous symmetry breaking in photonic lattices: Theory and experiment”, PHYSICS LETTERS A, 340(1-4): 275-280(2005)
14. Fedele F, Yang JK, Chen ZG, “Defect modes in one-dimensional photonic lattices”, OPTICS LETTERS 30 (12), 1506-1508(2005)
15. Yang J, Makasyuk I, Kevrekidis PG, et al., “Necklacelike solitons in optically induced photonic lattices”, PHYSICAL REVIEW LETTERS 94 (11), Art. No. 113902(2005)
16. Chen ZG, Martin H, Eugenieva ED, et al., “Formation of discrete solitons in light-induced photonic lattices”, OPTICS EXPRESS 13 (6), 1816-1826(2005)
17. Asaro M, Sheldon M, Chen ZG, et al., “Soliton-induced waveguides in an organic photorefractive glass”, Optics Letters 30 (5), 519-521(2005)
18. Ostroverkhova, W.E. Moerner, Z. Chen, M. Asaro, M. He and R. J. Twieg, “Recent Advances in Photorefractive Organic Materials”, OSA Trends in Optics and Photonics (TOPS) Vol.99, 307 (2005)
19. Zhigang Chen, Jingjun Xu, Jianke Yang, Controlling light in photonic lattices induced in photorefractive crystals, OSA Trends in Optics and Photonics (TOPS) Vol.99, 488 (2005)

20. Feng Gao, Jingjun Xu, Haijun Qiao, Qiang Wu, Yin Xu, Guoquan Zhang "Observation of superluminal and slowdown light 3 propagation in doped lithium niobate crystals", Optics Communications 257(1), 185-190(2006)
21. Feng Gao, Jingjun Xu , Boxia Yan, Jianghong Yao, Bo Fu, Zhenhua Wang, Jiwei Qi, Baiquan Tang and Romano A.Rupp, "Refractive index changes by electrically induced domain reversal in a c-cut slab", Appl. Phys. Lett. 87, 252905(2005)
22. Yuanmei Gao, SiminLiu, Ru Guo, Xiaohua Zhang, Yi Lu, "White-light photorefractive phase mask", App. Opt. 44(9),1533-1537(2005)
23. Chunfu Huang, Ru Guo, Simin Liu, Nan Zhu, Dayun Wang, Yuanmei Gao, Yi Lu, "Spatiotemporal coherence of white light beams trapped within dark spatial solitons", Opt. Commun.248(4-6), 449-457(2005)
24. Xiaohua Zhang, Simin Liu, Ru Guo, Dayun Wang, Zhaohong Liu, Yi Lu, "Interaction between a dark stripe and a two-dimensional photonic lattice with fully incoherent white light", Opt. Commun. 252(1-3), 84-90(2005)
25. Yuanmei Gao, Simin Liu, Ru Guo, Zhaohong Liu, Tao Song, "Transmission of digital images consisting of white-light dark solitons", APP. Opt, 44(32) (2005)
26. 朱楠, 郭儒, 刘思敏, 黄春福, 汪大云, 高垣梅, "光折变晶体中的光生伏打灰空间孤子", 中国激光 32(7), 903-907(2005)
27. Haijun Qiao, Jingjun Xu, Guoquan Zhang, Dengsong Zhu, Wei Li, Xuanyi Yu, Guangyin Zhang, and Y. Tomita, "On the dark-decay behaviors of photorefractive gratings in near-stoichiometric magnesium doped lithium niobate crystals at 351 nm", OSA Trends in Optics and Photonics (TOPS) Vol.99, 91 (2005)
28. Haijun Qiao, Y. Tomita, Jingjun Xu, Qiang Wu, Guoquan Zhang and Guangyin Zhang, "Observation of strong stimulated photorefractive scattering and self-pumped phase conjugation in LiNbO3:Mg in the ultraviolet", Optics Express 13, 7666(2005)
29. Xuanyi Yu, Jingjun Xu, Haijun Qiao, Baiquan Tang, Hua Yu, "The photo-assisted wet-etching effect in lithium niobate crystals by laser irradiation at different wavelengths", OSA Trends in Optics and Photonics (TOPS) Vol.99, 807 (2005)
30. Qiang Wu, Zhenhua Wang, Tiezheng Wang, Jingjun Xu, Romano Rupp, and Sveta Bugaychuk, "Coherent backscattering, phase conjugation, and waveguide in photovoltaic media", OSA Trends in Optics and Photonics(TOPS) , vol. 99, 391 (2005)
31. Wang Zhenhua, Zhang Xinzheng, Xu Jingjun, Wu Qiang, Qiao Haijun, Tang Baiquan, Rupp Romano, Kong Yongfa, Chen Shaolin, Huang Ziheng, Li Bing, Liu Shiguo, Zhang Ling, "Time-Resolved Femtosecond Degenerate Four-Wave Mixing in $LiNbO_3$:Fe,Mg Crystal", Chin. Phys. Lett. 22, 2831-2833(2005)
32. 王鲲, 张心正, 王振华, 唐莉勤, 吴强, 许京军, "时间分辨荧光光谱中信噪比与测量精度的提高", 激光技术 29(2), 126-129(2005)
33. 陆文强, 孙骞, 许京军, 崔国新, 齐继伟, 高国祥, 陈靖, "利用凹面镜抑制全息光栅叠置噪音", 光电子.激光 16(3), 152(2005)
34. Wenqiang Lu, Yudong Li, Jingjun Xu, Qian Sun, "The influence of wavefront of the writing beams on angle Bragg selectivity in volume holographic storage", SPIE 5636, 491-494(2005)
35. Wenqiang Lu, Yudong Li, Jingjun Xu, Qian Sun, "Noise-free readout in holographic storage by concave mirror", SPIE 5636,512-514(2005)

[**Bookmaking**]

1. 孔勇发, 许京军, 张光寅, 刘思敏, 陆猗, 《多功能光电材料——铌酸锂晶体》, 科学出版社 (2005)
2. Guoquan Zhang, Detlef Kip, David Nolte, Jingjun Xu, "Photorefractive effecs, materials, and devices", Optical Society of America (2005)

Conference

1. Guoquan Zhang, Fang Bo, Rong Dong, Jingjun Xu, "Phase coupling and control of light speed in photorefractive media", International Conference on Coherent and Nonlinear Optics, St. Petersburg, Russia, May 11-15(2005) (**invited talk**)
2. Guoquan Zhang, "Super- and subluminal light propagation in BSO crystals at room temperature", International workshop on atoms and photons for quantum information, Shanghai, China, July 25-26(2005) (**invited talk**)
3. Bo Fu, Guoquan Zhang, Lubing Zhao, Haijun Qiao, Qingjun Xu, Yan Shen, Jingjun Xu, Yongfa Kong, Jun Sun and Shaolin Chen, "Studies on the ultraviolet-light-induced ansorption changes in congruent $LiNbO_3$:Mg", The tenth International Conference on Photorefractive Effects, Materials, and Devices, Sanya, Hainan, China(2005)
4. Fang Bo, Guoquan Zhang, and Jingjun Xu, "Dispersive phase coupling induced superluminal gaussian light pulses in BSO crystals at room temperature", The tenth International Conference on Photorefractive Effects, Materials, and Devices, Sanya, Hainan, China(2005)
5. Qingjun Xu, Guoquan Zhang, Haijun Qiao, Bo Fu, Yan Shen, Jingjun Xu, Yongfa Kong, Jun Sun, and Shaolin Chen, "Studies on thermal activation energy of ultraviolet-induced small polarons O^- in damadge-resistant lithium niobate crystals", The tenth International Conference on Photorefractive Effects, Materials, and Devices, Sanya, Hainan, China(2005)
6. Ostroverkhova, W.E. Moerner, Z. Chen, M. Asaro, M. He and R. J. Twieg, "Recent Advances in Photorefractive Organic Materials", The tenth International Conference on Photorefractive Effects, Materials, and Devices, Sanya, Hainan, China(2005)
7. Z. Chen, "Spatial solitons in optically-induced photonic lattices", International Conference on Nonlinear Waves, Integrable Systems and Applications, Colorado Spring, CO, June(2005)
8. Z. Chen, "Discretizing light in light-induced photonic lattices", International Conferences on Coherent and Nonlinear Optics (ICONO-2005), St. Petersburg, Russia, May (2005)
9. Zhigang Chen, Jingjun Xu, Jianke Yang, "Controlling light in photonic lattices induced in photorefractive crystals", The tenth International Conference on Photorefractive Effects, Materials, and Devices, Sanya, Hainan, China(2005)
10. Haijun Qiao, Jingjun Xu, Guoquan Zhang, Dengsong Zhu, Wei Li, Xuanyi Yu, Guangyin Zhang, and Y. Tomita, "On the dark-decay behaviors of photorefractive gratings in near-stoichiometric magnesium doped lithium niobate crystals at 351 nm", The tenth International Conference on Photorefractive Effects, Materials, and Devices, Sanya, Hainan, China(2005)
11. Xuanyi Yu, Jingjun Xu, Haijun Qiao, Baiquan Tang, Hua Yu, "The photo-assisted wet-etching effect in lithium niobate crystals by laser irradiation at different wavelengths", The tenth International Conference on Photorefractive Effects, Materials, and Devices, Sanya, Hainan, China(2005)
12. Qiang Wu, Zhenhua Wang, Tiezheng Wang, Jingjun Xu, Romano Rupp, and Sveta Bugaychuk, "Coherent backscattering, phase conjugation, and waveguide in photovoltaic media", The tenth International Conference on Photorefractive Effects, Materials, and Devices, Sanya, Hainan, China(2005)
13. Cibo Lou, Liqin Tang, Jingjun Xu, Zhigang Chen and P.G.Kevrekides "Observation nonlinearity-induced symmetry breaking in a photorefractive waveguide lattice", The tenth International Conference on Photorefractive Effects, Materials, and Devices, Sanya, Hainan, China(2005)
14. Cibo Lou, Jingjun Xu, Zhigang Chen, "Novel discrete solitons in light-induced photonic lattices", International Symposium On Photonics, Biophotonics and Nanophotonics, Nanjing, Jiangsu, China (2005)
15. Cibo Lou , Jingjun Xu, Zhigang Chen, "Discrete solitons and symmetry breaking in a photonic

lattice", 第二十届国际光学会议(ICO20),长春(2005) (特邀报告)

The passive Q-switched microchip Er/Yb glass laser pumped by laser diode

Song Feng ,Wu Zhaohui, Liu Shujing, Cai Hong, Tian Jianguo, Zhang Guangyin

An analytical model of passively Q-switched diode-pumped Er-Yb:glass laser with a Co^{2+}:$MgAl_2O_4$ plate as a saturable absorber has been developed. Considering energy transfer between Er^{3+} and Yb^{3+}, upconversion luminescence and the transition processes of the Co^{2+} in the Co^{2+}:$MgAl_2O_4$ plate, rate equations of the passively Q-switched laser is presented and useful conclusions are drawn by numerical analysis in the paper. It is very useful to optimize these kind of lasers.

Erbium doped glass laser is attractive for its compactness, economy, high efficiency, simple structure, and eye-safe wavelength (around 1.54μm). Laser diode pumped 1.54μm passive Q-switched erbium doped glass laser was reported in this letter. A laser diode with wavelength of 973nm and output power of 1W was used to pump a 1mm Er/Yb co-doped phosphate glass. The concentrations of erbium and ytterbium are 1%wt and 21%wt respectively. A Co^{2+}:$MgAl_2O_4$ slab crystal was used to be a passive Q-switcher. Q-switched pulses with repetition frequency of 800Hz, width of 7.4ns,peakpower of 2.2Kw and average power of 13.3mW were obtained when absorbed pump power was 500mW. A sandwich structure of the Q-switched microchip Er/Yb glass laser has also been demonstrated, which shows shorter pulse widthof 6.8ns. What's more, we studied the dependence of pulse duration and repetition frequency on pump power.

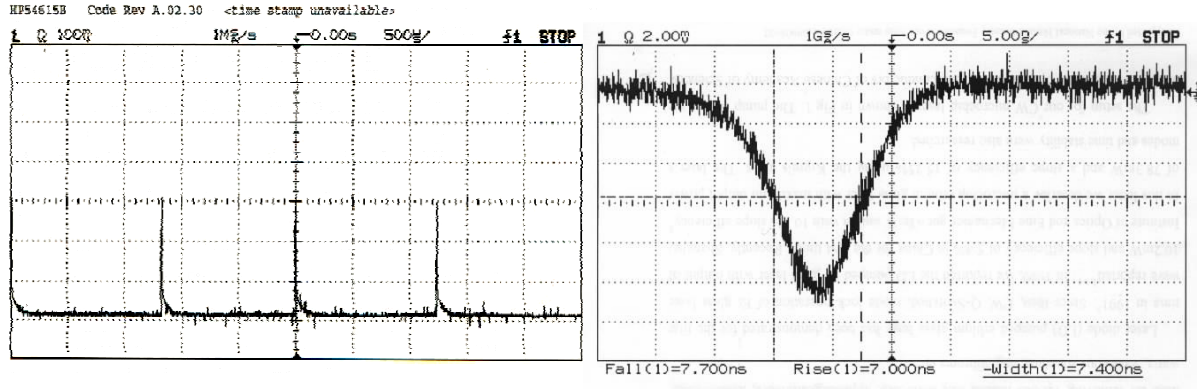

(a) (b)

Fig.3. output pulses of the 1.54μm laser(cavity length is about 3mm). (a) Output pulse train with the repetition rate of about 800Hz. (b) Single pulse with the width

References

[1] Laporta P, Silverstri S D, Magni V, and Svelto O 1991 *Opt. Lett.* **16** 1952

[2] Hutchinson J A, Toomas H A 1992 *Appl.Phys.Lett.* **60** 1424

[3] Song F, Chen X B, Myers M J et al 1999 *Chinese Journal of Lasers* **26** 790

Supported by the National Natural Science Foundation of China (Grant Nos.60377033, 60025512), Natural Science Foundation of Tianjin City, Program for New Century Excellent Talents in University, the Scientific Research Foundation for the Returned Overseas Chinese Scholars, State Education Ministry and the Excellent Young Teachers Program of MOE,P.R.C..

Spectral Performance and Intensive Green Upconversion Luminescence in Er^{3+}/Yb^{3+}-codoped $NaY(WO_4)_2$ Crystal

Song Feng, Han Lin, Su Jing

Using Czochralski (CZ) pulling method, an Er^{3+}/Yb^{3+}-codoped $NaY(WO_4)_2$ crystal was prepared. Absorption spectra, emission spectra and excitation spectra of this crystal were measured at room temperature. Some optical parameters, such as intensity parameters, spontaneous emission probabilities and lifetimes, were calculated from absorption spectra with Judd-Ofelt (J-O) theory. Upconversion luminescence excited by a 970*nm* diode laser was studied. In this crystal, green upconversion luminescence is particularly intensive. Energy transfer mechanisms that play an important role in upconversion processes were analyzed. Two cross-relaxation processes: $^4G_{11/2} + {}^4I_{9/2} \rightarrow {}^2H_{11/2}$ (or $^4S_{3/2}$) + $^2H_{11/2}$(or $^4S_{3/2}$), and $^4G_{11/2} + {}^4I_{15/2} \rightarrow {}^2H_{11/2}$(or $^4S_{3/2}$) + $^2I_{13/2}$, which contribute to the intensive green luminescence under 378*nm* excitation, were put forward. Background energy transfer $^4G_{11/2}(Er^{3+}) + {}^2F_{7/2}(Yb^{3+}) \rightarrow {}^4F_{9/2}(Er^{3+}) + {}^2F_{5/2}(Yb^{3+})$ was also demonstrated.

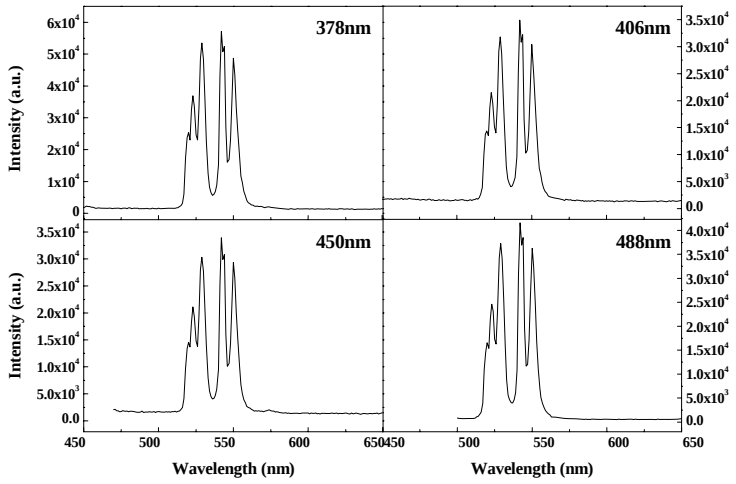

Fig. 1: Emission spectra when excitation wavelength is 378, 406, 450, and 488*nm*.

References

[1] T.J. Whitley, C.A. Millar, R. Wyatt, M.C. Brierley, *Electron. Lett.* **27** 1785 (1991).
[2] P.E.A. Mbert, E. Heumann, G. Huber, B.H.T. Chai, *Opt. Lett.* **22** 1412 (1997).
[3] A. Smith, J. P. D. Martin, M. J. Sellars, N. B. Manson, *Opt. Commun.* **188** 219 (2001).
[4] B.C. Hwang, S.B. Jiang, T. Luo, J. Watson, G. Sorbello, *J. Opt. Soc. Am. B* **17** 833 (2000).
[5] H. Lin, E.Y.B. Pun, S.Q. Man, X.R. Liu, J. Opt. Soc. Am. B **18** 602 (2001).
[6] Z. P. Cai, A. Chardon, H. Y. Xu, P. Féron, G. M. Stéphan, Opt. Commun. **203** 301 (2002).

The work is supported by the Program for New Century Excellent Talents in University and the Program for Excellent Young Teachers sponsored by State Education Ministry of China, Natural Science Foundation of Tianjin, and the Scientific Research Foundation for the Returned Overseas Chinese Scholars.

Gain characteristics of high-concentration Er^{3+}/Yb^{3+}-codoped phosphate fiber amplifier

Song Feng, Su Ruiyuan, Fu Qiang, Qin Bin, Tian Jianguo, Zhang Guangyin

The gain characteristics of high-concentration Er^{3+}/Yb^{3+}-codoped phosphate fiber amplifier pumped with 980nm wavelength are theoretically studied in this paper. In order to shorten the length of optical devices, high doping concentration is needed. But when the Er^{3+} concentration exceeds 1.0×10^{25}ions/m^3, the effects of up-conversion and cross-relaxation can't be neglected. In this analytical model, the up-conversion and cross-relaxation effects are taken into consideration. So it is suitable for analyzing the gain characteristics of high-concentration fiber amplifier.

With the rate equations and the propagation equation of Er^{3+}/Yb^{3+}-codoped phosphate fiber, we analyzed the effects of concentrations of Er^{3+} and Yb^{3+}, pump power, signal power and fiber length on the gain characteristics of the co-doped fiber amplifier. Comparison with single erbium-doped fiber amplifier was also made. It can be shown that the sensitization of Yb^{3+} decreases the cluster effect of erbium ions in the fiber and the gain and pump efficiency of Er^{3+}/Yb^{3+} co-doped fiber are apparently higher than that of single erbium-doped fiber. Numerical results also demonstrate that under suitable concentrations of Er^{3+} and Yb^{3+}, considerable signal gain, 10dB, can be achieved in a 3.2cm-long fiber amplifier with 20dBm(100mW) pumping power at 980 nm.

Figure 1 shows the gain as a function of the fiber length. Under different pump powers, the gain can reach the maximum at suitable length and then decrease for longer fiber.

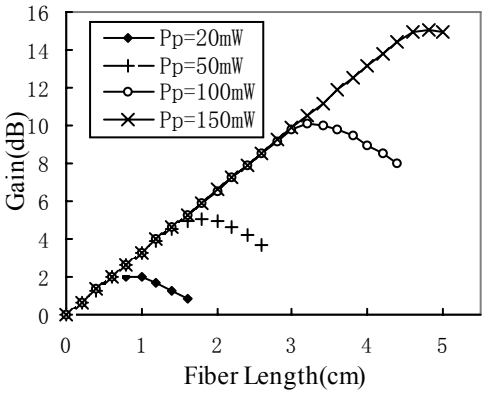

Fig.1 Gain versus

Reference

1. Yan Y C, Faber A J *et al* 1997 *Appl. Phys. Lett.* **71** 2922
2. Zhou X and Toratani H 1995 *Phys. Rev. B* **52** 15889
3. Pasquale F D and Federighi M 1994 *IEEE J. Quantum Electron.* **30** 2127
4. Laporta P, Taccheo S, Longhi S and Svelto O 1993 *Opt. Lett.* **18** 1232
5. Rany C and Desurvire E 1991 *J. Lightwave Technol.* **9** 271

Supported by the National Natural Science Foundation of China (Grant Nos.60377033, 60025512), Natural Science Foundation of Tianjin City, Program for New Century Excellent Talents in University, the Scientific Research Foundation for the Returned Overseas Chinese Scholars, State Education Ministry and the Excellent Young Teachers Program of MOE,P.R.C..

A Simplified transformation circle theory in analyzing laser resonator

Song Feng, Wu Yanxiong, Zhou Feng, Liu Shujing, Tian Jianguo, Zhang Guangyin

A method to analyze laser resonator, transformation circle theory is simpler. In this paper, further simplification was made and only . circles in the theory and simple mathematic knowledge were used to analyze the stability and calculate the parameters of the laser resonator, which further simplifies the transformation theory. The results agree with the well-known matrix theory. A two-mirror and three-mirror (including a thermal lens) laser resonators were illustrated to give the stability formula and the Guassian beam dimensions on the mirrors. Furthermore, we give a common used example when the laser medium is close to the cavity mirror.

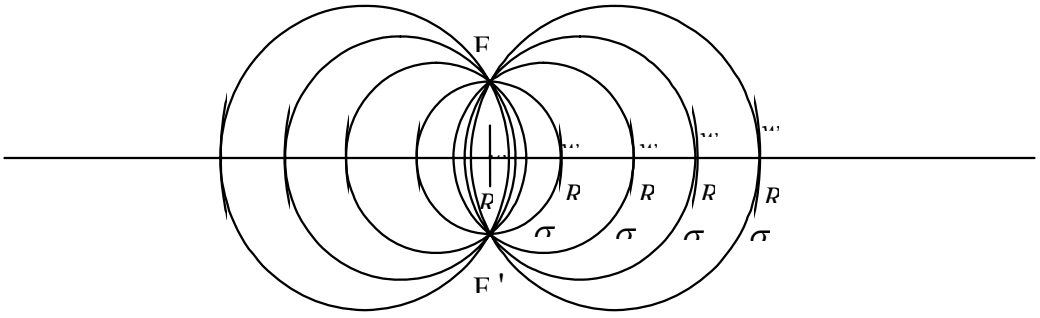

FIG.1. The changes of R and ω with the propagation of the Gaussian beam

The experiment set-up is as follow:

$F_1 F_1'$ is twice as long as the beam parameter b_0, circles represents the wave-front of the Gaussian beam, R is the curvature radius of circle, w is waist radius.

It is simple and direct to use the transformation circle theory to analyze the stability property of the two-mirror and three-mirror resonator. We only use circles and simple mathematic knowledge to calculate and the results agree with the well-known matrix theory. The formulas of the facula size on the mirrors can be analyzed and calculated with the Matlab program. We also analyze a common used example that the laser medium is close to the cavity mirror, and get the stability criterion and the formula of the facula size. In the end we give a method to measure the focal length of the thermal lens according to the stability of the resonator.

References

[1] Kogelink H,Li, Appl Opt **5**, 1550 (1966)

[2] Laures P, Appl Opt **6**, 747 (1967)

Project supported Program for New Century Excellent Talents in University, the Scientific Research Foundation for the Returned Overseas Chinese Scholars, State Education Ministry and the Excellent Young Teachers Program of MOE, P.R.C..

Coordinate transformation and coordinate mapping for numerical simulation of Z-scan measurements

Wei-Ping Zang, Jian-Guo Tian, Zhi-Bo Liu, Wen-Yuan Zhou, Feng Song, Chun-Ping Zhang

The beam propagation in thin nonlinear media has been analyzed and modeled extensively. But the analyses of beam propagation in thick nonlinear media are usually more complicated and difficult. In higher-power regimes, numerical techniques are usually applied. But for conventional numerical methods, a significant amount of computer CPU time is always required.

We apply CTM (coordinate transformation method) to improve the numerical efficiency of beam propagation and CMM (coordinate mapping method) to improve the numerical efficiency of numerical simulation of Z-scan measurements. The numerical analyses show that the numerical efficiency of the analyses on beam propagation enhances at least two orders of magnitude and total numerical efficiency of numerical simulation of Z-scan characteristics enhances at least three orders of magnitude, compared with that of CM (conventional method). For CW laser beam and pulsed laser beam, we applied these new methods to analyze the peak-to-valley normalized transmittance difference for closed-aperture Z-scan as the function of medium length and nonlinear refraction of medium.

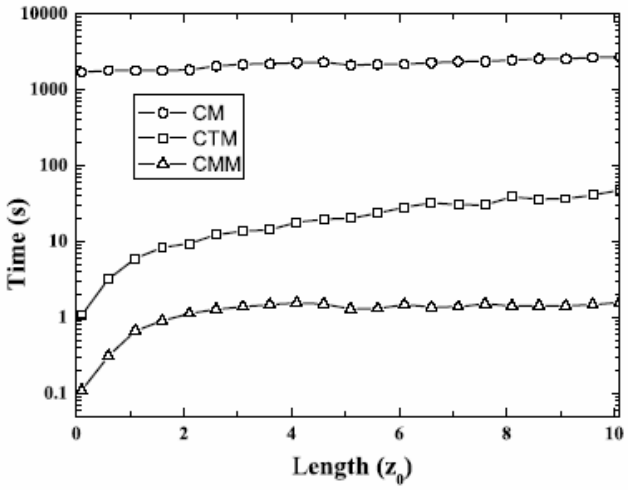

Fig. 1: Computational time taken by CM, CTM and CMM for numerical simulation of Z-scan measurements. The medium length is scaled by Rayleigh length z0, and the temporal unit is second.

References

[1] M. Sheik-Bahae, A.A. Said, T.H. Wei et al., IEEE. J. Quantum Electron. **26** (1990) 760.
[2] J.A. Hermann, J. Opt. Soc. Am. B **14** (1997) 814.
[3] W.-P. Zang, J.-G. Tian, Z.-B. Liu et al., Opt. Lett. **28** (2003) 722.

Supported by the Project 60025512 supported by the National Natural Science Foundation of China, Natural Science Foundation of Tianjin (Grant 0436012 11), a key project of the Ministry of Education (Grant 00026), the Foundation for University Key Teachers of the Ministry of Education, and the Fok Ying Tung Education Foundation (Grant 71008).
Published on Opt.Commun. **244**, 71-77(2005)

Effect of coupling between linear absorption and nonlinear absorption on Z-scan measurements

Wei-Ping Zang, Jian-Guo Tian, Zhi-Bo Liu, Wen-Yuan Zhou, Feng Song, Chun-Ping Zhang

The beam propagation in a thin nonlinear medium has already been analyzed and modeled extensively. But the analysis of Gaussian beam propagation in a thick nonlinear medium is usually more complicated. Some analytical approaches have been applied, most of them involve the aberrationless approximation, and the results are only correct to the first order in irradiance.

We have analyzed open-aperture Z-scan with multiphoton absorption by coordinate transformation. The approximate closed-form solution is obtained. The coupling between linear absorption and nonlinear absorption is also analyzed in detail. Results show that not only the magnitude of the absorption dip, but also the position of absorption dip of the normalized transmittance of open-aperture Z-scan is affected seriously by linear absorption coefficient.

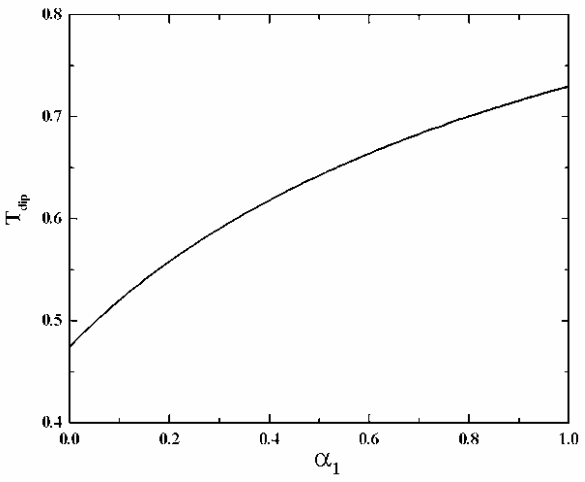

Fig. 1: The absorption dip of normalized transmittance versus the linear absorption coefficient. The real medium length is $4z_0$, and $\overline{\alpha}_2 = 1$.

References

[1] M. Sheik-Bahae, A.A. Said, T.H. Wei et al., IEEE. J. Quantum Electron. **26** (1990) 760.
[2] J.A. Hermann, J. Opt. Soc. Am. B **14** (1997) 814.
[3] W.-P. Zang, J.-G. Tian, Z.-B. Liu et al., Opt. Lett. **28** (2003) 722.

Supported by Supported by project 60025512 supported by National Natural Science Foundation of China, Natural Science Foundation of Tianjin (No. 0436012 11), and Fok Ying Tung Education Foundation (No.71008), and Innovation Foundation of Nankai University.
Published on Chinese Physics **14**, 546-550(2005)

Z-scan analysis for near top-hat beams

Yang Xin-Jiang, Zang Wei-Ping, Tian Jian-Guo, Liu Zhi-Bo, Zhou Wen-Yuan,Cao Pi-Jia, Zhang Chun-Ping, Zhang Guang-Yin

Using fast Hankel transform, we analyze the Z-scan theory of thin optically nonlinear medium. We discuss the characteristics of Z-scan curves under near top-hat beams. Meanwhile, the influence of the ratio (diaphragm-girdling ratio) of the limiting diaphragm radius to the expanded beams radius on normalized transmittance using near top-hat beams under closed-aperture is analyzed. Through theoretical analysis, the ratio with the best sensitivity is given. At last we analyze the influence of the size of the far field diaphragm on normalized transmittance under the experimental configure with the best sensitivity.

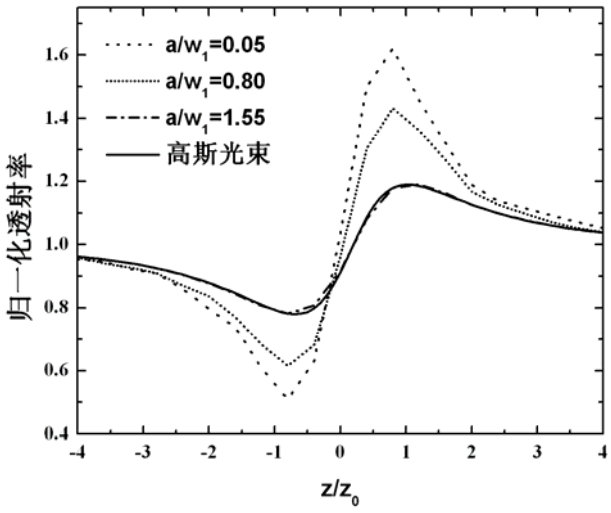

Fig. 1: The comparison of the normalized transmittance using near top-hat beams under different diaphragm-girdling ratios a/w_1 with the one using Gaussian beams for a nonlinear phase shift of 1.

References

[1] M. Sheik-Bahae, A.A. Said, T.H. Wei et al., IEEE. J. Quantum Electron. **26,** 760, (1990)

[2] W.Zhao et al, Appl.Phys.Lett. **63**, 1613, (1993)

[3] W.Zhao et al, Appl.Phys.Lett. **65**, 673, (1994)

Supported by the project 60025512 supported by National Natural Science Foundation of China, the Key Project of Chinese Ministry of Education (No.00026), the Foundation for University Key Teacher by the Ministry of Education, and Y. D. Huo Education Foundation Committee with grant No.71008.

Published on ACTA PHYSICA SINICA **54**(6), 2738 (2005)

Study on Z-scan characteristics for a large nonlinear phase shift

Shu-Qi Chen, Zhi-Bo Liu, Wei-Ping Zang, Jian-Guo Tian, Wen-Yuan Zhou,
Feng Song, Chun-Ping Zhang

To obtain unknown parameters reliably, it is necessary to make comprehensive analyses of Z-scan measurements. The Gaussian decomposition (GD) method has been usually used for analyses of Z-scan measurements with a thin nonlinear medium. However, the GD method for Z-scan is generally considered to be suitable only for the case of a small nonlinear phase shift and thin medium.

Using the Gaussian decomposition (GD) method, we here studied the characteristics of a Z scan for a thin nonlinear medium with a large nonlinear phase shift induced by a pulsed laser. It has been verified that the GD method is still valid for analyses of Z-scan measurements with a large nonlinear phase shift and is better than some others, i.e., Fresnel–Kirchhoff diffraction and the aberration-free approximation model. By comparing the peak-to-valley configuration of Z-scan curves for a large nonlinear phase shift induced by a pulsed laser with that by a cw laser, we found that some peak-to-valley features of Z-scan curves appear as the aperture size or the light intensity increases in the case of a large nonlinear phase shift. We carried out the Z-scan experiments of pure CS2 by a picosecond pulsed laser to verify the theoretical calculations in the case of a large nonlinear phase shift. The experimental results agree well with the theoretical calculations.

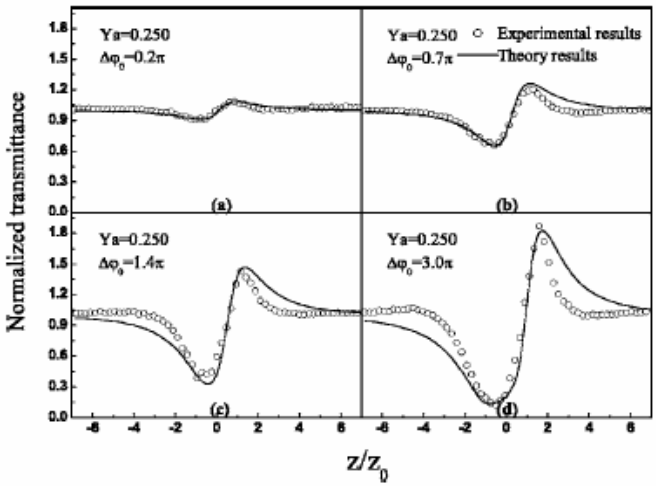

Fig. 1: Experimental and calculated Z-scan curves for different $\triangle\Phi_0$: 0.2 π, 0.7 π, 1.4 π, and 3.0 π. The dimensionless aperture radius Ya=0.250.

References

[1] M. Sheik-Bahae, A.A. Said, T.H. Wei et al., IEEE. J. Quantum Electron. **26,** 760, (1990)

Supported by the National Natural Science Foundation of China (60025512), Preparatory Project of the National Key Fundamental Research Program (2004CCA04400), Natural Science Foundation of Tianjin (043601211), and the Fok Ying Tung Education Foundation (71008).

Published on J. Opt. Soc. Am. B **22**(9), 1191 (2005)

Characteristics of co-existence of third-order and transient thermally induced optical nonlinearities in nanosecond regime

Zhi-Bo Liu, Wen-Yuan Zhou, Jian-Guo Tian, Shu-Qi Chen, Wei-Ping Zang, Feng Song, Chun-Ping Zhang

We report the experimental results on characteristics of co-existence of third-order and transient thermally induced optical nonlinearities using a nanosecond pulse laser and CS2 solutions of nigrosine. Results show that thermally induced optical nonlinearity is very sensitive to linear absorption, beam waist size and pulsewidth. Numerical simulations obtained by solving simultaneously acoustic and electromagnetic wave equations, agrees basically with experimental results. Meanwhile, the transition of optical nonlinearity from self-focusing pattern to self-defocusing pattern was observed when the contribution from thermally induced optical nonlinearity exceeds that from third-order optical nonlinearity.

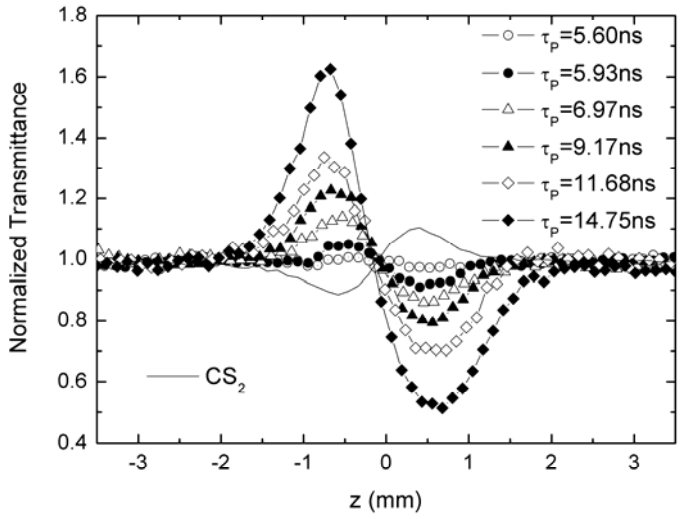

Fig. 1: Closed-aperture z-scan curves for different pulsewidth τ_p: 5.60*ns*, 5.93*ns*, 6.97*ns*, 9.17*ns*, 11.68*ns* and 14.75*ns*. The beam waist radius ω_0 is $9\mu m$, and linear absorption coefficient α_0 is $0.102cm^{-1}$. The solid line is the z-scan curve of pure CS_2.

References

[1] M. Sheik-Bahae, A.A. Said, T.H. Wei et al., IEEE. J. Quantum Electron. **26,** (1990) 760
[2] Dmitriy I.Kovsh, et al, *Appl. Opt.* **38** (1999) 5168
[3] Dmitriy I.Kovsh, David J.Hagan, Eric W.Van Stryland, *Optics Express* **4** (1999) 315

Supported by the Project 60025512 supported by the National Natural Science Foundation of China, a key project of the Ministry of Education (grant 00026), the Foundation for University Key Teachers of the Ministry of Education, and Fok Ying Tung Education Foundation (grant 71008).
Published on OPTICS COMMUNICATIONS 245 (1-6), 377 (2005)

Fabrication of Dammann Gratings in Silica Glass Using a Filament of Femtosecond Laser

Yudong LI, Wataru WATANABE, Takayuki TAMAKI, Junji NISHII and Kazuyoshi ITOH

The Dammann grating is one kind of useful binary optical elements. We fabricated a single-layer birefringence-free 5 _ 5 Dammann grating in silica glass using the filamentation of 800 nm femtosecond laser pulses. The diffraction efficiency of the Dammann grating reached 56%, which is close to the theoretical value of 77%.

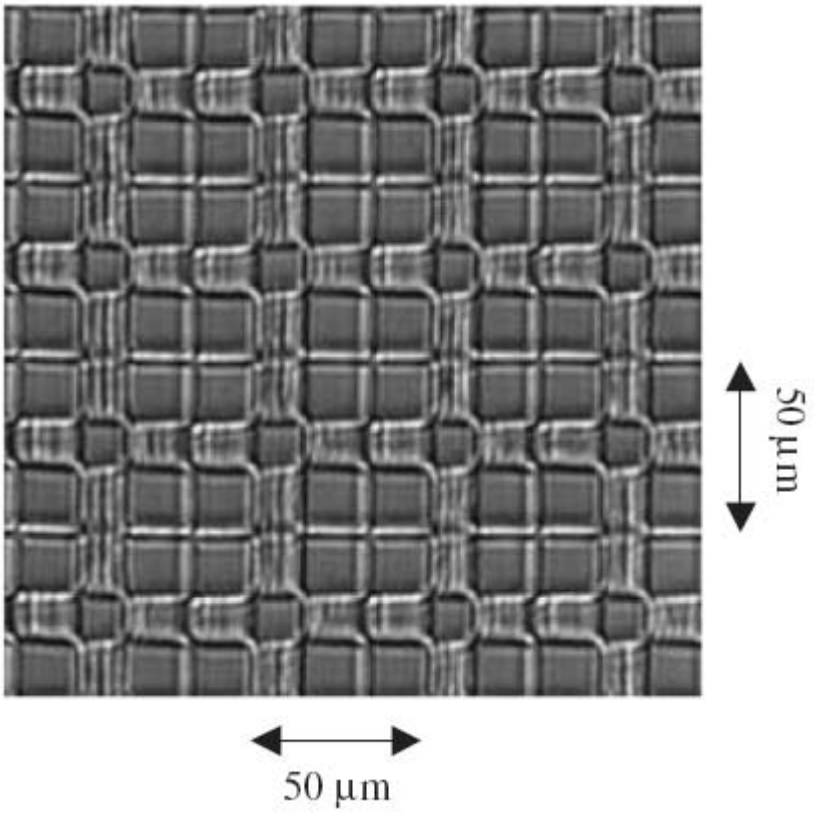

Fig. 1 Part of the fabricated 5×5 Damman grating

References

[1] K. M. Davis, K. Mura, N. Sugimoto and K. Hirao: Opt.Lett. **21**, 1729(1996)
[2] H. Dammann and E. Klotz: Opt. Acta 24, 505(1977).

Supported by the National Natural Science Foundation of China
Published on Jpn. J. Appl. Phys. 44(7A), 5014(2005)

Micro-fabrication by femtosecond laser pulses

Yudong Li, Jianguo Tian, Qian Sun

Optical microstructures are very important for the realization of multifunctional optics and photonics devices. In this paper, we reviewed the micro-fabricational technology by femtosecond laser pulses. Normal technologies, such as optical lithography, can only be used to introduce microstructures on plane surfaces of a limited number of materials. In the last decade, with the development of commercial femtosecond laser, it has been proven that micro-structuring with femtosecond laser pulses is an excellent tool for free design micro-fabrication of almost all kinds of materials. The high peak power of the incident femtosecond pulses makes nonlinear process occur not only in the light-sensitive polymerizations and metals (for example, copper) but also in the transparent media such as glass and crystals. When femtosecond laser pulses are tightly focused inside transparent materials, multi-photon absorption occurs and the micro-scale permanent structural modifications can be obtained. With the scanning of the focus of the femtosecond laser pulses, many types of 2 and 3-dimensional optical structures, including optical memory, waveguides, gratings and couplers, were produced successfully inside a wide variety of transparent materials. The surface micro-fabrication of transparent materials and metals can be realized by focusing or interfering the femtosecond laser pulses on the surfaces of the media.

References

[1] Hans Peter Herzig, Micor-optics, elements, system and applications, Taylor&Francis, 1997
[2] E. N. Glezer, and E. Mazur, “Ultrafast-laser driven micro-explosions in transparent materials”, Appl. Phys. Lett. Vol. 71, 882(1997)
[3] E. N. Glezer, M. Milosavljevic, L. Huang, R. J. Finlay, T.-H. Her, J. P. Callan, and E. Mazur, “Three- dimensional optical storage inside transparent materials”, Opt. Lett. Vol. 24, 2023(1996).
[4] M. Watanabe, H.-B. Sun, S. Juodkazis, T. Takahashi, S. Matsuo,Y. Suzuki, J. Nishii, and H. Misawa, “Three-dimensional optical data storage in vitreous silica,” Jpn. J. Appl. Phys., vol. 37, L1527(1998)

Supported by the National Natural Science Foundation of China
To be Published on SPIE 6149, (2005)

The influence of humidity on the shear-force between tip and sample in NSOM using piezo-electric fork

Tianhao Zhang, Zheyu Fang, Jianya Zheng, Limo Gao, Haidong Yang, Meirong Yin, Jia Yang, Yanzhen Luv, Huizhen Kang, Dapeng Yang, Huizhan Yang

The distanced between tip and sample can be regulated using piezo-electric quartz fork glued with micro optic fiber probe. In this work the relationships of the electric current flows through the fork vs. T-S distance under different humidity are measured. The *I-d* curve and the action distance for shear force are influenced by environment humidity. Furthermore, the intrinsic reasons for shear force damping between tip and sample have been confirmed and developed i.e. the water and hydrocarbon coupled between optic fiber probe and sample due to the capillary cohesion force.

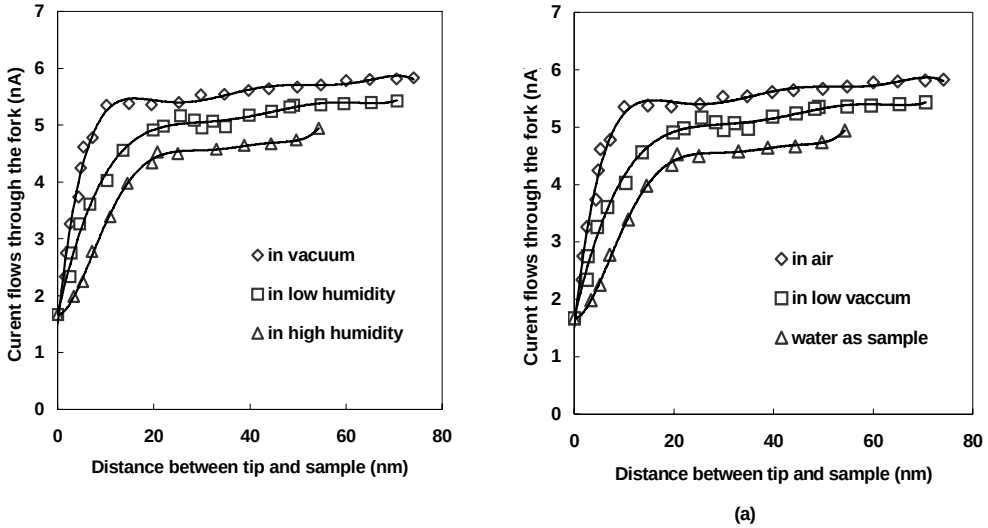

***I-d* curves under the condition of in vacuum, in low damp and in high damp condition.**

Reference:

[1] Zhang Shulin Near filed microscopes and application [M]. Beijing: Science publishing company, 2000,1-12

[2] K. Karrai, R. D. Grober. Piezoelectric tip-sample distance control for near field optical microscopes. *App. Phys. Lett.*, 1995, **66**: 1642-1644.

[3] X. Zhu, G. S. Huang, H. T. Zhou and Y. D. Dai. A novel ultrasonic resonance sample-tip distance regulation for near field optical microscopy and shear force microscopy [J]. *Solid State Comm.*, 1996; **98**:661-664

[4]P.Gunther, U. Ch. Fisher, and K. Dransfeld. Scanning near-Field Acoustic Microscopy [J]. *Appl. Phys. B*, 1989, 48:89-92

[5] Analysis of the regulation for tip-sample distance using piezo-electric quartz fork in SPM. Zhang Tianhao, Wu Zhaohui, Zhang Chunping, et al. J. of Optoelectronics Laser, 2003, **14** (1) :33-36

supported by the National Nature Science Foundation of China under Grant No. 60208002 and the Undergraduate Innovation Project of Nankai University.

published on Surface Review and Letters, Vol. 12, No. 4, 489-492 (2005)

Near-Field Scanning Optical Microscope with the application of Surface Plasma Resonance (SPR)

Zhang-Tianhao Fang-Zheyu Zheng-Jianya Gao-Limo Yin-Meirong Wu-Xue Jia-Feng

The NSOM based on SPR technique is established. A new kind of Kretschmann type of SPR is designed. The plasma with a gradient of thickness is fabricated using prism covered by gold film. The curve of SPR depending on the angel of incident beam is measured. The image of gold film on plasma is obtained at the SPR situation using this NSOM based on SPR technique. The experimental result indicates that the signal intensity and S/N ratio and the resolution for NSOM are greatly improved based on this type of technique.

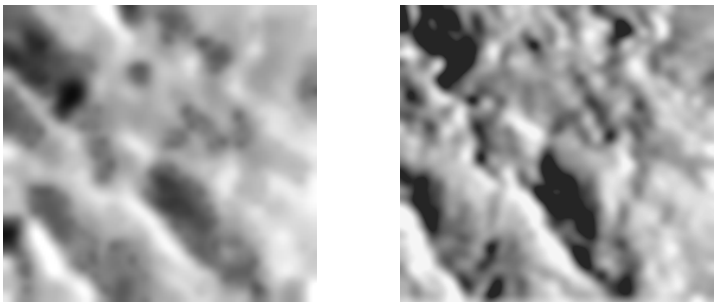

(a) **(b)**

the scanning images using NSOM

(a) Without SPR technique; (b) based on SPR technique

Reference:

[1] U.Ch. Fischer and D.W. Pohl. Observation of Single-Practice Plasmons by Near-Field Optical Microscopy. Physical Review Letters. 1989, 62(4):458-461

[2] O.Marti, H.Bielefeldt, B.Hecht,S.Herminghaus,P.Leiderer and J.Mlynek. Near-field optical measurement of the surface plasmon field[J]. Optics Communications. 1993, 96:225-228

[3] Bozhvolnyi S.I., Smolyaninov I.I., Zayats A.V. Near-field microscopy of surface-plasmon polaritons: Localization and internal interface imaging[J]. Phys Rev.B. 1995,51(24):17916-17924

[4] Igor I.Smolyaninov etc. Experimental study of surface-plasmon scattering by individual surface defects[J]. Physical Review B. 1997, 56(3):1601-1611

[5] M.Specht.J.D., Pedarnig.W.M. Heckl, and T.W. Hansch. Scanning Plasmon Near-Field Microscope[J]. Physial Review [1] Otto A. Excitation of radiative Surface Plasmon Waves in Silver by the Method of Frustrated Total Reflection[J]. Z.Physik. 1968, 216:398-410

[6] Kretschmann E.Die Bestim mung Optischer Konstanten Von metallen durch Anregung Von Oberflachen-plasm aschwinggungen[J]. Z.Physik, ,1971, 241:313-324

[7] Tianhao Zhang, Chunping Zhang, Guangyin Zhang, The Establ ishmen t ofM ult i-mode Scann ing ProbeM icroscope Ba sed on STM [J], Journal of Op to electronics·Laser, 2001, 12(2): 174-178.

---

supported by the National Nature Science Foundation of China under Grant No. 60208002 and the Undergraduate Innovation Project of Nankai University.

published on Surface Review and Letters, Vol. 12, No. 3, 355-358 (2005)

Experiment of $SrBaNbO_3$ PR SEW

Zhang Tian-hao, Lu Yan-zhen, Kang Hui-zhen, Yang Da-peng, Zheng Jian-ya, Fang Zhe-yu, Lou Ci-bo, Yang Jia, Yang Hui-zhan, Yin Mei-rong

Photorefractive surface electromagnetic wave (PR SEW) at the interface between SBN crystal and air based on drift and diffusion mechanism was observed experimentally for the first time. PR SEW can be formed when laser beam was incident at an angle of 55^o in proper ratio of signal beam to background beam, and the intensity of PR SEW increases along with the increasing of additional electric field.

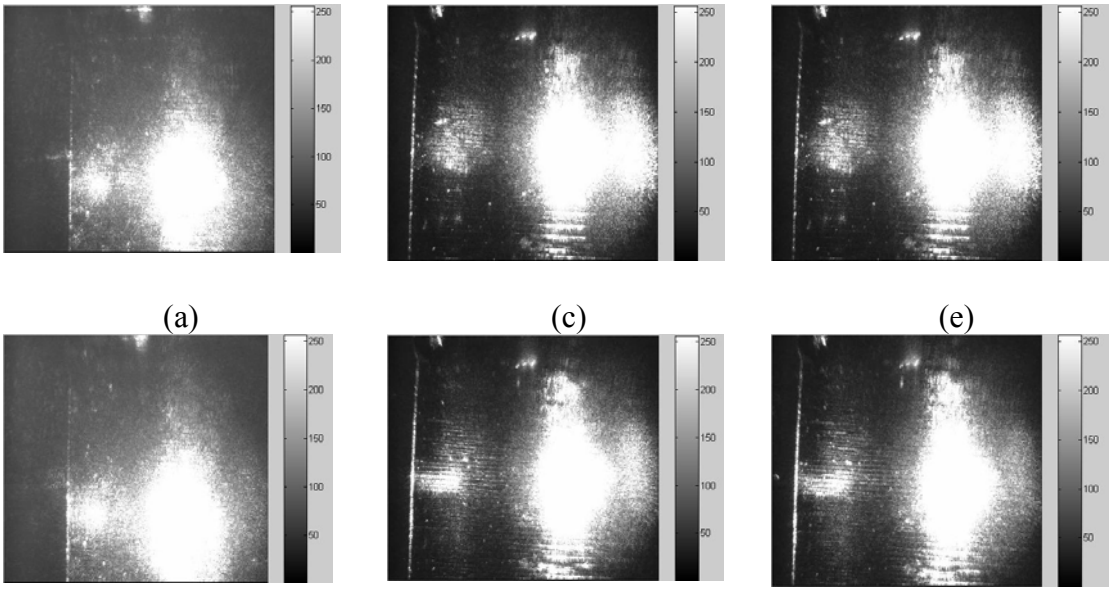

PR SEW at the interface between SBN crystal and air. PR SEW is generated at the place where the narrow long facula is in (b), (d), (f). (a), (c), (e)are the images of the surface 2 without additional electric field; (b), (d), (f) are the images of the surface 2 with 3880V/cm, 5600V/cm and 5800V/cm additional electric field after 40 minutes respectively, and

Reference:

[1] She W L，Li R J 2001 *Acta Phys. Sin.* **50** 886 (in chinese)

[2] Belyi V N，Khilo N A 1997 *Tech. Phys. Lett.* **23** 467

[3] Zimin A B，Petrov N S 2001 *Optics and Spectroscopy* **90** 896

[4] Aleshkevich V A，Vysloukh V，Kartashov Y 2001 *Optical and Quantum Electronics* **33** 1205

[5] Aleshkevich V A，Kartashov Y，Egorov A 2001 *Phys. Rev. E* **64** 056610

supported by the National Nature Science Foundation of China under Grant No. 60208002 and the Undergraduate Innovation Project of Nankai University.
published on Acta Phys. Sin., 54(10)：245-248(2005)

Theoretical Research of PR SEW at the $LiNbO_3$-Air Interface

Tianhao Zhang, Dapeng Yang, Yanzhen Lu, Huizhen Kang,
Zheyu Fang, Zhijian Hu, Xiangkui Ren

The nonlinear photorefractive surface electromagnetic waves (PR SEW) based on PV effect at the $LiNbO_3$-air interface is analyzed theoretically for the first time to our known. We show theoretically that when an extraordinarily polarized signal beam and an ordinarily polarized background beam are launched onto the interface between air and $LiNbO_3$ crystal whose $\kappa_{311}>\kappa_{333}$, the refractive-index change Δn (induced by PV effect) reverses its polarity. We have solved the equations numerically and the stationary solution of the signal beam is obtained, which decays from the crystal-air interface to the bulk of the crystal.

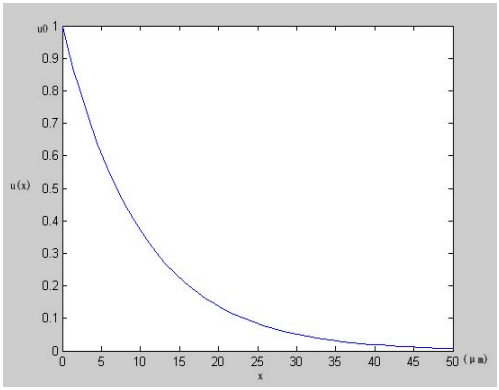

The optical field distribution of the PR SEW along the x axis at the $LiNbO_3$-air

References:

[1] George C.valley, Mordechai Segev, Bruno Crosignani, Amnon Yariv, M.M.fejer, and M. C. Bashaw, "Dark and bright photovoltaic spatial solitons", Phys. Rev. A **50** R4457-R4460 (1994).
[2] M.Taya, M. C. Bashaw, M. M. fejer, et al, "Y junctions arising from dark-soliton propagation in photovoltaic media", Opt. Lett. **21** 943 (1996).
[3]Mordechai Segev, George C. valley, Matthew. C. Bashaw, Minoru Taya, and Martin. M. fejer, "Photovoltaic spatial soliton", J. Opt. Soc. Am. B **14** 1772-1780 (1997).
[4] S. Bian, J. Frejlich, K. H. Ringhofer, "Photorefractive Saturable Kerr-Type Nonlinearity in Photovotaic", Phys. Rev. Lett. **78** 4035-4038 (1997).
[5] Z. Chen, M. Segev, D. Wilson, R. Muller, and P. Maker, "Self-trapping of an optical vortex by use of the bulk photovoltaic effect", Phys. Rev. Lett. **78** 2948 (1997).

supported by the National Nature Science Foundation of China under Grant No. 60208002.
published on Proceeding Volume (OSA), Trends in Optics and Photonics Series, Photorefractive Effects, Materials, and Device, 451-456(2005)

Photorefractive Surface Electromagenetic Waves at the Interface between SBN Crystal and Air

Tianhao Zhang, Huizhen Kang, Yanzhen Lu, Dapeng Yang, Jianya Zheng, Cibo Lou, Jia Yang, Huizhan Yang and Meirong Yin

It is the first time to experimentally observe Photorefractive surface electromagnetic waves at the interface between SBN and air with a drift-diffusion mechanism. The condition to produce this type of electromagnetic wave is : incident beam at an angle of 55^{o} in proper ratio of signal beam to background beam, and the intensity of PRC SEW increases along with the increasing of additional electric field.

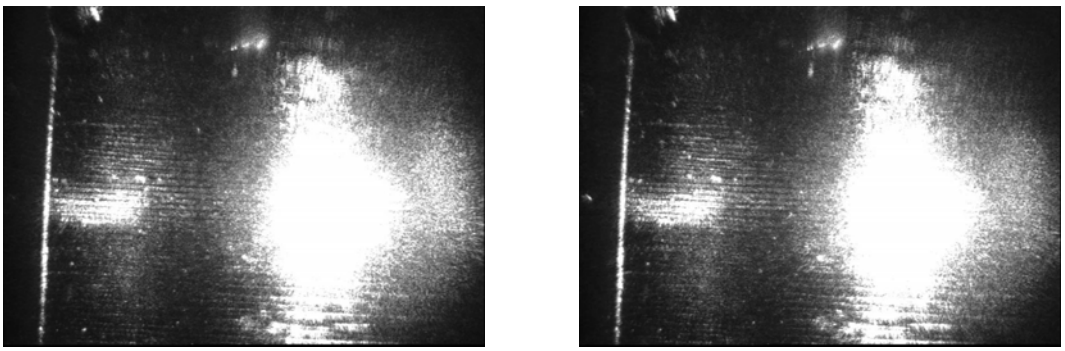

(a)

Images when an electric field 5800kv/cm is applied for 10mins and 40mins respectively. (a) is the image for 10mins, and (b) is the image for 40mins.

References:

[1] V. N. Belyi and N. A. Khilo, Tech. Phys. Lett, **23,** 467 (1997)
[2] A. B. Zimin and N. S. Petrov, Optics and Spectroscopy **90,** 896 (2001)
[3] V. Aleshkevich, V. Vysloukh, and Y. Kartashov, Optical and Quantum Electronics**, 33,** 1205 (2001)
[4] V. Aleshevich, Y. Kartashov, and A. Egorov, Phys. Rev. E **64**, 056610 (2001)
[5] N. S. Petrov, Optics and Spectroscopy, **93**, 84 (2002)
[6] Igor I. Smolyaninov and Christopher C. Davis, Opt. Lett. **24,** 1367 (1999)

supported by the National Nature Science Foundation of China under Grant No. 60208002.
published on Proceeding Volume (OSA), Trends in Optics and Photonics Series, Photorefractive Effects, Materials, and Device, 412-416(2005)

Publication

1. Weiping Zang, Jianguo Tian, Zhibo Liu, Wenyuan Zhou, Feng Song and Chunping Zhang, “The coordinate transformation and coordinate mapping for numerical simulation of Z-scan measurements”, Opt.Commun. 244, 71-77(2005)
2. Weiping Zang, Jianguo Tian, Zhibo Liu, Wenyuan Zhou, Feng Song and Chunping Zhang, “Effect of coupling between linear absorption and nonlinear absorption on Z-scan measurements”, Chinese Physics 14, 546-550(2005)
3. Weiping Zang, Jianguo Tian, Zhibo Liu, Wenyuan Zhou, Feng Song, Chunping Zhang, “Modified local one-dimensional beam-propagation method based on the Douglas scheme”, Optics Communications 256, 210-215(2005)
4. Xinjiang Yang, Weiping Zang, Jianguo Tian, Zhibo Liu, Wenyuan Zhou, Chunping Zhang andGuangyin Zhang, “Z scan analysis for near top-hat”, ACTA PHYSICA SINICA 54(6), 2738 (2005)
5. Shuqi Chen, Zhibo Liu, Weiping Zang, Jianguo Tian, Wenyuan Zhou, Feng Song and Chunping Zhang, “Study on Z-scan characteristics for a large nonlinear phase shift”, J.Opt.Soc.Am.B22(9), 1191-1196 (2005)
6. Xu T, Zhang CP, Chen GY, Tian JG, Zhang GY, Zhao CM, “Theoretical and experimental study of the intensity distribution in biological tissues”, Chinese Physics 14 (9), 1813-1820(2005)
7. Chen GY, Zhang CP, Guo ZX, Wang XY, Tian JG, Song QW, “Time-dependent all-optical logic gates based on two coupled waves in bacteriorhodopsin film”, Journal of Applied Physics 98 (4): Art. No. 044504(2005)
8. Yang XQ, Zhang CP, Qi SW, Chen K, Tian JG, Zhang GY, “All-optical Boolean logic gate using azo-dye doped polymer film”, OPTIK 116 (6), 251-254(2005)
9. Xu T, Zhang CP, Tian JG, Song F, Wang XY, Zhao CM, “Experimental study of effect of medium boundary on light distribution in tissue phantoms”, Chinese Physics Letters 22 (7),1660-1663(2005)
10. Chen GY, Guo ZX, Chen K, Zhang CP, Tian JG, Song QW, “Time-dependent all-optical logic-gates with bacteriorhodopsin film”, OPTIK 116 (5), 227-231(2005)
11. Qi SW, Yang XQ, Chen K, Zhang CP, Zhang LS, Wang XY, Xu T, Liu YL, Zhang GY, “Photoinduced birefringence in an azo-dye-doped polymer”, ACTA PHYSICA SINICA 54 (7), 3189-3193(2005)
12. Yang XJ, Zang WP, Tian JG, Liu ZB, Zhou WY, Zhang CP, Zhang GY, “Z scan analysis for near top-hat beams”, ACTA PHYSICA SINICA 54 (6), 2735-2738 (2005)
13. Yang XQ, Qi SW, Chen K, Zhang CP, Tian JG, Wu Q, “Optical limiting characteristics of mercury dithizonate in polymer film”, Optical Materials 27 (8), 1358-1362(2005)
14. Chen GY, Zhang CP, Shang XD, Guo ZX, Wang X, Tian JG, Song QW, “Real-time intensity-dependent all-optical switch of reverse image converter from wavelength to wavelength based on bacteriorhodopsin film”, Optics Communications 249 (4-6), 563-568(2005)
15. Zhang LX, Zhang CP, Feng JC, “Numerical simulation of TiC cermet/iron joint brazed with Ag-Cu-Zn filler metal”, TRANSACTIONS OF NONFERROUS METALS SOCIETY OF CHINA 15,30-34 Sp. Iss. 2(2005)
16. Wang XY, Zhang L, Zhang CP, Xu T, Zhang LS, Tian JG, “Simulation of light propagation in bio-tissue under cylindrical boundary condition”, JOURNAL OF MODERN OPTICS 52 (6), 885-895(2005)
17. Wang YQ, Zhang CP, “Preparation and characterization of magnetic norfloxacin gelatin microspheres”, JOURNAL OF INORGANIC MATERIALS 20 (1), 77-82 (2005)
18. Guo ZX, Chen GY, Wang Y, Gu LQ, Zhang CP, Tian JG, Zhang GY, Song QW, Shen B, Fu

GH, “Characters for optical filter of removing bright-background based on bacteriorhodopsin film”, JOURNAL OF INFRARED AND MILLIMETER WAVES 24 (1), 56-60(2005)

19. Zhang CP, Chen GY, Wei X, Guo ZX, Tian JG, Wang XY, Zhang GY, Song QW, “Optical novelty filter using bacteriorhodopsin film”, OPTICS LETTERS 30 (1), 81-83(2005)
20. Liu ZB, Zhou WY, Tian JG, Chen SQ, Zang WP, Song F, Zhang CP, “Characteristics of co-existence of third-order and transient thermally induced optical nonlinearities in nanosecond regime”, OPTICS COMMUNICATIONS 245 (1-6), 377-382(2005)
21. Chen GY, Zhang CP, Guo ZX, Xu T, Liang X, Wang XY, Tian JG, Song QW, “Relationship between parameters of bacteriorhodopsin film and behavior of optical novelty filters”, APPLIED OPTICS 44 (30), 6373-6379(2005)
22. 王晓阳, 徐艳梅, 张春平, 莫越奇, 吴宏滨, 曹镛, 俞钢, “MEH-PPV 薄膜的光学性质”, 光子学报 34, 746-749(2005)
23. Yudong Li, Wataru Watanabe, Takayuki Tamaki, Junji Nishii and Kazuyoshi Itoh, “Fabrication of Dammann Gratings in Silica Glass Using a Filament of Femtosecond Laser”, Jpn. J. Appl. Phys. 44(No.7A), 5014-5016(2005)
24. Yudong Li,Wataru Watanabe, Qian Sun, Takayuki Tamaki, Junji Nishii and Kazuyoshi Itoh, “Fabrication of Dammann Gratings in Silica Glass”, Chin. Opt. Lett. Supplement 3, S57-S59(2005)
25. Yasunobu Iga, Wataru Watanabe, Yudong Li, Yan Li, and Kazuyoshi Itoh, “Generation of debris in water-assisted femtosecond laser drilling of silica glass”, Jpn. J. Appl. Phys. 44(11), 8013(2005)
26. Yudong Li, Jianguo TIAN, Qian SUN: “Micro-fabrication by femtosecond laser pulses”, SPIE 6149(2005)
27. 宋峰, 苏瑞渊, 傅强, 覃斌, 田建国, 张光寅, “高浓度镱铒共掺磷酸盐光线放大器增益特性”, 物理学报 11, 5228(2005)
28. 吴朝晖, 宋峰, 刘淑静, 覃斌, 苏静, 田建国, 张光寅, “上转换对 Er^{3+}:Yb^{3+}共掺磷酸盐玻璃激光器输出的影响”, 物理学报 12, 121(2005)
29. Tianhao Zhang, Dapeng Yang, Yanzhen Lu et al, “Theoretical research of PR SEW at the LiNbO3-Air interface”, OSA Trends in Optics and Photonics (TOPS) Vol.99,451 (2005)
30. Tianhao Zhang, Huizhen Kang, Yanzhen Lu et al, “Photorefractive surface wave at the interface between SBN crystal and air”, OSA Trends in Optics and Photonics (TOPS) Vol.99, 412 (2005)
31. 张天浩，路彦珍，康慧珍等，铌酸锶钡光折变表面电磁波实验，54(10), 245-248(2005)
32. Tianhao Zhang，Zheyu Fang ，Jianya Zheng ，Limo Gao，Meirong Yin，“Near-Field Scanning Optical Microscope With THe Application Of Surface Plasma Resonance (SPR)”，Surface Review and Letters, Vol. 12, No. 4, 489-492 (2005)
33. 张天浩, 尹美荣, 方哲宇, 杨海东, 杨嘉, 路彦珍, 杨会战, 康慧珍, 杨大鹏, “表面等离子体共振技术的一些新应用物理”, Vol.34, 12(2005)
34. Tianhao Zhang, Zheyu Fang, Jianya Zheng, Limo gao, Haidong Yang, Meirong Yin, Jia Yang, Yanzhen Lu, Huizhen Kang, Dapeng Yang, Huizhan Yang, “The Influence Of Humidity On The Shear Force Between Tip and Sample In Nsom Using Piezoelectric Fork”，Surface Review and Letters, Vol. 12, No. 3, 355-358 (2005)

Conference

1. Yudong Li, Wataru Watanabe, Qian Sun, Takayuki Tamaki, Junji Nishii and Kazuyoshi Itoh, “Fabrication of Dammann Gratings in Silica Glass”, International Symposium On Photonics, Biophotonics and Nanophotonics, Nanjing, Jiangsu, China (2005)
2. Yudong Li, Jianguo TIAN, Qian SUN: “Micro-fabrication by femtosecond laser pulses”, The 2nd International Symposiun on Advanced Optical Manufacturing and Testing Technologies (AOMATT), Xian, China (2005)
3. Zhi-Bo Liu, Jian-Guo Tian, Wei-Ping Zang, Wen-Yuan Zhou, Feng Song, Chun-Ping Zhang, “Investigation on effect of nonlinear refraction to reverse saturable absorption by variational approach”, International Symposium On Photonics, Biophotonics and Nanophotonics, Nanjing, Jiangsu, China (2005)
4. Zhang Chunping， Qi Shengwen , Yang Xiuqin , Chen Kuan , Zhang Lianshun, Liu Yongliang，Liang Xing，Xu Tang， Tian Jianguo, “Nonlinear Optical Properties of Cong red solution and doped PVA film”, The 5th Conference on Transient optics and photonic technology, Xishuangbanna, Yunnan(2005)
5. Tianhao Zhang, Dapeng Yang, Yanzhen Lu et al, “Theoretical research of PR SEW at the LiNbO3-Air interface”, The tenth International Conference on Photorefractive Effects, Materials, and Devices, Sanya, Hainan, China(2005)
6. Tianhao Zhang, Huizhen Kang, Yanzhen Lu et al, “Photorefractive surface wave at the interface between SBN crystal and air” , The tenth International Conference on Photorefractive Effects, Materials, and Devices, Sanya, Hainan, China(2005)

Patent

1. 张天浩，“一种扫描探针显微镜压电扫描器的电压配置方式”， 02148631.X

Photonics Materials and Advanced Fabrication Techniques

In the field of Photonics Materials and Advanced Fabrication Techniques, we mainly focused on the nonlinear optical crystals, glass ceramics, nanoparticulate films, and photonic microstructure. More than 20 papers were published in international academic journals, one US and four national patents were issued, and one academic book was published.

In 2005, we obtained some important results, such as tetravalent ions, Hf^{4+}, doped $LiNbO_3$ crystals were grown, which had high resistance against optical damage as highly MgO doped crystals when the doped concentration up to 4 mol%, and the OH^- absorption peak corresponding to $(Hf_{Nb}^{4+})^{-}$-OH^- located at 3500 cm^{-1}. The glass ceramics with the composition of $30SiO_2 \cdot 15Al_2O_3 \cdot (50\text{-}x)\ PbF_2 \cdot xCdF_2 \cdot 4ErF_3 \cdot 1YbF_3$ were prepared. Under the condition of optimization Pb/Cd ratio, the intensity of up-conversion luminescence increases 20 times than former reported compositions of PbF_2 and CdF_2 in glass ceramics. TiO_2 nanoparticle films were prepared by plasma-enhanced chemical vapor deposition. Experiments of phenol photodegradation show that the TiO_2 film treated by O_2 plasma presents much higher photocatalytic activity than that treated by $TiCl_4$ plasma.

A novel all-optical wavelength conversion (AOWC) based on the cascaded sum-frequency generation (SFG) and difference-frequency generation (DFG) in $LiNbO_3$ waveguides was theoretically studied. The domain reversal characteristics of the MgO-doped $LiNbO_3$ single crystals with different Mg doping levels have been investigated, and the switching field is found to decrease with the increasing of Mg concentration. A nonlinear dependence of switching field on the concentration of anti-site niobium Nb_{Li}^{4+} ions was observed. This nonlinear relationship was explained by a two-dimensional model based on the dynamics of the domain wall. A parameter of θ_c, denoting the critical position of the domain wall round Nb_{Li}^{4+} ions, was introduced to describe domain reversal.

These researches were supported by the National Natural Science Foundation of China, the Ministry of Education of China, the Natural Science Foundation of Tianjin and Nankai University.

In 2005, three new projects were funded by the National Natural Science Foundation of China. Associate professor Lijuan Zhao came back form Germany after two years post-doctor research, and Dr Li Wu joined our team after graduated from the Institute of Physics, Chinese Academy of Sciences.

Prof. Yongfa Kong
2006-1-22

The H+ related defects involved in domain reversal for both near-stoichiometric and heavily Mg-doped lithium niobate crystals

W. Yan, Y. Kong, L. Shi, J. Yao, S. Chen, L. Sun, D. Zhao, J. Xu, and G. Zhang

Domain reversal was performed on both near-stoichiometric and heavily Mg-doped lithium niobate crystals. H^+ related defect structures in these two types of crystals were studied through the infrared absorption spectra. It is found that the intensity of some decomposed peaks of absorption band change apparently during domain reversal for near-stoichiometric lithium niobate crystals but not for heavily Mg-doped lithium niobate crystals. According to these experimental results, distinct models about H^+ related defect structure in $LiNbO_3$ lattice were supposed for them. Nb_{Li}^{4+} and Mg_{Nb}^{3-} were considered as the centers of H^+ related defect complex for near-stoichiometric and heavily Mg-doped lithium niobate crystals respectively. Different behavior of them was used to explain the difference of infrared absorption spectra during domain reversal between two types of crystals.

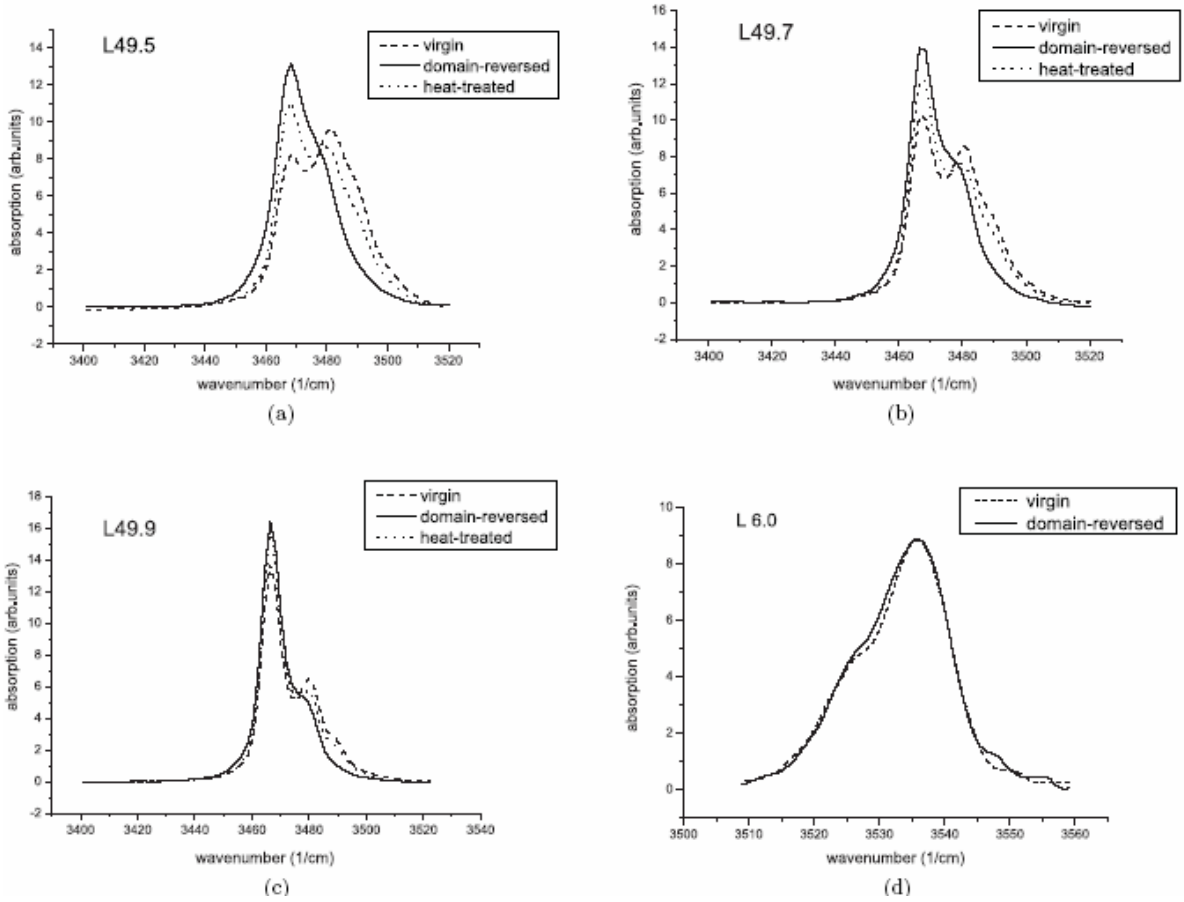

Fig. 1. The OH− absorption spectra of near-stoichiometric LN and heavily Mg-doped LN: (a), (b), (c), (d) are corresponding to samples L49.5, L49.7, L49.9 and L6.0; the dash, solid and dot curve denote different sample status of virgin, domain-reversed, and heat-treated, respectively.

Supported by the National Natural Science Foundation of China (60108001)
Published on Eur. Phys. J. B **43**, 347 – 353 (2005)

The composition dependence and new assignment of the Raman spectrum in lithium tantalate

Lihong Shi, Yongfa Kong, Jun Sun, Shaolin Chen, Jingjun Xu, and Guangyin Zhang

The Raman scattering spectra of lithium tantalate crystals with different compositions were investigated. The comparison of the Raman data obtained for the congruent and the near-stoichiometric crystals reveals some differences in the shape and the number of Raman peaks, which lead to a new assignment of the long-wavelength optical phonons. And quantitative relationships between the linewidth of Raman peaks (142 cm^{-1} for E-phonon and 861 cm^{-1} for A_1-phonon) and the crystal composition were firstly presented. Two local Raman lines, 278 cm^{-1} and 750 cm^{-1}, were found for the congruent crystals and attributed to the intrinsic defects, Li vacancy and anti-site Ta ion, respectively.

Table 1 The new assignment of E phonon characteristics for $LiTaO_3$

E(TO)	142	190	208	251	314	378	462	591	661
E(LO)	142	190	280	314	343	380	462	661	865

The dependence of Li_2O composition C_{Li} on the halfwidth Γ of Raman bands are

$C_{Li} = 51.45 - 0.2945\,\Gamma$ (for the 142 cm^{-1} phonon)

and $C_{Li} = 52.42 - 0.1380\,\Gamma$ (for the 861 cm^{-1} band),

where C_{Li} is in mol% and Γ in cm^{-1}.

The dependence of concentration of V_{Li}^{-} and Ta_{Li}^{4+} on the integral area of Raman peak are

$$C_{V_{Li}} = 30.67 \times S_{normal}^{278}$$

and $$C_{Ta_{Li}} = 182.01 \times S_{normal}^{750}$$

References

[1] X. Yang, G. Lan, B. Li, and H. Wang, Phys. Sta. Sol. B 141 (1987) 287.

[2] C. Raptis, Phys. Rev. B 38 (1988) 10007.

[3] A.Ridah, P.Bourson, M.D.Fontana, G.Malovichko, J. Phys.: Condes. Matter. 9 (1997) 9687.

[4] Y. Kong, J. Xu, X. Chen, C. Zhang, W. Zhang, and G. Zhang, J. Appl. Phys. 87 (2000) 4410.

Supported by the National Natural Science Foundation of China (60108001)

Published on Solid State Communications 135 (2005) 251–256

Photorefractive properties of near-stoichiometric lithium niobate crystals doped with iron

Hongde Liu, Xiang Xie, Yongfa Kong, Wenbo Yan, Xiaochun Li, Lihong Shi
Jingjun Xu, and Guangyin Zhang

Near-stoichiometric lithium niobate crystals doped with iron were prepared by vapor transport equilibration (VTE) method. The gain coefficient of these samples were measured and compared to the near-stoichiometric lithium niobate crystals prepared by double-crucible method, and the diffraction efficiency, recording time and erasing time were also done. The dynamic range coefficient (M/#) and homogeneity of the composition in the crystals were investigated too. The results showed that VTE method effectively improve the photorefractive response speed of iron-doped congruent crystals, which was helpful in applying lithium niobate crystals in volume holographic storage processing.

Table 1. The composition and gain coefficient of of lithium niobate crystals used in this study

No.	Sample	Li_2O concentration (x_c : %)	Gain coefficient (Γ : cm^{-1})
1C	0.02wt% Fe-doped CLN	48.38	34
1S	0.02wt% Fe-doped SLN	49.96	38
2C	0.025wt% Fe-doped CLN	48.38	33
2S	0.025wt% Fe-doped SLN	49.97	40
3C	0.03wt% Fe-doped CLN	48.38	35
3S	0.03wt% Fe-doped SLN	49.93	42

Table 2. The photorefractive properties of congruent and stoichiometric lithium niobate crystals with different doping composition.

No.	Diff. efficiency (η : %)	Recording time (τ_r : s)	Erasing time (τ_e : s)	Dynamic range (M/#)
1C	45	125	630	2.29
1S	55	70	545	3.75
2C	45	80	450	1.82
2S	56	35	255	2.82
3C	49	55	380	1.89
3S	57	35	245	3.79

Supported by the National Natural Science Foundation of China (60108001), the National Advanced Materials Committee of China (2001AA313020), and China Key Basic Research Project (G199903004).
To be published on Optical Materials 28 (2006) 212 – 215

The relationship between the switching field and the intrinsic defects in near-stoichiometric lithium niobate crystals

Wenbo Yan, Yongfa Kong, Shaolin Chen, Ling Zhang, Ziheng Huang, Shiguo Liu
Jingjun Xuand Guangyin Zhang

Several near-stoichiometric lithium niobate ($LiNbO_3$) plates were prepared by the vapour transport equilibrium technique. Domain reversal was carried out on these samples by electric field poling. A nonlinear dependence of switching field on the concentration of anti-site niobium (Nb_{Li}^{4+}) ions was observed. This nonlinear relationship was explained by a two-dimensional model based on the dynamics of the domain wall. A parameter of θ_c, denoting the critical position of the domain wall round Nb_{Li}^{4+} ions, was introduced to describe domain reversal. The domain wall energy per unit area for near-stoichiometric lithium niobate was also roughly calculated to be larger than 0.27 Jm^{-2}.

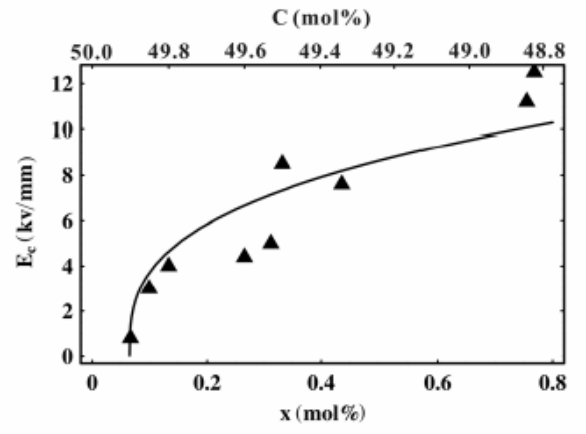

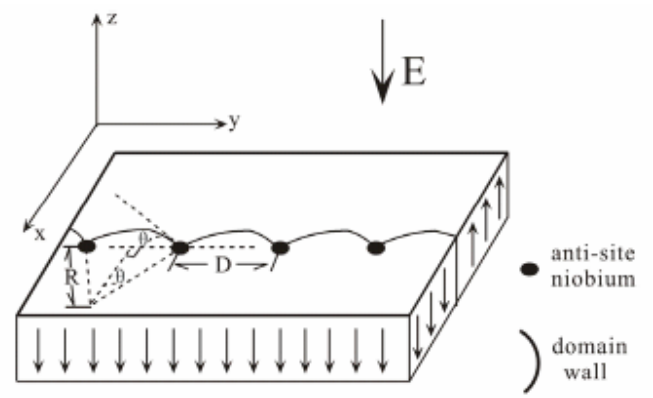

Figure 1. The switching field E_c as a function of Li composition C (top *x*-axis) and the Nb_{Li}^{4+} concentration *x* (bottom *x*-axis) in the crystal.

$E_c = 11.4\ (x - 0.06)^{1/3}$

Figure 2. The schematic of a two-dimensional model of a pinned domain wall under an applied electric field.

$$E_c = \frac{\sigma_w \sin\theta_c}{P_s d} x^{1/3}$$

where P_s is the spontaneous polarization, *d* the distance between two Li^+ ions along the *y*-axis and σ_w the domain wall energy per unit area.

Supported by the National Natural Science Foundation of China (60108001)
To be published on J. Phys. D: Appl. Phys. **39** (2006) 21–24

The optical damage resistance and absorption spectra of $LiNbO_3$:Hf crystals

Shiguo Liu, Shuqi Li, Yongfa Kong, Ling Zhang, Ziheng Hang, Shaolin Chen and Jingjun Xu

Highly HfO_2 doped lithium niobate crystals have been grown. The experimental results indicate that $LiNbO_3$: Hf (up to 4 mol%) can withstand the same light intensity of 5×10^5 W/cm^2 as $LiNbO_3$: Mg (6.5 mol%). And the OH^- absorption bands of these $LiNbO_3$: Hf crystals shift to 3487 cm^{-1} from 3484 cm^{-1} of congruent pure $LiNbO_3$. The difference spectra and fitting treatments show the OH^- absorption peak corresponding to (Hf_{Nb}^{4+})-OH^- locates at 3500 cm^{-1}.

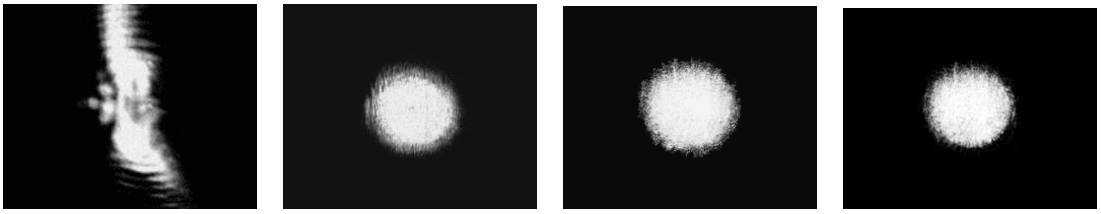

(a) (b) (c) (d)

Figure 1. Distortion of transmitted argon laser beam spot. (a) 2mol% Hf; (b) 4mol% Hf; (c) 6mol% Hf; (d) 6.5mol% Mg. The light intensity for (a) is 10^4W/cm^2 and 5×10^5W/cm^2 for (b), (c), and (d).

Table 1. The maximum change of refractive index (Δn_{sat}) of Hf-doped and Mg-doped lithium niobate crystals.

Sample No.	Doping level	Δn (10^{-5})
LN:Hf_2	2.0mol% Hf	2.2
LN:Hf_4	4.0mol% Hf	0.87
LN:Hf_6	6.0mol% Hf	0.84
LN:$Mg_{6.5}$	6.5mol% Mg	0.78

Table 2. The position of component peaks in the OH^- absorption spectra of Hf-doped lithium niobate crystals.

Sample	Position of peaks (cm^{-1})			
LN:Hf_2	3469.0	3480.2	3489.2	
LN:Hf_4 (the top part)		3481.2	3490.2	3500.2
LN:Hf_4 (the bottom part)		3481.1	3490.1	3500.6
LN:Hf_6		3481.1	3490.2	3500.1

Supported by Program for Changjiang Scholars and Innovative Research Team in University and the National Natural Science Foundation of China (60578019).

Effect of plasma treatment on surface properties of TiO2 nanoparticulate films

Yaan Cao

TiO_2 nanoparticle films were prepared by plasma-enhanced chemical vapor deposition, and subsequently, their surfaces were treated by $TiCl_4$ and O_2 plasmas, respectively. Experiments of phenol photodegradation show that the TiO_2 film treated by O_2 plasma presents much higher photocatalytic activity than that treated by $TiCl_4$ plasma. X-ray photoelectron spectral analyses indicate that more active species, such as O_2-, are formed on surface of the film treated by O_2 plasma than that treated by TiCl4 plasma. The energy levels of the surface species and the photogenerated electronic transitions via these surface species are further investigated by surface photovoltage spectra and electric field-induced surface photovoltage spectra.

References

[1] M.S. Vohra, K. Tanaka, Environ. Sci. Technol. 35 (2001) 411.
[2] O.V. Makarova, T. Rajh, M.C. Thurnauer, A. Martin, P.A. Kemme, D. Cropek, Environ. Sci. Technol. 34 (2000) 4797.
[3] A. Linsebigler, G. Lu, J.T. Yates, Chem. Rev. 95 (1995) 735.
[4] G. Lu, A. Linsebigler, J.T. Yates, J. Chem. Phys. 102 (1995) 3005.
[5] D.D. Beck, J.M. White, C.T. Ratcliffe, J. Phys. Chem. 90 (1986) 3132.

Supported by the National Natural Science Foundation of China (Grant No. 50472035) and Natural Science Foundation of Tianjin City (Grant No. 043612411).
To be published on Colloids and Surfaces A.262 (2005) 181–186

Light Induced Interfacial Electron Transfer in Phenylcapped Aniline Tetramer /TiO_2/ ITO Film Electrode

Yaan, Cao

TiO_2 monolayer film and TiO_2 sensitized with phenylcapped aniline tetramer (Pat) complex film(Pat/TiO_2), were prepared by the rolling coat and soak method respectively. By means of surface photovoltage spectroscopy, cyclic voltammograms with irradiation(CAGI) and the photocurrent action spectra(PAS), the band gap and energy level of surface states of TiO_2 monolayer film, the energy level of ground state, energy level gap(HOMO~LUMO) and energy level of dual polarons of phenylcapped aniline tetramer and the properties of photo-to-electric conversion of Pat/TiO_2 complex film were investigated. By the results of SPS, CAGI and PAS and the energy band structure of the Pat/TiO_2 complex film, the reasonable mechanism of interfacial electron transport in TiO_2 sensitized with phenylcapped aniline tetramer film electrode was analysed.

References

[1] A. Hagfeldt, M. Grätzel, *Chem. Rev.* [J], 1995, **95**: 49
[2] R. Grunwald, H. Tribusch, *J. Phys. Chem. B* [J], 1997, **101**: 2564
[3] P. Wang, S. M. Zakeeruddin, P. Comte, I. Exnar, and M. Grätzel, *J. Am. Chem. Soc.* 2003, **125**:1166-1167
[4] A. Zaban and Y. Diamant，*J. Phys. Chem. B* [J], 2000, **104**: 10043-10046

Supported by the National Natural Science Foundation of China (Grant No. 50472035) and Natural Science Foundation of Tianjin City (Grant No. 043612411).
To be published on Chem. J. Chin. Univ. 26 (2005) 1677–1681

All-optical wavelength conversion and the domain reversal of Mg:LN

Yunlin Chen, Yongfen Luo, Juan Guo, Jianwei Yuan, Weiguo Yan, Binbin Zhou, Shaolin Chen, Jingjun Xu, Guangyin Zhang

A novel all-optical wavelength conversion(AOWC) based on the cascaded sum-frequency generation(SFG) and difference-frequency generation(DFG) in $LiNbO_3$ waveguides have been theoretically studied. This novel wavelength convertor employing two pump sources place the input two pump wavelengths outside the optical communication band. It is easily realizing optimum coupling between punp wavelengths and signal wavelength since their wavelengths are relatively close to each other and the pump wavelenths don't occupy the the communication band and the convertor have a characteristic of polarization-insensitive. Firstly, we established the theoretical model of the AOWC and gave out the coupled-mode equations of optical interaction in waveguide. Then we detailed deduced the coupled-mode equations step by step and gained an electric field expression of clear physical insight. Finally we analyzed the relation between the conversion efficiency and the device length, the pump powers ,and optimized the fabrication parameters for stable and high efficiency AOWC.

Quasi-phase-matched second harmonic generation(SHG) in bulk periodically poled $LiNbO_3$(PPLN) was studied , the coupled-wave equations for quasi-phase-matched SHG was accurately resolved, and the formula for calculating SHG conversion efficiency under focusing Gauss beams was given． The relations between focusing beam's waist and crystal length were analyzed． Furthermore, the SHG cavity was optimized to obtain the maximum conversion efficiency．

MgO-doped $LiNbO_3$ crystal has been produced using the Czochralski method. The domain reversal characteristics of the MgO-doped $LiNbO_3$ single crystals with different Mg doping levels have been investigated, and the switching field is found to decrease with the increasing of Mg concentration. The switching field for the domain reversal in the MgLN crystal doped with 6.5 mol.% MgO was ~4.6 KV/mm. This is about one fifth of the switching field for the congruent crystal. The resistance of the poling MgLN crystals as a function of Mg concentration was measured，and the influence of doping Mg on domain reversion for Mg-doped $LiNbO_3$ is discussed, and explain the physical mechanism of the polarization switching of the MgLN crystals.

Supported by the National Natural Science Foundation of China (No.10174040, 90101022) and the Key Natural Science Foundation of Tianjin (033800111) and International Cooperation project of Tianjin.

Effect of Nanocrystals on Up-conversion Luminescence of Er^{3+}/Yb^{3+}-Codoped Glass Ceramics*

Hua Yu, Lijuan Zhao, Jie Meng, Qin Liang, Xuanyi Yu, Baiquan Tang, Jingjun Xu

The oxyfluoride glass ceramics is a promising material for optical amplifiers and laser up-conversion applications[1,2]. These glass-ceramics shown efficient infrared-to-visible up-conversion luminescence under the infrared laser excitation. Most of investigations were focused on preparing of transparent glass-ceramics and up-conversion properties of rare earth ions under the infrared laser excitation. However, the properties of nanocrystals, which are decided by the stoichoimetric and treatment process, are very important to prepare high efficiency up-conversion glass-ceramics. There are no publications about stoichiometric proportion of nanocrystals and related up-conversion luminescent intensities.

The glass ceramics with the composition of $30SiO_2 \cdot 15Al_2O_3 \cdot (50\text{-}x)PbF_2 \cdot xCdF_2 \cdot 4ErF_3 \cdot 1YbF_3$ (x= 0, 10, 22) were prepared. The crystallizability of the glass ceramics doped with Er^{3+} and Yb^{3+} ions is best when x=0, which means the rare earth ions doped in the PbF_2 nanocrystals. The relative intensity of the red luminescence of Er^{3+} ions in the glass ceramics increases with decreasing of Cd content. The intensity of the up-conversion fluorescence could be decided mainly by the stoichiometric proportion of the nanocrystals. The suitable contend of CdF_2 could modify crystal lattice field of the nanocrystals in the glass ceramics. The optimization ratio of PbF_2 and CdF_2 is found, which value is 40:10 in the oxyfluoride glasses. Under the condition of optimization Pb/Cd ratio, the intensity of up-conversion luminescence increases 20 times than former reported compositions of PbF_2 and CdF_2 in glass ceramics.

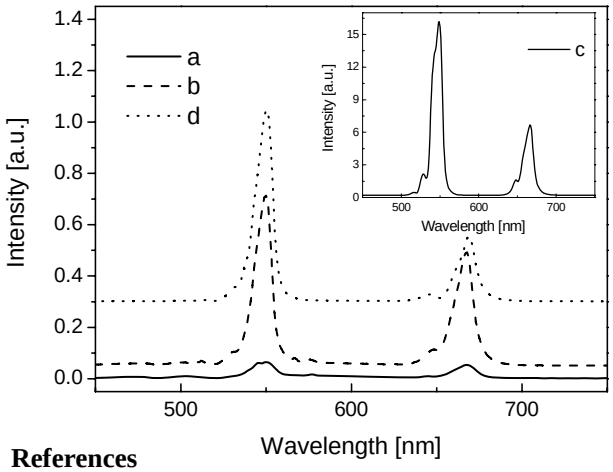

Fig.1 Up-conversion luminescent spectra of Er^{3+} ions in the glass ceramics with the different compositions of $(50\text{-}x)PbF_2 \cdot xCdF_2$ for (b)x=0, (c)x=10, (d)x=22, sample a which was not heat-treated, is the same compositions as sample d

References

[1] P. A. Tick, N. F. Borrelli, L. K. Cornelius, et. al., J. App. Phys. **78**(11), 6367 (1995)
[2] Yuhu Wang and Junichi Ohwaki, Appl. Phys. Lett. **63**, 3268 (1993)

* Supported by the National Natural Science Foundation of China(No. 60178024) and the Cultivation Fund of the Key Scientific and Technical Innovation Project, Ministry of Education of China(NO. 704012)..
* Published on Chin. Opt. Lett. 3(8): 469-71 (2005)

Publication

1. Wenbo Yan, Yongfa Kong, Lihong Shi, Xiaochun Li, Xiang Xie, Jingjun Xu, Cibo Lou, Hongde Liu, Guangyin Zhang, “The dependence of the switching field on the intrinsic defects in lithium niobate crystals”, SPIE 5646, 568-576 (2005)
2. W. Yan, Y. Kong, L. Shi, J. Yao, S. Chen, L. Sun, D. Zhao, and J. Xu, “The H+ related defects involved in domain reversal for both near-stoichiometric and heavily Mg-doped lithium niobate crystals”, Eur. Phys. J. B 43, 347-353 (2005)
3. Lihong Shi, Yongfa Kong, Wenbo Yan, Hongde Liu, Xiaochun Li, Xiang Xie, Di Zhao, Lei Sun, Jingjun Xu, Jun Sun, Shaolin Chen, Ling Zhang, Ziheng Huang, Shiguo Liu, Wanlin Zhang, Guangyin Zhang, “The composition dependence and new assignment of the Raman spectrum in lithium tantalite”, Solid State Commun. 135, 251–256 (2005)
4. Huang Hui, Jingjun Xu, Yongfa Kong, Guoquan Zhang, Yongchun Shu, Jun Sun, Xiaoxuan Xu, Guangyin Zhang, “Observation of Fractal Geometry in Lithium Niobate Crystal”, Journal of Synthetic Crystals 33(4), 647-650(2004)
5. Yongfa Kong, Jun Sun, Ling Zhang, Wenbo Yan, Jingjun Xu, and Guangyin Zhang, “The growth of large-diametered nearly stoichiometric lithium niobate crystals by double crucible technique”, OSA Trends in Optics and Photonics (TOPS) Vol.99, 50 (2005)
6. 谢翔, 黄自恒, 孔勇发, 张玲, 刘士国, 陈绍林, 李晓春, 赵迪, 许京军, “钛酸钡钙晶体的生长及其基本光学性能研究”, 人工晶体学报 34(2), 242 (2005)
7. 陈云琳, 刘晓娟, 吴朝晖, 宋峰, 罗勇锋, 楼慈波, 张万林, 陈绍林, 许京军, “准相位匹配周期极化掺镁铌酸锂 490nm 倍频连续输出”, 光子学报 34(1), 29-31(2005)
8. 陈云琳, 罗勇锋, 袁建伟, 张万林, 陈绍林, 黄自恒, 许京军, 张光寅, “准相位匹配周期极化高掺镁铌酸锂 532nm 倍频准连续输出研究”, 光学学报 25(1), 63-66(2005)
9. 陈云琳, 袁建伟, 罗勇锋, 郭娟, 张万林, 许京军, “准相位匹配 PPLN 倍频理论研究与优化设计”, 物理学报 54(5), 119-123(2005)
10. 罗勇锋, 陈云琳, 袁建伟, 闫卫国, 周斌斌, 张万林, 郭娟, 陈绍林, “准相位匹配级联二阶非线性全光波长转换研究”, 光学学报 25(4), 651-654(2005)
11. Yunlin Chen, Weiguo Yan, Juan Guo, Shaolin Chen, Guangyin Zhang, “Effect of Mg concentration on the domain reversal of Mg-doped $LiNbO_3$”, Appl. Phys. Lett. 87(21), 2904(2005)
12. 孙军, 张玲, 孔勇发, 乔海军, 刘士国, 黄自恒, 陈绍林, 李剑韬, 许京军, “大直径高掺镁铌酸锂晶体的生长及其紫外光折变性能研究”, 人工晶体学报 34(4) 576 (2005)
13. Yu Hua, Zhao Lijuan, Meng Jie, Liang Qin, Yu Xuanyi, Tang Baiquan, Xu Jingjun, “Nanocrystal formation and structure in oxyfluoride glass ceramics”, Chin. Phys. 14(9), 1799-1802(2005)
14. Yu Hua, Zhao Lijuan, Liang Qin, Meng Jie, Yu Xuanyi, Tang Baiquan, Tang Liqin, Xu Jingjun, "Red up-conversion luminescence process in oxyfluoride glass ceramics doped with Er^{3+}/Yb^{3+}", Chin. Phys. Lett. 22(6), 1500-3(2005)
15. Yu Hua, Zhao Lijuan, Meng Jie, Liang Qin, Yu Xuanyi, Tang Baiquan, Xu Jingjun, “Effect of nanocrystals on up-conversion luminescence of Er^{3+},Yb^{3+} co-doped glass-ceramics”, Chin. Opt. Lett. 3(8), 469-71(2005)

16. 孟婕, 赵丽娟, 余华, 唐莉勤, 梁沁, 禹宣伊, 唐柏权, 苏静, 许京军, “微晶结构对氟氧化物玻璃陶瓷发光特性的影响”, 物理学报 54(3), 1442-6(2005)
17. 刘永胜, 余华, “BaFBr:Eu^{2+}中 Al^{3+}的最佳掺杂浓度研究”, 光电子激光, 16(4), 444-6(2005)
18. Tang Li-qin, Zhao Li-jian, Zhang Xin-zheng, Yu Hua, Meng Jie, Liang Qin, Xu Jing-jun, Kong Yong-fa, “Luminescent Enhancement in Mg^{-} and Er^{-} Codoped $LiNbO_3$ Crystals”, Chinese Physics Letters 22(3), 588-590(2005)
19. Lijuan Zhao, J. Luis Pérez Lustres, Vadim Farztdinov and Nikolaus P. Ernsting, “Femtosecond fluorescence spectroscopy by upconversion with titled gate pulses”, Phys. Chem. Chem. Phys. 7(8), 1716-1725(2005)
20. Yaan Cao, “Effect of plasma treatment on surface properties of TiO2 nanoparticulate films”, Colloids and Surfaces A 262, 181–186(2005)
21. Yaan Cao, “Light Induced Interfacial Electron Transfer in Phenylcapped Aniline Tetramer /TiO_2/ ITO Film Electrode”, Chem. J. Chin. Univ.26, 1677–1681(2005)

[**Bookmaking**]

1. 孔勇发, 许京军, 张光寅, 刘思敏, 陆猗, 《多功能光电材料——铌酸锂晶体》, 科学出版社 (2005)

Conference

1. Yongfa Kong, Jun Sun, Ling Zhang, Wenbo Yan, Jingjun Xu, and Guangyin Zhang, “The growth of large-diametered nearly stoichiometric lithium niobate crystals by double crucible technique”, The tenth International Conference on Photorefractive Effects, Materials, and Devices, Sanya, Hainan, China(2005)

Patent

1. 陈云琳, 孔勇发, 许京军, 张光寅, “掺镁化学比铌酸锂周期极化微结构晶体的制备工艺”, ZL 02 1 00623.7
2. 陈云琳, 刘晓娟, 楼慈波, 许京军, 陈绍林, 黄自恒, “周期极化掺镁铌酸锂全光开关及其制备工艺”, ZL 03 1 02423.8
3. 孔勇发, 许京军, 张光寅等, “Doubly doped lithium niobate crystals”, US 6835368 B2
4. 陈绍林, 许京军, 孔勇发等, “准确定向切割晶体的方法”, ZL03121582.3
5. 陈绍林, 许京军, 孔勇发等, “平行度优于 1 秒的晶体材料偏心抛光方法”, ZL03121583.1

Annual report of fields in Spectral Characterization and Sensor Techniques

In 2005, in the field of Spectral Characterization and Sensor Techniques, our group had published 25 papers in international reviewed academic Journals. Our research topics focus in the follow area:

1、 RAMAN and FTIR spectroscopy in medicine application.
Following papers are in this topic:

- Studies on breast tumor tissues with ATR-FTIR spectroscopy
- Studies on Breast Cancer Tissues With ATR-FTIR Spectroscopy
- Investigation of Human Breast Tumors Tissues With ATR-FTIR Spectroscopy in Vitro
- Confocal Raman Microspectroscopic Study of Human Breast Morphological Elements

2、 Multi-dimensional spectroscopy and imaging spectra.
Following papers are in this topic:

- Three-dimensional fluorescence spectra of mineral oil and extraction method of characteristic parameters
- Application of Depth-Analysis of Confocal Raman Micro-Spectroscopy to Chirography Identification
- The Three-dimension Spectral Subtraction Fluorescence to Check Adulteration of Petrol by 120# solvent naphtha
- Microscopic Raman imaging spectra of PbS and its photo-oxidation products

3、 The spectroscopy research of phase change in solid material.
Following papers are in this topic:

- Studies on Photoluminescence Characteristics of 1-An ilinonaphthalene-8-Sulfonate in Solid Matrixes
- Microscopic Raman imaging spectra of PbS and its photo-oxidation products

4、 RAMAN spectroscopy research of semiconductor and OLED.
Following papers are in this topic:

- Raman spectra of annealed self-assembled quantum dots
- Performance Improvement of Polymer Light-emitting Diodes with Metal Fluoride Cathode
- Study of Poly(3,4-ethylene dioxythiophene):Poly (styrene sulfonate) by In-situ resonance Raman spectroscopy

5、 Fluorescent characteristic of micro-mineral oil in water and solid powder.
Following papers are in this topic:

- Laser-induced fluorescent characteristic of micro-mineral oil in water
- Fluorescence spectra of mineral oil-water intermixture

- Fluorescence Measurement of Oil Micro-contamination in Water with Optical Fiber Technique and it s Application
- Solid Powder Fluorescence of Oil Cuttings
- Spectra Study on the Quality Change of Deep Frying Edible Oils by Synchronous Scan Fluorescence Spectra

6、 Near infrared spectroscopy experiment and algorithm research
Following papers are in this topic:

- Adopting the Method of Correlation Coefficient to Improve the Accuracy of the Xylene Isomer's Prediction Model
- Improving the Accuracy of Isomer's PLS Prediction Model in Near Infrared Spectrum Analysis by Subtractive Spectra Technology
- The application of Cross-correlation analysis in near infrared spectrum pretreatment
- Adopting the method of near infrared spectrum to measure the ratio of primary hydroxyl group and second hydroxyl group in polyether polyol
- Adopting cross-correlation algorithm for optimizing Model Transfer of Near infrared spectrum
- The Orthogonal Polynomial Regression Method of M wavelength ult i—Radiation Thermometry

7、 Other application spectroscopy research ,method and experiment.
Following papers are in this topic:

- The Optimum Design and Radiation Characteristics Research of Indoor Gas Infrared Source in the FTIR Emission Spectrometric Method.
- The Measurement of Tumor Auto-fluorescence Spectra with Fiber Optical Biosensor

Studies on breast tumor tissues with ATR-FTIR spectroscopy

Ge Yu ,Jialin Xu Yun Niu Cunzhou Zhang ,Chunping Zhang

The original and deconvoluted spectra of Attenuated Total Reflection (ATR) FTIR have been determined for both benign and malignant tumor tissues samples and the spectral differences have been investigated between the two types of samples. In comparison with the benign samples, the characteristic changes of malignant ones mainly involve: The prominent bands 1652 and 1645cm-1 due to the proteins in the α-helical and the unordered-random-coils substructures become stronger compared to those in the β-sheet and the turns substructures, suggesting that the former type of proteins increase in content in contrast to the later. The phospodiester band 1083 cm-1 of the nucleic acids becomes strongest on cancer tissues spectra and its area ratio to the amide II band 1548cm-1 rises greatly, indicating that the DNA content rises remarkably. The collagen proteins reduce in content while phosphorylated ones rise, and some hydrogen bonding is nearly broken in amino acid residue C-O (H) groups. The glycogen content decreases, and the CH2 content is higher than CH3 one. These results suggest that ATR-FTIR spectroscopy has the potential to become a powerful tool for biochemical studies and in vivo diagnosis of human breast cancers.

Supported by Zhenxing Project of the Chinese Ministry of Education,A01504
Published on Proceedings of SPIE,5360,796-801（2005）

Raman spectra of annealed self-assembled quantum dots

Bin Wang, Xiao xuan Xu, Yong chun Shu, Jiang hong Yao

We have measured Raman spectra of annealed self-assembled In0.65Al0.35As quantum dots. The samples are annealed at either 600K or 700K; the annealed time is either 30 minutes or 60 minutes. We have systematically analyzed the changes of Raman spectra between the samples annealed and not annealed, and further studied the new characteristics of semiconductor quantum dots. It found that:

1) After the structure of the annealed quantum dots is reorganized, the peak of like AlAs LO mode near 382cm-1 disappears, and the peak of the like InAs LO mode or TO mode near 200cm-1 appears. It shows that the original quantum dot disappears and the new quantum dot is created after annealing.

2) After the quantum dots is annealed, the Raman spectra peaks' move is much more than that which is came form confinement effects in quantum dots by the phonon.

3) The enhanced Raman phenomena exist universally in quantum dots. It shows that Raman spectrum is one of the powerful methods to examine the growth and components of quantum dots.

Supported by Zhenxing Project of the Chinese Ministry of Education,A01504
Published on Proceedings of SPIE,5360,796-801（2005）

Three-dimensional fluorescence spectra of mineral oil and extraction method of characteristic parameters

Liping Shang ， Xianyong Liu ， Xiaoxuan Xu， Jingjun Xu

To realize the on-line fluorescence monitoring of mineral oil pollution in water, three-dimensional spectral characteristic of oil-water intermixtures must be studied and the characteristic must be extracted. Using excitation wavelength, fluorescence wavelength and fluorescence intensity as three-dimensional system of coordinate, through sampling and surface fitting, three-dimensional fluorogram is gotten, which can provide gist for oil discrimination when presented in contour chart (finger-print map of oils). But there is little difference between characteristics of three-dimensional fluorogram because of the similarity of constituent and structure of similar oils. Therefore this paper introduces quantitative analysis method-characteristic parameter method which starts with analyzing statistical characteristic of three-dimensional fluorogram. Using RFPC fluorescence spectrometer (Shimadzu, Japan), three-dimensional fluorescence spectra of diesel oil, machine oil, gasoline oil, crude oil are measured and parameterized. The result shows that as a quantitative classified discrimination method of three-dimensional fluorescence spectra, the parameter of characteristic parameter method possesses definiteness for three-dimensional fluorescence spectra, and it is applicable, available when used in oil discrimination.

Published on Proceedings of SPIE,5634，153－159（2005）

.Laser-induced fluorescent characteristic of micro-mineral oil in water

Liping Shang ， Xinzheng Zhang ， Jingjun Xu，Na Zhang

Laser-induced fluorescence emission contains information about both spectra and time, so the different shapes, intensities and fluorescent lifetimes of fluorescence emission spectra can be used to measure the categories and contents of fluorescent substances with high sensitivity and good selectivity. To measure the oil micro-contamination in water, we utilized femtosecond ultraviolet laser pulse (fs Laser: MaiTai, Spectra Physics, US) as driving source and gated enhanced type ICCD (Time-resolved Fluorescence Spectroscopy, Lavision, German) as detector. We carried through laser-induced fluorescence measurement on DaGang crude oils and machine oils, accomplished data processing, and analyzed the differences of shapes of fluorescence spectra and lifetimes between crude oil and refined oil.

Published on Proceedings of SPIE,5627，265－269（2005）

Fluorescence spectra of mineral oil-water intermixture

Liping Shang ， Xiaoxuan Xu ， Jingjun Xu ， Daying Xia ， Jinshan Shi

Using highly pure water disposed by Milli-Qlabo purifying system of United States as background water, employing RF540 fluorescence spectrometer and selecting fourteen wavelengths as excitation wavelengths, this paper measured and analyzed excitation spectra and fluorescence spectra of oil-water intermixtures with different concentrations from eight domestic mineral crude oils, seven imported mineral crude oils and eight mineral product oils. Experiment results show that: all of these oils can emit fluorescence in broad range of excitation spectra, but the fluorescence quantum efficiency is different; optimal excitation wavelength is 254nm, while more effective excitation wavelength is 360nm, and the corresponding optimal fluorescence detection wavelengths are 360nm and 460nm; with the increment of concentration, relative intensities of fluorescence also increase linearly, which shows that they have obvious positive correlation and the correlation coefficient is above 0.9. Thus using fluorescence method to directly measure the content of mineral crude oil and product oil in water is feasible. Based on the experimental work, combining transfer characteristic of optical fiber, the ranges of optimal excitation wavelength and detection wavelength of mineral oil in water are confirmed, which founds for the on-line fluorescence measurement with optical fiber of micro-content of mineral oil in water.

Published on Proceedings of SPIE,5627，265－269（2005）

Application of Depth-Analysis of Confocal Raman Micro-Spectroscopy to Chirography Identification

Lin Haibo , Xu Xiaoxuan , Wang Bin, Yang Yanyong, Zhang Cunzhou, Yu Gang, Li Jie

Depth analysis of confocal Raman micro-spectroscopy was applied to chirography identification. The result indicated that depth analysis has potential application to forensic science field , especially in longitudinal identification of ink and inkpad. No matter what the spatial distributions of the signature pen and inkpad are , confocal Raman micro-spectroscopy can longitudinally distinguish those spatial differences. All those suggested that confocal Raman micro-spectroscopy is a fast ,simple , high sensitive and non-destructive technique.

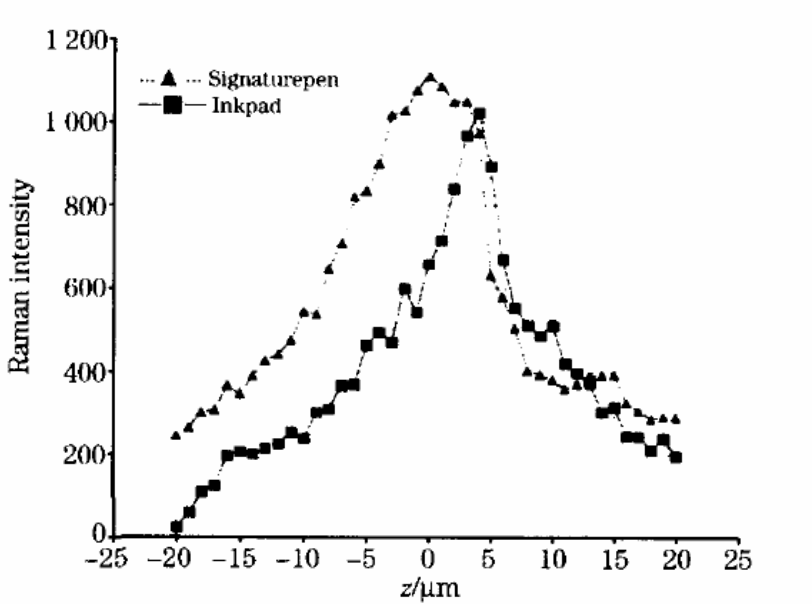

Fig. 1 Raman spectrum intensity in z-direction mapping of the sample

References

[1]Wu Jin-guang. The Technique and Application of Modern Fourier Tranform Infrared Spectroscopy. Beijing : Science and Technology Document Press ,. 1994.227.

[2]Wang Jian , Sun Su-qin , Luo Guo-an , Wang Yan-ji , Wang Yan , Wang Jing-han . Spectroscopy and Spectral Analysis, 19 (6) , 834(1999) .

[3]Xu Xiao-xuan , Lin Hai-bo , Wu Zhang-chen , Yang Yan-yong , Zhang Chun-zhou . Chinese Journal Infrared and Millimeter Waves , 22 (1) , 63(2003).

[4]XU Xiao2xuan et al . Chinese Journal Infrared and Millimeter Waves, 20 (3), 169(2001).

Supported by Zhenxing Project of the Chinese Ministry of Education,A01504
Published on Spectroscopy and Spectral Analysis,25(1),51(2005)

Studies on Photoluminescence Characteristics of 1-An ilinonaphthalene-8-Sulfonate in Solid Matrixes

Yang Ren-Jie, Xu Xiao-xuan, Shang Li-ping, Xu Jialin, Yang Yanyong, Zhang Cunzhou

The photoluminescence characteristics of 12 anilinonaph thalene282sulfonatein (ANS) in solid matrixes were studied. The fluorescence peak of ANS shifted to shorter wavelength in solid matrix compared with that in m ethanol solution, which is probably single molecular luminescence due to the limit to the motion of ANS molecules in solid environment, while the fluorescence peak of pure ANS powder shifted to longer wavelength due to the in ten se interaction among ANS molecules. The emission maximum in solid paraffin is the largest red shifted one due to the non-polar environments, while on the polar talcum surface there is a blue shifted one, which shows the solid microcosmic environments effects upon the properties of ANS fluorescence. Fluorescence lifetime is shortened because of the larger fluorescent emission rate in solid substrates. Relative quantum yields obviously increase due to the limit of the ANS molecules motion in solid environment, and the decrease of collision quenching. The results are important to obtain composition and physical properties of solid substrates, and significant to study the phenomenon of energy transfer in photochemical reaction.

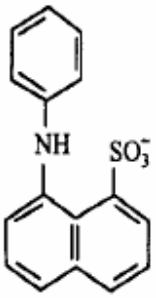

Fig. 1 ANS

References

[1] Kosower E M. Photophysics of Phenylaminonaph thalene-Sulfonates: A Paradigm for Excited State In tramolecular Electron Transfer [J]. Acc. Chem. Res., 15: 259-266(1982).

[2] Buschmann H J, Wo lff T. F luo rescence of 12A nilinonaph thalene282Sulfonate in Solid M acrocyclic Environments [J]. J. P hotochem. Photobiol. A: Chem., 121: 99—103(1999).

[3] KashaM, Raw I H R, A sh raf E G et al. The Exciton Model in Mo lecular Spectro scopy [J]. P ure Appl. Chem., 11 (5):371—392(1965).

Supported by Zhenxing Project of the Chinese Ministry of Education,A01504
Published on Chinese Journal of Spectroscopy Laboratory, 22(2),230(2005)

Fluorescence Measurement of Oil Micro-contamination in Water with Optical Fiber Technique and it s Application

Shang Li-ping, Xu Xiao-xuan, Xu Jing-jun, Shi Jinshan, Xia Daying

Based on the theoretic analysis and experimental research of fluorescence spectral characteristic of mineral oil in water, a fluorescence measuring system of oil micro2contamination in water with optical fiber is developed and accomplished. The system performance test and experimental research in situ is carried out. The experimental results show that the application of the fiber optic sensing and transmitting technique to fluorescence oil measuring instrument is correct theoretically and reasonable schematically. This research provides a novel technical means for oil contamination in water monitoring.

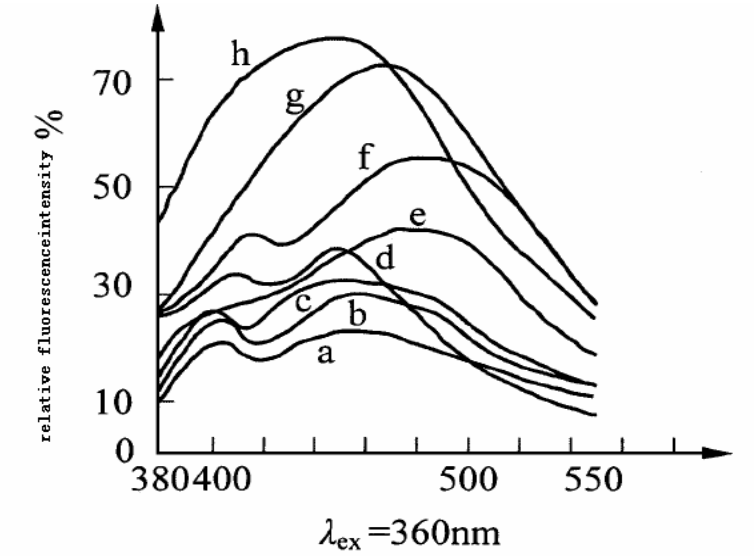

Fig. 1 fluorescence spectral of oils in different producing area
a —Da Gang; b —Qing Hai; c —Xin Jiang; d —Sheng Li;
e —Sheng Li mixed oil; f —Hui ZHou; g —the Central of Bo Hai; h —Qi Kong

References

[1] Wang guo-tai, Yi Xiu-fang, Wang Li-li. Robot, 19(6), 474～478(1997).
[2] Cheng Xiong-biao, Yuan Zhe-jun, Yao Ying-xue. Robot, 19(1), 7～11(1997).
[3] Wu Juan, Cao Xiao-yin, Song Ai-guo, et al. Transaction of Sensor Tech, (3), 181～185(2001).

Supported by the National Natural Science Foundation of China,40106011
Published on ACTA METROLOGICA SINICA,26(1),81(2005).

Adopting the Method of Correlation Coefficient to Improve the Accuracy of the Xylene Isomer's Prediction Model

Wu Zhongchen, Xu Xiaoxuan, Li Qinan, Yu Gang, Zhang Cunzhou

The concentration of the Benzene and its homologue's mixture is measured by near infrared. Based on the fingerprint infrared spectrum database, array of correlation coefficient was first used to identify traditional para-xylene, meta-xylene, ortho-xylene's mixture rapidly. This paper focuses on the detailed researches on the correlation coefficient in Near Infrared spectrum and point out it's characteristics with multi-component solution; The paper also prove the principle which obtain the much accurate results when using high correlation coefficient for model building and give a practical experiment to test the conclusions by using para-xylene, meta-xylene, ortho-xylene's mixture.

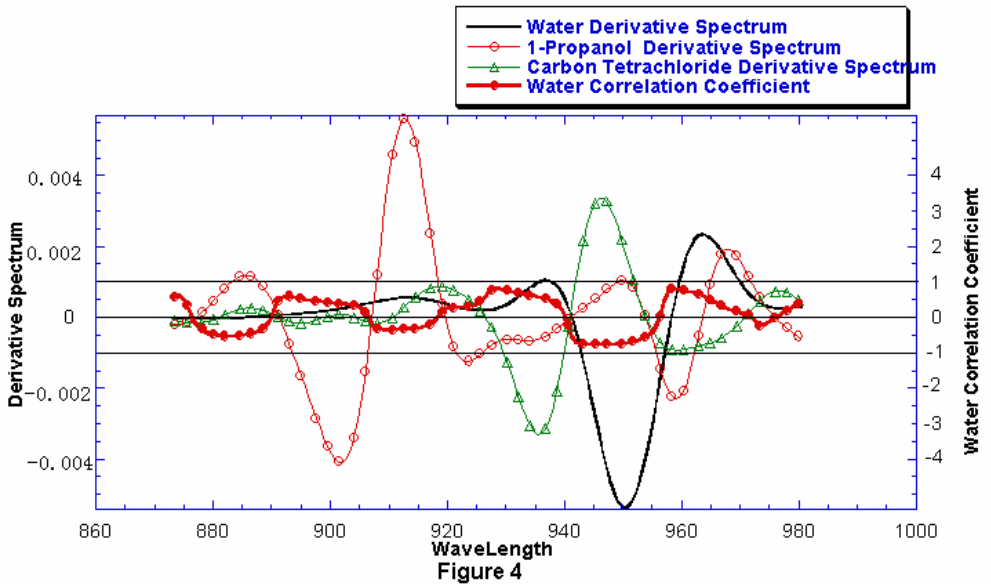

Fig.1: Derivative spectrums and water correlation coefficient.

References

[1] Special Guest Editorial, Applied Spectroscopy,1991; 45（1）:14A

[2] Xu Yong-qin, Sun Su-qin, XU Jin-wen, Chinese Journal of Spectroscopy Laboratory, 2002; 19(5): 606-610

[3] Hu Wei, Tang Wan-ying, Zhou Shen-fan, Chinese Journal of Analytical Chemistry, 1997; 25（5）: 614

Supported by Zhenxing Project of the Chinese Ministry of Education, A01504
Published on Spectroscopy and Spectral Analysis. 25(1):136-140(2005)

Solid Powder Fluorescence of Oil Cuttings

Yang Ren-jie,Xu Xiao-xuan, Shang Li-ping, Xu Jia-lin, Yang Yan-yong, Zhang Cunzhou

The solid powder fluorescence of oil cuttings was studied and we drawn a conclusion that in the range of certain oil concentration, the fluorescence intensity of the solid powder is linear with oil concentration in the powder of cuttings, with a regression coefficient of 0. 9936. But when the heavy oil concentration in the sample reaches a certain degree, the fluorescence intensity does not vary with oil concentration in the powder of cuttings, but its value does not equal zero. At the same time, the fluorescence quenching phenomena of oil cuttings were studied and the high concentration of heavy oil is the primary factor of the fluorescence quenching, which will causes non2linear relation between the fluorescence intensity and oil concentration in the powder of cuttings and results in false analytical data and error characters of spectra. From the study on the mechanism of concentration quenching of fluorescence, we obtained that the concentration quenching is mainly induced by the organic molecular interaction, such as formation of excimer and dimmer, intercrossing relaxation, etc. A comparison was made between the concentration quenching of solid powder fluorescence and the concentration quenching in solution. This showed that (1) when oil concentration of sample reaches a certain degree, the intensity of fluorescence keep s a constant in solid powder, but it equals zero in solution. (2) fluorescence peak of heavy oil locates at shorter wavelength in solid powder than that in solution. (3) the fluorescence quantum yield of heavy oil is larger in solid powder than that in solution. The study is important to develop a new analytical technique of quantitative fluorescence detector which can be app lied to the analysis of solid samples with pretreatment, and is significance for quantitative fluorescence logging and organic geochemistry.

References

[1] Lu J ingci, Yong Kelan. Study on the fluorescence quench phenomena in three2dimension fluorescence determination of crude oils [J]. Analytical Laboratory, 17 (6): 28231 (1978).

[2] Chen Guozhen, Huang Xianzhi, Zheng Zhuzi. Spectrofluorimetry [M]. Beijing: Science Press, 10220(1990).

[3] Huang Qiaosong, Xu Xiaoxuan, Xu Jialin, et al. Microscopic fluorescence imaging spectra of oily core [J]. Chin. J.Lum in. 25 (2): 2022206 (2004).

Supported by Zhenxing Project of the Chinese Ministry of Education,A01504
Published on CHINESE JOURNAL OF LUMINESCENCE, 26(1),131(2005)

Improving the Accuracy of Isomer's PLS Prediction Model in Near Infrared Spectrum Analysis by Subtractive Spectra Technology

Wu Zhongchen, Xu Xiaoxuan, Zhang Jing, Li Qinan, Zhang Cunzhou, Yu Gang

The mixture of xylene's isomer is quantificationally measured by near infrared spectrum in this paper. The accuracy of three different ways PLS modeling building, namely full spectrum modeling building, selecting the spectrum bands which have high correlation coefficient and selecting the spectrum bands which show a great difference by using subtractive spectra technology, are compared. The result show that the accuracy is much better than others by using the spectrum bands which is selected by subtractive spectra technology, because it can markedly overcome the overlapping of the isomer's near infrared spectrum.

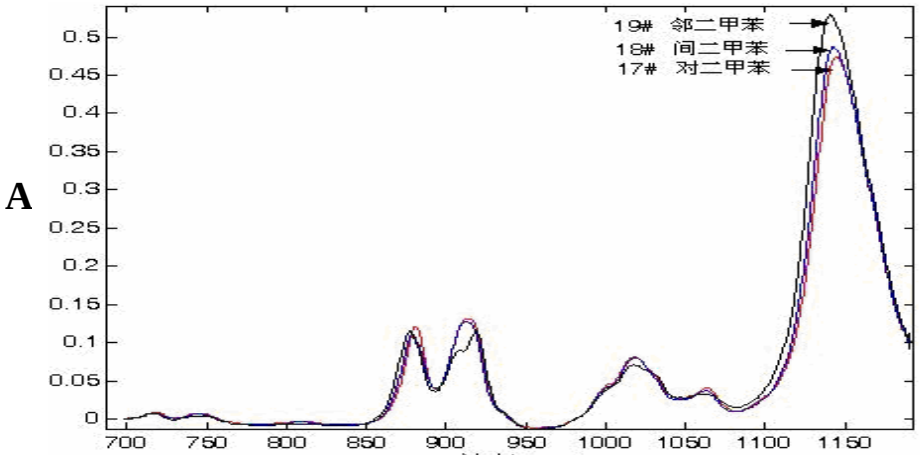

Fig.1: NIR spectra recorded on benzene and its homologue's mixture in the wavelength range 700 to 1200 nm

References

[1] Yanlu YAN , Longlian ZHAO , Junhui LI. Information Technology of Modern NIR Spectral Analysis, Spectroscopy and Spectral Analysis,2000:20(6)777-780

[2] Shen Han-xi, Cai Shuo-wei , Solution of Morbid Spectra data Systems by Ridge Regression Method and Its Application for Analysis of Complex Vitamins B. Chinese Journal of Analytical Chemistry, 1994: 22(7)720-723

[3] D. Jouan-Rimbaud, B. Walczak, D. L. Massart. Comparison of multivariate methods based on latent vectors and methods based on wavelength selection for the analysis of near-infrared spectroscopic data. Analytica Chimica Acta. 1995：304(3)285-295

Supported by Zhenxing Project e Chinese Ministry of Education, A01504
Published on Chinese Journal of Spectroscopy Laboratory, 22(1), 38(2005)

The application of Cross-correlation analysis in near infrared spectrum pretreatment

Wu Zhongchen, Xu Xiaoxuan, Zhang Jing, Li Qinan, Zhang Cunzhou, Yu Gang

From the point of view of signal analysis, a new way to feature extraction of near infrared reflection spectroscopy by the correlation analysis theory was discussed. The benzene's concentration is quantitatively measured adopting cross-correlation analysis with simple linear regression using near infrared spectrum, and the relation that the signal's amplitude transformed by cross-correlation analysis is proportional to the concentration of the measured component is proved. The advantages and disadvantages of the cross-correlation analysis were discussed. Figure 1 shows that NIR spectra recorded on benzene samples in the wavelength range 700 to 1150 nm

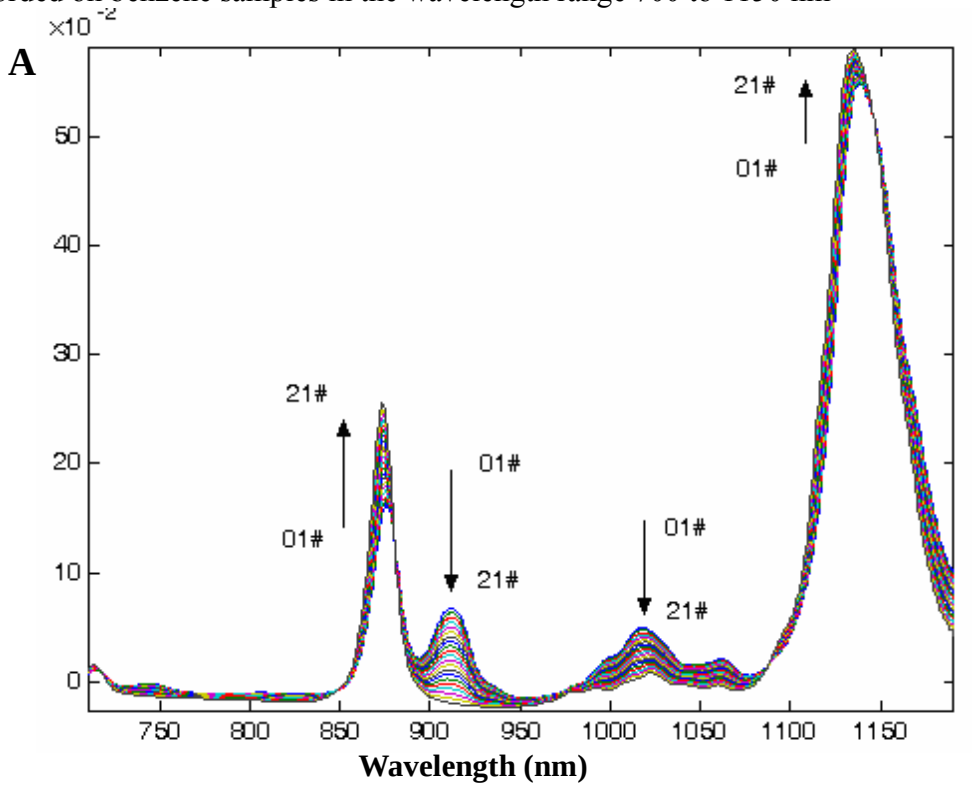

Fig.1: NIR spectra recorded on benzene samples in the wavelength range 700 to 1200 nm

References

[1] C. K. Mann, J. R. Goleniewski, and C. A. Sismanidis Spectrophotometric Analysis by Cross-correlaton, Applied Spectroscopy, 1982：36（3）223～227

[2] LU Ya-Guang, Adaptive Wavelet Thresholding Deno is ing Used in Spectra l Signal, Chinese Journal of Spectroscopy Laboratory, 2004, vol21, No. 3

Supported by Zhenxing Project e Chinese Ministry of Education, A01504
Published on Chinese Journal of Spectroscopy Laboratory, 22(1), 126(2005)

Adopting the method of near infrared spectrum to measure the ratio of primary hydroxyl group and second hydroxyl group in polyether polyol

Zhang Jing, XU Xiaoxuan, Wu Zhongchen, Yang Renjie, Yu Gang, Zhang Cunzhou

This paper describes the application of infrared spectroscopy in examination the hydroxyl value of poyether polyol. The method of near infrared spectrum, combing with derivative spectrum and multiple linear regression, is applied to measure the ratio of primary hydroxyl group and second hydroxyl group in polyether polyol. We obtain the good predictive results by using the method in this experiment. The work is very helpful for the on-line measurement of polyether polyol.

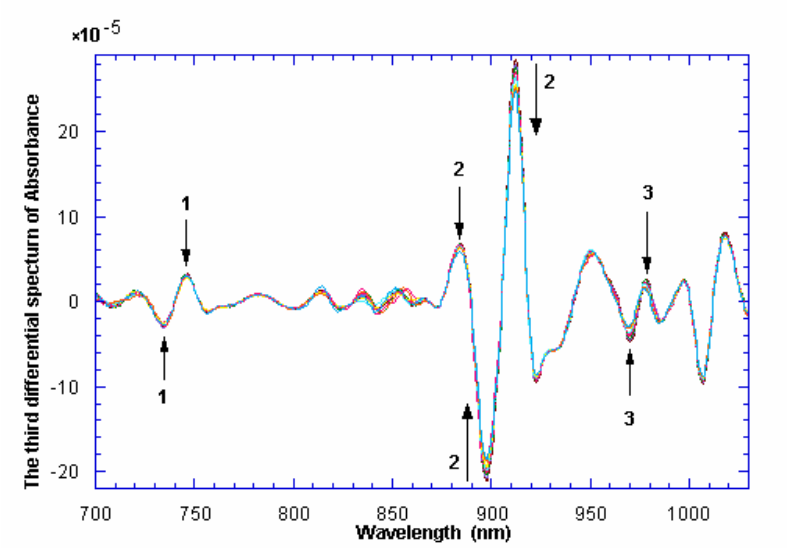

Fig. 1: The third differential spectrums of PPG

References

[1] Song Li.Jiangsu Chemical Industry.2001:29(5)18-24
[2] Gangliang Hu,XiuYang Lv,Ke Cheng,Dan Qing Liu.China Journal of Chinese Materia Medica.2003:28(12)1117-1119
[3] Guoan Luo,Jiaxue Qiu,Yiming Wang · Quantitative ananlysis and computer application in visible and ultraviolet spectrum,(shanghai)： (Shanghai Scientific and Technical Documents Fublishing House)，1988：75
[4] Yongnian Ni.The application of chemometrics in analytical chemistry .（BeiJing）: (Science Press).2004:135

Supported by ZhenXing project of the Chinese Ministry of Education, A01504
To be published on Spectroscopy and Spectral Analysis, 26(1) (2006)

Performance Improvement of Polymer Light-emitting Diodes with Metal Fluoride Cathode

Lin Hai-bo, Xu Xiao-xuan, Wu Hongbing, Wang Bin,Yu Gang, Zhang Cunzhou

The electronic and optical performances of polymer light-emitting diodes of inserting lithium fluoride insulating layer between the metal cathode and active polymer are studied. As for the polymer light-emitting diodes, optimization of charge injection lies in the dominant factors for substantive improvement performance. Since it is minority carriers dominate the combination thus the radiation, heir injection takes priority over that of majority carriers. Generally insemiconducting polymers, holes are majority carriers while electrons minority, the carrier misbalance between electrons and holes further deteriorate in the fact that hole usually take possession of higher mobility and smaller injection barrier. To balance injection charge carriers and facilitate the electron injection, there are two commonly used stratagems in cathode fabrication. One is to employ low work function metals such as barium and calcium as cathode though they are susceptible to degradation upon water vapor and oxygen. The other choice is proposed to insert an insulating thin layer lithium fluoride between polymer/ electrode interfaces to build a bilayer cathode. As show in the experiment result, the LiF/Al double-layer-cathode devices are capariable with

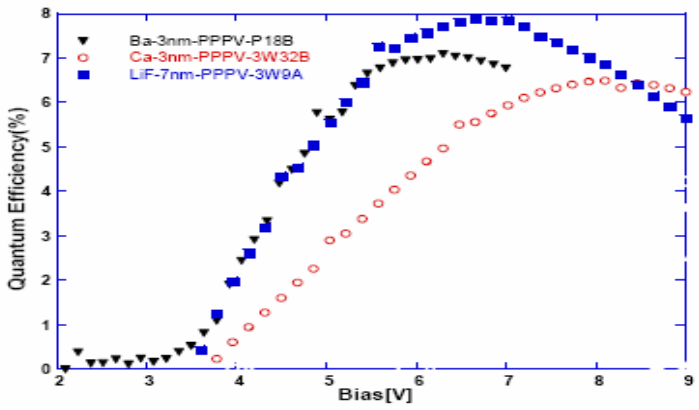

Fig. 1 External quantum efficiency curves of different-cathode PLEDs with P-PPV as active layer

References

[1] A. Kohler, D. A. dos Santos, D. Beljonne, Z. Shuai, J. -L. Bre´das, A.B.Holmes, A. Kraus, K.Mu¨llen & R. H. Friend, Charge separation in localized and delocalized electronic states in polymeric semiconductors, Nature, 392, 903-906(1998)

[2] R. H. Friend, R. W. Gymer, A. B. Holmes, J. H. Burroughes, R. N. Marks, C. Taliani, D. D. C. Bradley, D. A. D. Santos, J. L. Brÿdas, M. Lˆgdlund,W. R. Salaneck, Electroluminescence in conjugated polymers, Nature 397, 121-128(1999).

Supported by Zhenxing Project of the Chinese Ministry of Education, A01504
Published on Chinese Journal of Luminescence, 26（4）469-472（2005）

Adopting cross-correlation algorithm for optimizing Model Transfer of Near infrared spectrum

Wu Zhongchen, Xu Xiaoxuan, Yang Renjie, Zhang Jing, Yu Gang, Zhang Cunzhou

This paper introduces an algorithm used for resolving calibration transfer in multivariate calibration of chemometrics. Model transfer is researched by cross-correlation in near infrared spectrum .The hypothesis that this is an inherent proportional constant between the two spectrums for model building measured by two different spectrometers after cross correlation analysis is put forward and approved. The compatibility of two models is enhanced after making up the proportional constant. So the good results are got. The figure 1 shows that the difference between two kinds of spectrometer was made up by adopting the cross-correlation analysis.

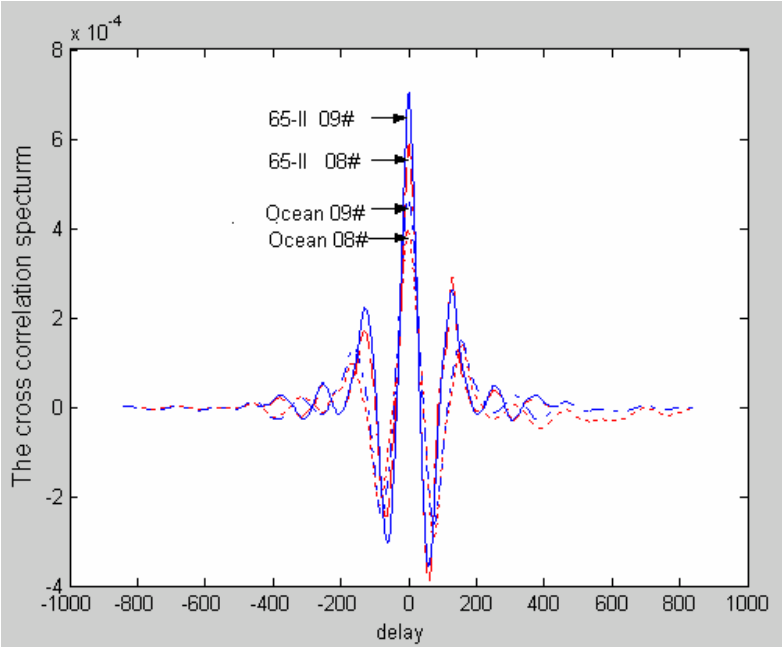

Fig.1: The Cross-correlation spectrum of Partial samples

References

[1] Gary E Ritchie, Emil W Ciurczak, Howard Mark. Books of Abstracts Presented at PITTCON, 2000, 460.

[2] XiaoLi Chu，HongFu Yuan，WanZhen Lu．Spectroscopy and Spectral Analysis.2001：21（6）：881-885

[3] XiaoLi Chu，HongFu Yuan，WanZhen Lu．Chinese Journal of Analytical Chemistry．2002：30（1）：114-119

[4] Gary Horlick．Analytical Chemistry．1973：45（2）319-324

Supported by the National Natural Science Foundation of China'A01504
To be published on Spectroscopy and Spectral Analysis, 25(12) (2005)

Studies on Breast Cancer Tissues With ATR-FTIR Spectroscopy

Yu Ge , Lu Shuhua , Xu Jialin, Zhang Cunzhou, Zhang Chunping

Attenuated total reflection (ATR) FTIR spectra of benign and malignant breast tumor tissues from 32 female patients have been determined and investigated. The spectral differences and changes (shape, peak position and relative intensities) have been observed between these two types of samples. In comparison with the benign tumor tissues, the mainly characteristic changes of malignant breast tissues involve: 1) The secondary structure of proteins in malignant tumor tissues is composed mainly ofα2helix and random coil, in whichα2helix structure is dominant. 2) The absorption band near 1160 cm- 1 due to the C2O (H) stretching modes of serine, threonine, tyrosine group s evidently shifted to a higher wavenumber, suggesting that the intermolecular hydrogen bonds were nearly broken, and the collagen absorption peaks at 1205 cm- 1 , 1278 cm- 1 and 1338 cm- 1 became lower or disappeared, showing its relative contents decreased. 3) The bands from the symmetric and asymmetric stretching modes of the PO2 of the phosphodiester group s in nucleic acid shifted to 1083 cm- 1 and 1242 cm- 1 , respectively, and became stronger. All these indicated that the relative content of nucleic acid increased greatly. 4) The A2852 /A2870 and A2923 /A2958 absorbance ratio were significantly higher for malignant tumor tissues than for benign breast tumor tissues. This suggested that there were changes in the conformational structure of the methylene chains of membrane lip ids. These results showed that ATR-FTIR spectroscopy was able to become a powerful tool for the biochemical study and the vivo diagnosis of human breast cancers.

References

[1] Wang S C, He J F, Peng J F, et al. Acta Photonics S inica,33 (7) : 871～ 876(2004).
[2] Xu T, Zhang C P, Wang X Y, et al. Acta Photonics S inica,32 (5) : 571～575(2003).
[3] Rigas B, Wong P T T. Human colon adenocarcinoma cell lines display infrared spectroscopy features of malignant colon tissues. Cancer Research, 52 (1) : 84～ 88(1992).
[4] Benedetti E, TeodoriL, TrincaM L, et al. A new approach to human solid tumor cells. Applied Spectroscopy, 44(8) : 1276～1280(1990)

Supported by Zhenxing Project of the Chinese Ministry of Education,A01504
Published on ACTA PHOTON ICA SIN ICA,34(3),390(2005)

Investigation of Human Breast Tumors Tissues With ATR-FTIR Spectroscopy in Vitro

Yu Ge, Lu Shuhua, Xu Jialin, Zhang Chunping, Zhang Guangyin

Attenuated total reflection (ATR)FTIR spectra of breast tumor tissues from 38 female patients have been determined and investigated. In comparison with the benign and normal tumor tissue, the mainly characteristic changes of these malignant tumor tissues in the spectra were observed in the symmetric and asymmetric stretching band of phosphodiester groups, which shifted to short wavenumber about 6cm-1 invas PO2- , and 1220cm-1 band appeared in the corresponding second derivative spectra, which intensity increased. And also integral area ratiodisplayed and order of normal <benign <malignant. The absorption band near 1162cm-1 due to the C-O(H)stretching modes of serine, threonine, tyrosine groups evidently shifted to a higher wavenumber about 6cm-1,and the collagen absorption peaks at 1204cm-1,1281cm-1and 1339cm-1became lower or disappeared. The symmetric stretching modes of PO2-3 at 970 cm-1 from the phosphorylated proteins became stronger. The absorbance intensity ratio A1045/A1083,decreased,the A2852 /A2873 ，A2923/A2958 evidently increased.

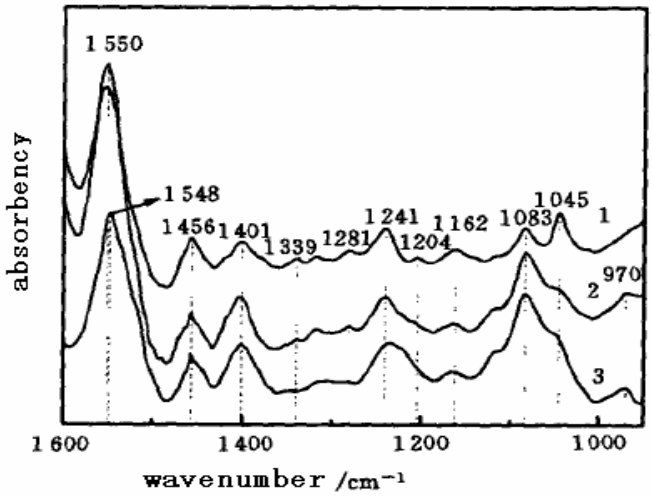

Fig. 1 ATR-FTIR spectra in the frequency region 1600 to 950 cm^{-1} of human breast tissue

References

[1] Shafer-Peltier K E, Haka A S,Fitzmaurice M,et al. Raman microspect rosdopic model of human breast: implications for breast cancer diagnos is in vivd[J]. Journal of Raman Spectro scopy,33:552~563(2002).

[2] Rigas B, Wong P T T. Human colon adenocarcinoma cell lines display infrared spectroscopy features of malignant colon tissues[J].Cancer Research,52:84~88(1992)

. Supported by Zhenxing Project of the Chinese Ministry of Education,A01504
Published on Acta Scientiarum Naturalium Universitatis Nankaiensis,38(1),53(2005)

Confocal Raman Microspectroscopic Study of Human Breast Morphological Elements

Yu Ge, XU Xiao-xuan, LU Shu-hua, Song Zengfu, Zhang Cunzhou, Zhang Chunping

Breast tissue sections were examined by means of confocal Raman spectroscopy with an excitation wavelength of 633nm. Acquired using a microscopic mapping approach with the sample volume ~2μm3, these spectra were compared with the ones of the commercially available actin, DNA, collagen (type I), triolein etc. Some spectra were distinguished and identified to be from and characterize the morphological elements like cell cytoplasm, extracellular matrix etc. The cell nucleus spectrum was also obtained by K-means cluster analysis. The correlation analysis showed that the spectrum from a morphological element is highly correlated with that from the corresponding purified chemical. The spectroscopic characterization of these morphological elements was then investigated. This study is helpful to understanding the chemical/morphological basis of the Raman spectrum and designing the Raman microspectroscopic model of human breast tissue.

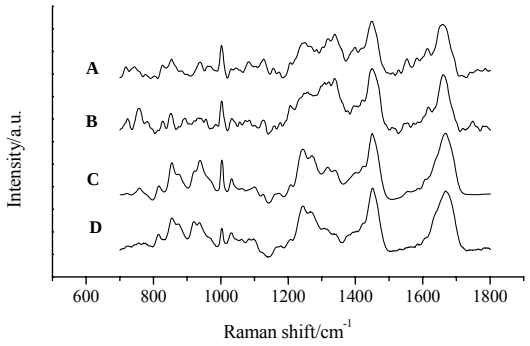

Fig.1 Comparison of (A) cell cytoplasm and (B) actin;
(C) extracellular matrix and (D) purified collagen (type I).

References

[1] Johnson J, Dalton R, Wester S, Landercasper J, Lambert P. Archives of Surgery ,134: 712(1999).
[2] Alfano R R, Liu C H, Sha W L, Zhu H R, Akins D L et al. Lasers Life Sci., 4: 23(1991).
[3] Frank C J, Redd D C B, Gansler T S et al. Analytical Chemistry, 66(3): 319(1994).

Supported by Zhenxing Project of the Chinese Ministry of Education,A01504
To be published on Spectroscopy and Spectral Analysis,26( ) .(2006)

The Three-dimension Spectral Subtraction Fluorescence to Check Adulteration of Petrol by 120# solvent naphtha

Yang Renjie, Xu Xiaoxuan, Shang Liping, Xu Jialin, Yang Yanyong, Zhang Cunzhou

Studying on characteristics of a adulterated sample of diesel by 120# solvent naphtha by three-dimension Spectral Subtraction Fluorescence technique, we described that the technique may analyse fastly whether there is a adulterated sample of 120# solvent naphtha in diesel. At the same time, measuring the volume of three-dimension Spectral Subtraction Fluorescence graph, we find that this total volume is directly related to the concentration of the adulterant present in the sample. The study is important for us to analyse whether there is a adulterated sample of 120# solvent naphtha in diesel. and is significance for us of maintaining the stable of market.

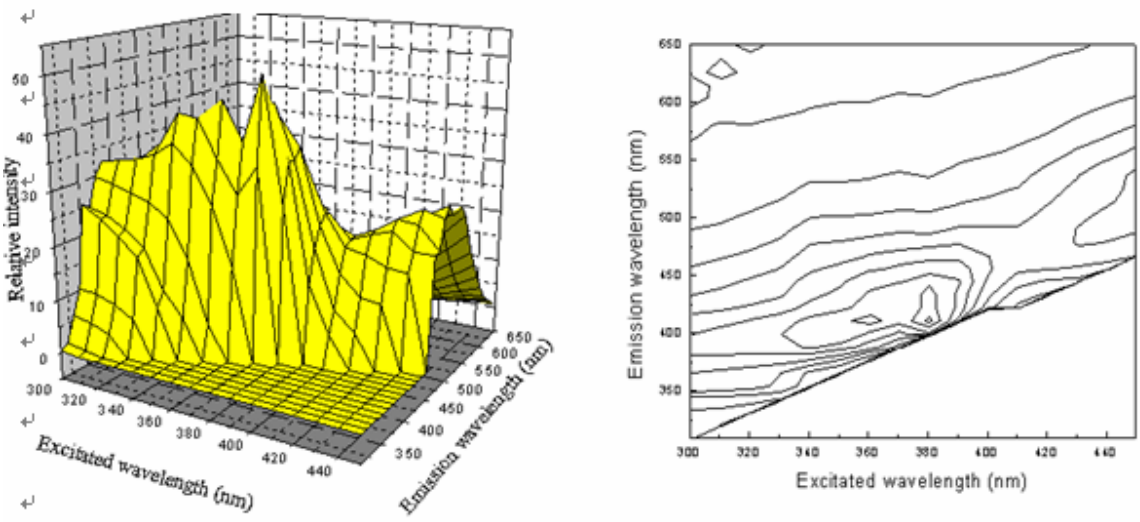

Fig. 1 The three-dimension fluorescence spectrum and fluorescence contour spectra of diesel oil

References

[1]Liu Zhihong, Cai Ruxiu, Journal of analytical science, 1994, 16(6): 516
[2]N.R.Gray, S.J.Mcmillen, A.G.Requejo, J.M.Kerr, G.Denoux,and T.J.McDonald, SPE 25900,465(1993)
[3]J.L.Beltran, R.Feffer, and J.Guiteras, Anal.Chem. Acta 373,311(1998)
[4]R.D.JiJi, G.A.Copper, and K.S.Booksh, Anal.Chem. Acta 397, 61(1999)
[5]A.E.Dudelzak, S.M.Babichenko, L.V.Poryvikina, and K.J.Saar, Appl.Opt.30, 453(1991)

Supported by Zhenxing Project of the Chinese Ministry of Education, A01504
To be published on Spectroscopy and Spectral Analysis, 26(1), (2006)

Study of Poly(3,4-ethylene dioxythiophene):Poly (styrene sulfonate) by In-situ resonance Raman spectroscopy

Lin Haibo, Xu Xiaoxuan, Wang Bin, Wu Binlin, Xu Jialin, Yu Gang, Yang Yanyong

Poly (3,4-ethylene dioxythiophene)(PEDOT): Poly (styrene sulfonate)(PSS) has due to good stability and hig electronic conductivity in its doped state attracted a lot of interest for application in organic electronics. Indeed, thin layers of PEDOT: PSS are regularly used in light emitting diodes (PLEDs) as hole injection and transportation layer. Here, Doping and dedoping states of PEDOT:PSS are studied by absorbance spectra and Raman spectra. A new absorption band centered at 620 nm is observed on dedoped PEDOT: PSS. Consistently, Raman signals of dedoped PEDOT: PSS are resonantly intensified since the Raman excitation wavelength (633nm) is set in the enhanced absorption band. So it gives a sensitive way to study the doping and dedoping states of PEDOT: PSS. Furthermore, for the encapsulated polymer light-emitting diodes, Raman spectroscopy is a powerful way to study the polymer layers inside the devices.

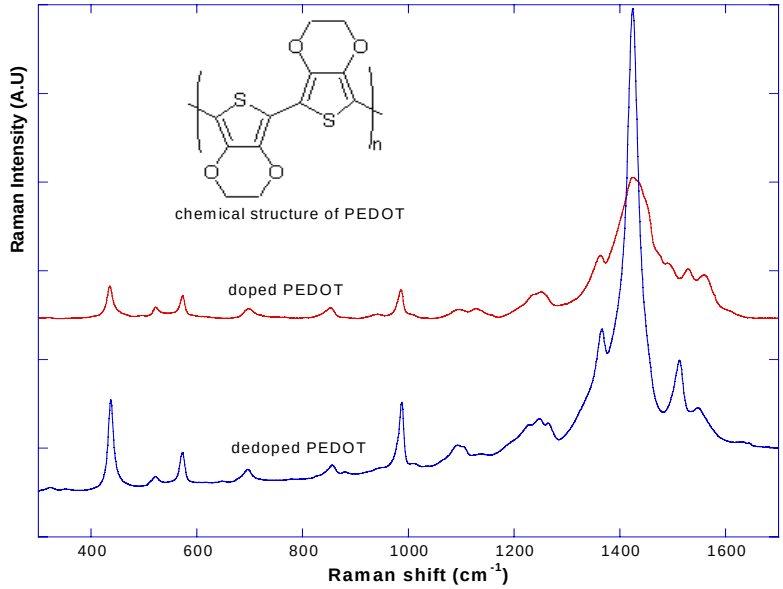

Fig.2: Raman spectral comparison between doping and dedoping PEDOT: PSS. Chemical structure of PEDOT is shown in the insert.

References

[1] A.C. Arias et al. Phys. Rev. B 60 (1999) 1854–1860.
[2] A.van Dijken et al. Organic Electronics 4 (2003) 131–141
[3] F.Louwet et al. Synthetic Metals 135–136 (2003) 115–117
[4] Y. Cao et al. Synthetic Metals, 87(1997) 171–174.

Supported by ZhenXing project of the Chinese Ministry of Education,A01504
To be published on Spectroscopy and Spectral Analysis.,26 (2006)

The Orthogonal Polynomial Regression Method of M wavelength ult i—Radiation Thermometry

Li Qinan, Xu Xiaoxuan, Wu Zhongchen, Song Ning, Zhang Cunzhou, Yu Gang

A new data processing method of multi—wavelength radiation thermometry—the orthogonal polynomial regression method—was brought forward in this article on the base of variable emissivity. Comparing this method with the tradition data processing methods, it has the merit of simple principle, small operation and the small error of fitting true temperature, it can fit the true temperature of object fast and the result is accurate.

true temperature of tungsten sueface （K）	Step regression method		orthogonal polynomial regression method	
	fitting temperature （K）	Relative error	fitting temperature （K）	Relative error
1600	1608.9	0.56%	1603.2	0.20%
1800	1807.9	0.44%	1803.1	0.17%
2000	2002.3	0.12%	2002.7	0.13%
2200	2182.2	0.81%	2201.8	0.08%
2400	2375.0	1.04%	2400.3	0.01%

Table 1: The fitting result comparison of tungsten surface

References

[1]MENG Jian Ping，YANG Jing Guo，TAN Hua，HU Shao Lou.Spectroscopy and Spectral Analysis,2002，22（5）：721.

[2]ZHAN Chun Lian，LI Yan Mei，LIU Jian Ping，YANG Zhao Jin，FAN Ji Hong，LI Zheng Qi.Journal of Applied Optics,2002，23（6）：39.

[3]SUN Xiao Gang，DAI Jing Min，CONG Da Cheng，CHU Zai Xiang. Journal of Infrared and Millimeter Waves,1998，17（3）：221.

[4] DAI Jing Min.Theory and Practice of Multi-spectral Thermometry. Beijing：Higher Education Press，2002：11.

[5]ZHOU Ji Xiang.Practical Regression Analysis Method.Shanghai：Shanghai Scientific and Technical Publishers，1990：77.

[6] GE Shao Yan，NA Hong Yue. The Character and Measurement of Heat Radiation.Beijing：Science Press，1989：243.

Supported by ZhenXing project of the Chinese Ministry of Education, A01504
To be published on Spectroscopy and Spectral Analysis.26 (2006)

Microscopic Raman imaging spectra of PbS and its photo-oxidation products

Xu Jia-lin, Xu Xiao-xuan, Zhang Pan, Zhang Cunzhou, Yu Gang

Spatially resolved molecular information on galena (PbS) crystals was obtained by microspectrometric Raman mapping through a high numerical aperture objective. Different experimental conditions were used: excitation power and crystal size. Spatially guided analysis was obtained from the spectra recorded in the point-by-point microprobe mapping mode with 0.5 μm spacing between the points. Multivariate data processing yielded the characteristic spectra of PbS and its degradation products. The Raman features of PbS were found to be weak under non-damaging excitation conditions. The laser-induced photochemical effect generates complete and irreversible oxidation reaction of PbS to a-PbO for particles of size of the order of micrometres. For larger PbS crystals, several lead oxysulphates including 4PbO·PbSO4, 3PbO·PbSO4 and PbO·PbSO4 were located by Raman mapping in the vicinity of the illuminated spot.

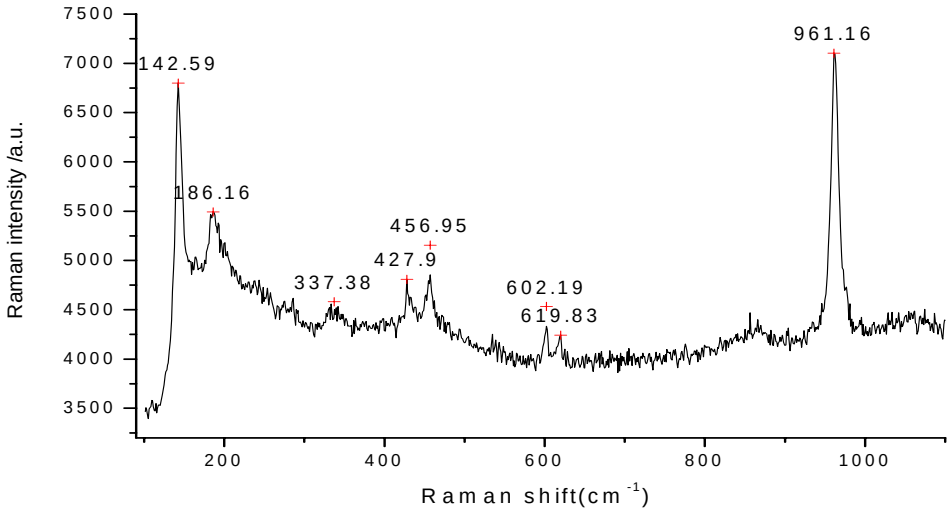

Fig.1: Raman spectrum (Stokes) of freshly cleaved galena recorded of an increase in laser power.

References

[1] K.K.Nanda, S.N.Sahu, R.K.Soni, Raman spectroscopy of PbS nanocrystalline semiconductors, Phys. Rev.B, 1998, 58:15405.
[2] J.G.Shaper, M.H.Brooker, W.M.Skinner, Observation of the oxidation of galena using Raman spectroscopy,Int.J.Miner.Process, 2000, 60: 199-211.
[3] Todd D. Krauss, Frank W. Wise, Raman-scattering study of exciton-phonon coupling in PbS nanocrystals, 1997, 55: 9860.
[4] Janet L.Machol, Frank W.Wise, Ramesh C.Patel, et al..Vibronic quantum beats in PbS microcrystallites, 1993, 48:2819.

Supported by the National Natural Science Foundation of China, A01504
To be published on Chinese Journal of Light Scattering, 18(3) (2006)

The optimum design and radiation characteristics research of indoor gas infrared source in the FTIR emission spectrometric method

Li Qinan, Xu Xiaoxuan, Wu Zhongchen, Song Ning, Zhang Cunzhou, Yu Gang

In this paper，the start point is to measure the emission spectra of the indoor high-temperature gas using the FTIR spectrometer；the geometric parameters of the gas radiation source are optimized under the condition that the spectrometer has certain resolution and can receive the fullest extent of radiation energy. The condition of gaining the non-continual and continual spectrum is discussed quantitatively in this article. In the end, the radiation characteristics of high-temperature gas are discussed.

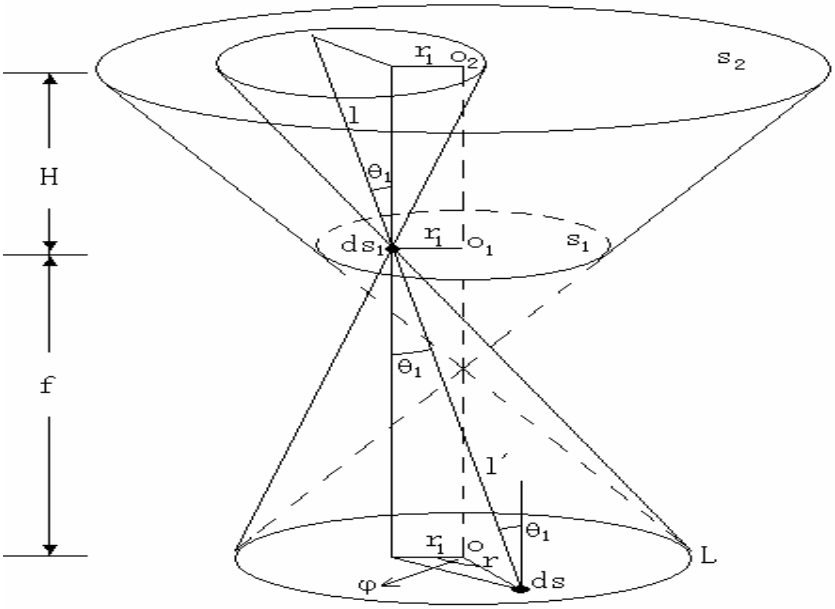

Fig.2 The calculation of the energy that enters into the FTIR spectrometer

References

[1] WU Jin-guang.The Technique and Application of Modern Fourier Tranform Infrared Spectroscopy.Beijing：Science and Technology Document Press, 1994.19

[2] Flanigan D F. Detection of organic vapors with active and passive sensors: a comparison. Applied Optics, 1986, 25（23）: 4253～4260

[3] ZHANG Jun, XUN Yu-long.Real-time remote detection of weak-spectra of chemical vapors using subtractive spectroscopy techniques.Spectroscopy and Spectral Analysis，1998, 18（6）: 649～653 2000.485

Supported by ZhenXing project of the Chinese Ministry of Education, A01504
To be published on Journal of Infrared and Millimeter Waves.,25(3)(2006)

The Measurement of Tumor Auto-fluorescence Spectra with Fiber Optical Biosensor

Zhang Pan, Yu Ge, Xu Xiao-xuan, Liu Yan-nan, Liang Jun, Zhang Cunzhou

Fiber optical biosensor is a significant kind of modern biosensor systems. At present, many fiber optical biosensor systems depending on detecting fluorescence have been on sale. However, the fiber optical biosensor systems that could get the bio-informatics directly from the auto-fluorescence spectrum of biologic samples have not come into the market. In this situation, the author started some research on the samples of fresh human breast tissues by a self-made three-dimensional fluorescence fiber optical spectrometer. The peak value in normal tissue is on the position of 511nm, while it is on the position of 513nm around the cancerous tissue, 518nm in the core of cancerous tissue. We can observe that the position of peak value has a trend to shift to right side from normal to cancerous tissues. On the other side, the intensity ratio of two primary peaks in normal tissue is 0.77, while it is 0.64 around the cancerous tissue and 0.58 in the core of cancerous tissue. We can observe that there is a decreasing trend from normal to cancerous. Furthermore, the article analyzes the source of the spectral difference and the origin of different fluorescent bands. Although there are still much work to do and lots of elements to reveal, it is definitely obvious that the fluorescence spectrum technique combined with fiber optical sensors technique would make great progress in on-line diagnosis of human cancer in near future.

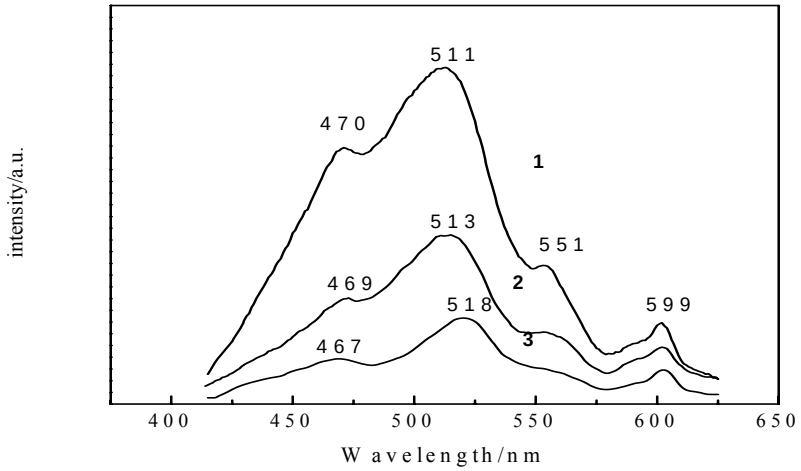

Fig.1: The auto-fluorescence spectrum of human breast tissues:(1) normal tissues, (2)beside the cancerous tissues, (3)in the center of the cancerous tissues

References

[1] Wu Baoli, Zhang Guomei, Gao Chunguang, Shuang Shaomin. Application and Development of Biosensors. CHINA BIOTECHNOLOGY, 2004, 24(7):65-69 (in Chinese)

[2] Wolfbeis OS(Ed). Fiber Optic Chemical Sensors and Biosensors[M], 1991,Vol Ⅰ & Ⅱ, CRC Press(Boca Raton ,Florida)

Supported by ZhenXing project of the Chinese Ministry of Education, A01504
To be published on Chinese Journal of Luminescence, 27(3) (2006).

Spectra Study on the Quality Change of Deep Frying Edible Oils by Synchronous Scan Fluorescence Spectra

Jia Yan-hua,Xu Xiao-xuan, Yang Ren-jie, Liang Jun, Deng Dawei, Yang Yanyong, Zhang Cunzhou

Several oils including oils that were not fried and fried oils were analyzed and studied by synchronous scan fluorescence spectra, and combined with infrared absorption spectra. Synchronous scan fluorescence giver a narrower and simpler spectrum and is of extensive use for multi-fluorescence analysis. In this method, both excitation and emission monochromators are scanned simultaneously keeping a fixed wavelength interval($\Delta\lambda$)between them (constant $\Delta\lambda$ mode).In our experiment, the optimization $\Delta\lambda$ is 10nm. The synchronous scan fluorescence was obtained in the emission wavelength range of 250nm－700nm. Compared with fresh oils, in the fluorescence spectra image of fried oils, fluorescence peak value in 370-380nm disappeared, and two fluorescence peak value in 461nm and 479nm emerge. In 1745cm^{-1}, the intensity of infrared absorption increase. All of this indicate that the number of carbonyl(C=O) increase, which is the same to chromatogram approximately.

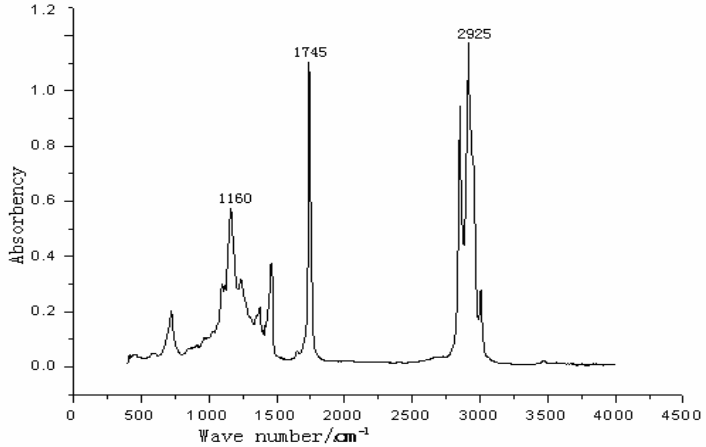

Fig.1 Difference of Infrared absorption spectrum of fried and unfried peanut attemper oil

References

[1] Chen Jie. Grease Chemistry. Chemical Publishing house, 2: 1～43(2004)

[2] Lai, Y. W., Kemsley, E. K., Wilson, R. H., et al. Potential of Fourier transform infrared spectroscopy for the authentication of vegetable oils. Journal of Agricultural and Food Chemistry. 42, 1159(1994)

[3] Bertran. E., Coello,J., Iturriaga,H., et al. Determination of olive oil free fatty acid by Fourier transform infrared spectroscopy. Journal of the American Oil Chemists Society. 76,611～616(1999)

Supported by Zhenxing Project of the Chinese Ministry of Education, A01504
To be published on ACTA PHOTON ICA SINICA, 35 (2006)

[d] 光谱表征及传感技术

[d]Spectral Charaterization and Sensing Techniques

1. 林海波, 徐晓轩, 王斌, 杨延勇, 张存洲, 俞钢, 李杰, “共焦显微拉曼光谱深度剖析法在笔迹鉴定中的应用”, 光谱学与光谱分析 25(1), 51-53(2005)
2. 武中臣, 徐晓轩, 李奇楠, 俞钢, 张存洲, “提高二甲苯三种同分异构体预测模型准确性的相关系数法”, 光谱学与光谱分析 25(1), 136-140(2005)
3. 武中臣, 徐晓轩, 张静, 李奇楠, 张存洲, 俞钢, “近红外差谱法选择信息区提高同分异构体预测模型准确度”, 光谱实验室 22(1), 38-41(2005)
4. 武中臣, 徐晓轩, 张静, 李奇楠, 张存洲, 俞钢, “互相关分析在近红外光谱预处理中的应用”, 光谱实验室 22(1), 126-129(2005)
5. 杨仁杰, 徐晓轩, 尚丽平, 许家林, 杨延勇, 张存洲, “1-苯胺基萘-8-磺酸盐在各种固体基质中发光特性的研究”, 光谱实验室 22(2), 230-234(2005)
6. 杨仁杰, 徐晓轩, 尚丽平, 许家林, 杨延勇, 张存洲, “含油岩屑固体粉末荧光的研究”, 发光学报 26(1), 131-134(2005)
7. 林海波, 徐晓轩, 吴宏滨, 王斌, 俞钢, 张存洲, “绝缘层 LiF/Al 电极对提高 P-PPV 发光器件发光性能的研究”, 发光学报 26(4), 469-472(2005)
8. 于舸, 吕淑华, 许家林, 张存洲, 张春平, “衰减全反射红外光谱用于人乳腺癌组织的研究”, 光子学报 34(3), 390-394(2005)
9. 尚丽平, 徐晓轩, 许京军, 史锦珊, 夏达英, “水中微量矿物油污染光纤荧光监测技术及应用研究”, 计量学报 26(1), 81-85(2005)
10. 于舸, 吕淑华, 许家林, 张春平, 张光寅, “人乳腺离体肿瘤组织的 ATR-FTIR 谱鉴别方法的探索”,南开大学学报 38(1), 53-56(2005)
11. 武中臣, 徐晓轩, 杨仁杰, 俞钢, 张存洲, “互相关分析在近红外光谱模型传递中的应用”, 光谱学与光谱分析 25(12)(2005)

Investigation of mode-locking mechanism and resonator design of ultrashort pulse lasers

Zhang Guangyin, Zhang Xiaohua, Yan Caifan, Gu Xuewen, Wu Dinger

This dissertation describes some work on the mode-locking and resonator design of ultrashort pulse lasers. The main points are as follows:

1. The luminescence dynamics of X-folded cavity Ti:sapphire femto-second laser has been measured, and the self-mode-locking mechanism and process of femto-second laser has been investigated systematically by means of propagation-circle and transform-circle graphic method.A new mode-locking mechanism, self-pulsing Kerr-lens and magnifying mode-locking have been put forward.

2. The sensitivity of Kerr-lens self-mode-locked dynamic sensitive resonator has been analyzed. Combined with dual-U curves denoting dynamic state, we analyzed the design and choice process of Kerr-lens self-mode-locked dynamic sensitive resonator. At the same time, we point that the Kerr-lens effect of lasing medium is the trigger factor for mode-locking operation.

3. The Kerr-lens mode-locking mechanism and process of Ti:sapphire femtosecond laser and pulsed Nd:YAG laser passively mode-locked with Cr^{4+}:YAG has been discussed, and a new mode-locking mechanism, self-pulsing Kerr-lens switching and magnifying mode-locking resulted from optics chaos, has been put forward, which the mode-locking mechanism of the two kinds of ultra-short pulse laser.

4. Three kinds of self-mode-locked resonator, equivalent nearly symmetrical resonator, equivalent asymmetrical resonator and resonator with mode-locked area magnified effectively, have been analyzed through transform-circle graphic theory. And the last kind of resonator which is easy to start and collimate has good stability. So it’s a novel kind of resonator that should be generalized.

Publication

1. 张晓华, 张光寅, 焦志勇, 顾学文, 颜彩繁, “钛宝石飞秒激光器的锁模机理探讨”, 物理学报 54(3), 1213-1217(2005)
2. 焦志勇, 张光寅, 张晓华, 颜彩繁, “激光二极管侧向泵浦的 Nd:YAG 激光器的热效率”, 南开大学学报, 38(2), 1-4(2005)
3. Gu xuewen, Zhang qiulin, Zhang dongxiang, Feng baohua, Zhang xiaohua, Zhang Guangyin, “Antiphase State in Passively Q-Switched Yb:YAG Microchip Lasers with a Nd, Cr:YAG as Saturable Absorber”, Chin. Phys. Lett. 22(6), 1416-1419(2005).

Semiconductor Growth Technology and Devices

The progress in the area of semiconductor growth technology and devices is summarized as follows.

1. Prof. Yongchun Shu et al., has grown GaAs material with high electron mobility, using a molecular beam epitaxy instrument.
2. Prof. Yongchun Shu et al., has grown AlAs/GaAs distributed Bragg reflection mirrors.
3. Prof. Zhangcheng Xu et al., has studied the carrier dynamics of submonolayer InGaAs/GaAs quantum dots, using low-temperature time-resolved photoluminescence. The results are very useful for understanding the corresponding devices based on submonolayer quantum dots.
4. Prof. Zhangcheng Xu et al. started to build the lab of nano-photonics in 2005. In this lab, electro deposition of nano-Cu thin films on Si substrate was realized. The set-ups of studying the surface voltage spectrum and modulated reflectance spectrum of quantum dots, are built. The technique of using the Anodic Aluminum Oxide template to control the growth of ordered nano-structures has been developed. ZnCdS/Si heterojuctions have been fabricated via electro-deposition.

In summary, we have just started to challenge in the area of semiconductor nano-material and devices. We believed that more promising progress will be made in the near future.

Carrier Dynamics of Submonolayer InGaAs/GaAs Quantum-Dot-Quantum-Well Heterostructures

Zhangcheng Xu, Yating Zhang, Jingjun Xu

Submonolayer (SML) deposition is an alternative way of growing self-assembled quantum dots (QDs) [1]. It was verified that SML QD heterostructure is a structure with quantum dots embedded in a quantum well, i.e., a quantum-dot-quantum-well (QDQW) [2,3,4]. Here we study the carrier dynamics by means of time-resolved photoluminescence at 5 K, which is crucial to understand the corresponding devices.

According to the growth mechanism of SML QDs, the smallest QDs are formed by perfectly vertically correlated 2D InAs islands, and have the lowest In content, while slight deviation from the perfect vertical correlation produces larger QDs with lower In content. The transient PL at different detection energies are shown in Fig. 1. The energy dependence of the PL decay and rise time is shown in Fig. 2. The larger QDs with higher emission energies have shorted exciton lifetime, due to the enhancement of the overlap of electron-hole wave-functions. The capture time of carriers into larger QDs are longer, which is consistent with the theoretical prediction on the size dependence of Auger capture of carriers to QDs.

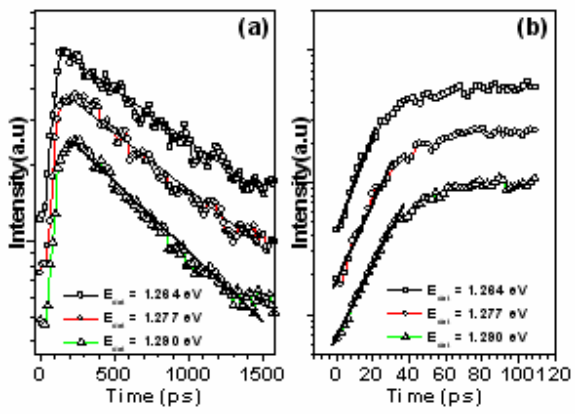

Fig.1 The transient PL of SML QDs at 5K

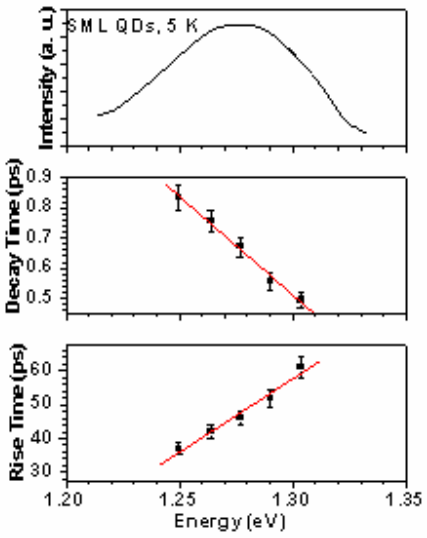

Fig. 2 The energy dependence of PL decay and rise time

References

[1] Mikhrin et al, Semicond. Sci. Technol. **15**, 1062(2002)
[2] Zhangcheng Xu, et al., Appl. Phys. Lett. **82**, 3859(2003)
[3] Zhangcheng Xu, et al., Appl. Phys. Lett. **85**, 3259(2004)
[4] Zhangcheng Xu, et al., Nanotechnology **14**, 1259(2003)

Supported by the National Natural Science Foundation of China (60444010, 60506013)

MBE Growth of High Electron Mobility InP and GaAs Epilayers

Shu Yongchun, Yao Jianghong, Lin Yaowang, Xing Xiaodong, Pi Biao

The molecular beam epitaxial growth of high quality epilayers on (100) InP substrate using a valve phosphorous cracker cell over a wide range of P/In BEP ratio (2.0~7.0) and growth rate (0.437 and 0.791μm/h).Experimental results show that electrical properties exhibit a pronounced dependence on growth parameters, which are growth rate, P/In BEP ratio, cracker zone temperature, and growth temperature. The parameters have been optimized carefully via the results of Hall measurements. For a typical sample,77K electron mobility of $4.57\times10^4 cm^2/(V\cdot s)$ and electron concentration of $1.55\times10^{15} cm^{-3}$ have been achieved with an epilayer thickness of 2.35μm at a growth temperature of 370℃ by using a cracking zone temperature of 850℃.

Modulation doped AlGaAs/ GaAs st ructures were grown on GaAs (100) substrate by solid source molecular beam epitaxy (SSMBE) system. The factors which influence the electron mobility were investigated. After growing InP based materials, growth conditions were deteriorated , but by an appropriate method and using reasonable process high electron mobility(77 K) of more than 1.50×10^5 $cm^2/(V\cdot s)$ can still be obtained. The structures and growth conditions have been studied and optimized via Hall measurements. For a typical sample, 2.0 K electron mobility as high as 1.78×10^6 $cm^2/(V\cdot s)$ is achieved , and the quantum Hall oscillation phenomena can be observed.

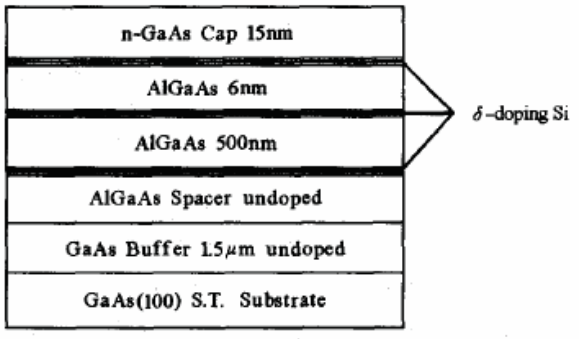

Fig.1:δ-doping Si structure

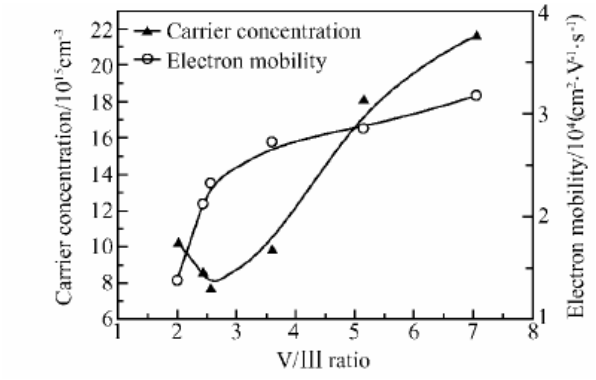

Fig.2: Electron mobility and concentration of

References

[1] Shu Yongchun, Pi Biao, Lin Yaowang, Xing Xiaodong, Yao Jianghong, Wang Zhanguo and Xu Jingjun. Trans. Nonferrous Met. Soc. China, Vol.15 (2), 332-335 (2005).

[2] Shu Yongchun, Yao Jianghong, Lin Yaowang, Xing Xiaodong, Pi Biao, Xu Bo, Wang Zhanguo and Xu Jingjun, Chinese Journal of Semiconductors，Vol. 36(8), (2005).

[3] Zhang Guanjie, Shu Yongchun, Pi Biao, Xing Xiaodong, Lin Yaowang, Yao Jianghong, Wang Zhanguo and Xu Jingjun, Journal of Synthetic Crystals, Vol.34 (3), 395-398(2005).

Supported by National Nature Science Foundation of China (Grant No. 60476042) and Teda College.

The study of Optically Pumped Semiconductor (OPS) Vertical-External-Cavity Surface-Emitting Lasers (VECSEL)

Liu Rubin, Zhang Guanjie, Yao Jianghong, Lin Yaowang Shu Yongchun,

Optical pumping semiconductor vertical-external-cavity surface-emitting lasers which incorporate the properties of conventional semiconductor lasers and semiconductor vertical cavity surface emitting lasers have many advantages such as high quality of output beam, high power and small bulk. As a result, this kind of laser has great and has attracted much attention. In this article, the properties and advantages of optical pumping semiconductor vertical-external-cavity surface-emitting lasers are introduced and the newest device developments are demonstrated. On the basis of these analyses, we point out the application potential and technology direction in the areas.

Optically pumped semiconductor vertical-external-cavity surface-emitting lasers (OPS-VECSEL) which could generate the ultra-short pulse are presented. The characteristics and development of OPS-VECSEL are demonstrated about the laser's pulse width, average output power, output wavelength and pulse repetition frequency. Furthermore, we point out the further development direction in the area.

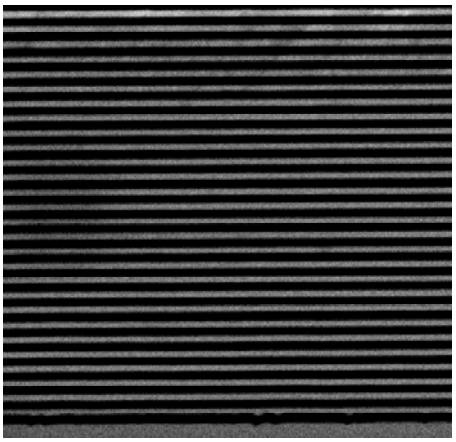

Fig.1: the SEM image of DBR

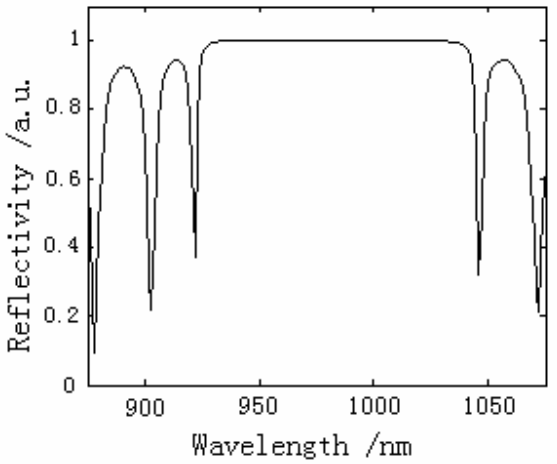

Fig.2: Reflectance spectrums of AlAs/GaAs DBR (30 pairs, wavelength: 980nm)

References

[1] Liu Rubin, Shu Yongchun, Zhang Guanjie, Shu Qiang, Lin Yaowang, Yao Jianghong, Wang Zhanguo and Xu Jingjun, Laser Journal. Received.
[2] Zhang Guanjie, Shu Yongchun, Pi Biao, Yao Jianghong et.al. 34(6), (2005)
[3] Zhang Guanjie, Shu Yongchun, Liu Rubin, Shu Qiang et. al , Received.

Supported by National Nature Science Foundation of China (Grant No. 60476042) and Teda College.

The study of persistent photoconductivity and subband electronic properties of the two-dimensional electron gas in modulation doped GaAs/AlGaAs structure

Shu Qiang, Lin Yaowang, Yao Jianghong, Shu Yongchun

The electronic properties of GaAs/AlGaAs 2DEG have been studied by Quantum Hall effect and Shubnikov-de Haas (SdH) oscillation measurements. We found that the electron concentrations of two subbands increased simultaneity with the increasing total electron concentration, and the electron mobilities also increased clearly after illuminated. At the same time, we also found that the electronic quantum lifetime was becoming shorter, and the theoretical analysis was shown through the widths of integral quantum Hall plateaus.

By low-temperature Hall and Shubnikov-de Hass (SdH) measurements. We obtained that quantum lifetimes related to all-angle scattering events reduced from 0.64 ps to 0.52 ps after the sample was illuminated. However transport lifetimes related to large-angle scattering events increased from 42.3 ps to 67.8 ps. This indicated that small-angle scattering events became stronger. At the same time, the widths of the plateaus have become narrower. We believed that small-angle scattering events caused the varieties of the widths of the quantum Hall plateaus.

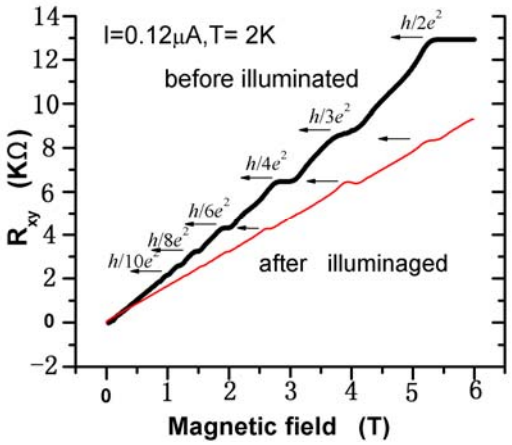

Fig.1: The Quantum Hall effect curves for sample

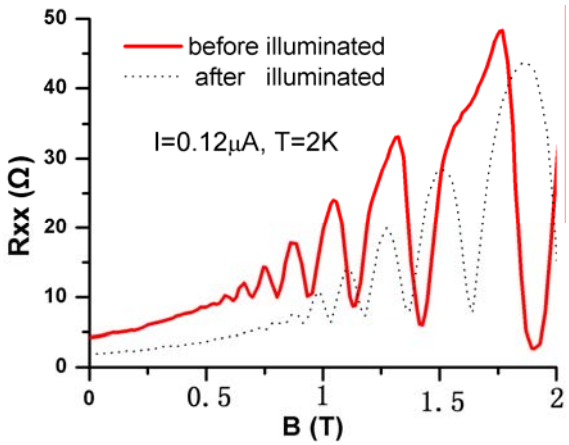

Fig.2: SdH oscillation spectrum of the sample

References

[1] Shu Qiang, Shu Yongchun, Zhang Guanjie, Liu Rubin, Yao Jianghong, Pi Biao Xing Xiaodong, Lin Yaowang, Xu Jingjun and Wang Zhanguo, Acta Phys. Sin. 55, 368 (2006).

[2] Shu Qiang, Lin Yaowang, Xing Xiaodong, Yao Jianghong, Pi Biao, Shu Yongchun, Wang Zhanguo, Xu Jingjun, Chin. Phys. Lett, 23, 436 (2006).

Supported by National Nature Science Foundation of China (Grant No. 60476042) and Teda College.

The study of quantum dot infrared photodetector and Raman spectroscopy

Zhang Guanjie, Shu Yongchun, Yao Jianghong, Wang Zhanguo

Quantum dot infrared photodetectors (QDIPs) ideally have several advantages over quantum well infrared photodetectors. We discuss the theoretical advantages of QDIPs including their normal incidence response, lower dark current, higher responsivity and detectivity, etc. The newest experimental results in this area are also reported. Finally we point out some approaches that can further improve the capabilities of such devices.

Raman scattering of InAs self-assembled quantum dots (QDs) with different thicknesses are performed at 77K. The vibrational mode which can be assigned to phonons of the dots was observed between the GaAs TO and the bulk InAs LO modes. The influence of strain effect and confinement effect were estimated from experimental result and calculated value. As the InAs deposited thickness L increases, the InAs-like LO mode shows a downward frequency shift, which can be attributed to the relaxation of the strain in the QD layer. In another experiment about samples with InAlAs strain buffer layer, the AlAs-like LO mode shows a blue shift as L increases, which indicates that the cladding layer on the islands also participates to the strain relaxation.

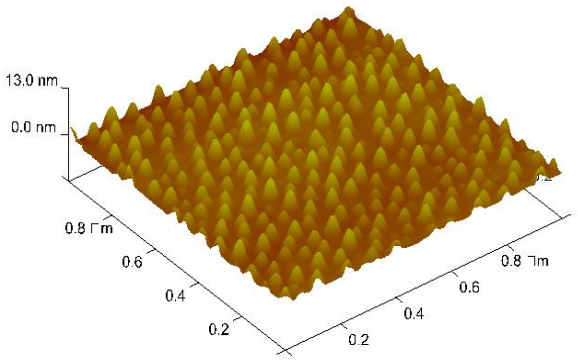

Fig.1: the AFM image of quantum dot

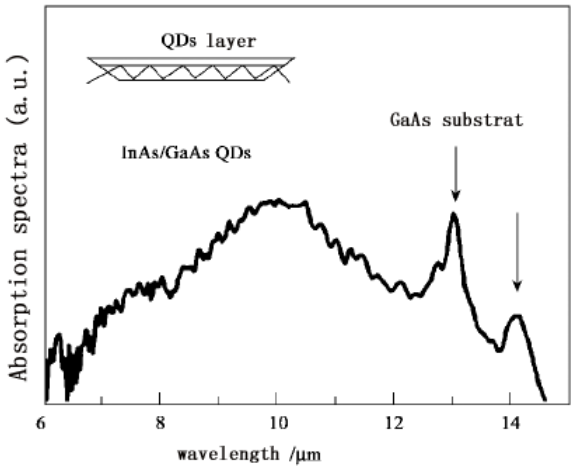

Fig.2: Infrared absorption spectra of quantum dot

References

[1] Zhang Guanjie, Shu Yongchun, Yao Jianghong, Shu Qiang, Deng Haoliang, Jia Guozhi and Wang Zhanguo, Physics. 9,510 (2005)

[2] Zhang Guanjie, Xu Bo, Chen Yonghai, Yao Jianghong et.al. , submitted to Chinese Journal of Semiconductors.

Supported by National Nature Science Foundation of China (Grant No. 60476042) and Teda College.

Publication

1. 徐章程, 贾国治, 孙亮, 姚江宏, 许京军, J. M. Hvam, 王占国, “亚单层 InGaAs/GaAs 量子点-量子阱异质结构的时间分辨光致发光谱”, 物理学报 54, 5367-5371(2005)
2. Shu Yongchun, Pi Biao, Lin Yaowang, Xing Xiaodong, Yao Jianghong, Wang Zhanguo and Xu Jingjun, “High electron mobility of modulation doped GaAs after growing InP by solid source molecular beam epitaxy”, Trans. Nonferrous Met. Soc. China, 15 (2), 332-335(2005).
3. Shu Yongchun, Yao Jianghong, Lin Yaowang, Xing Xiaodong, Pi Biao, Xu Bo, Wang Zhanguo and Xu Jingjun, “MBE growth of high electron mobility InP epilayers, Chinese Journal of Semiconductors”, Chinese Journal of Semiconductors, 36(8), 1085-1088(2005)
4. Zhang Guanjie, Shu Yongchun, Pi Biao, Xing Xiaodong, Lin Yaowang, Yao Jianghong, Wang Zhanguo and Xu Jingjun, “Compatibility study on growing high quality modulation doped GaAs and InP/InP epi-layers by solid source molecular beam Epitaxy”, Journal of Synthetic Crystals, 34(3), 395-398(2005)
5. 张冠杰, 舒永春, 姚江宏, 舒强, 邓浩亮, 贾国治, 王占国, “量子点红外探测器的特性与研究进展”, 物理 9, 510(2005)
6. 张冠杰, 舒永春, 皮彪, 姚江宏, 林耀望, 舒强, 刘如彬, 王占国, 许京军, “AlAs/GaAs 分布布拉格反射镜（DBR）的反射谱拟合与优化生长”, 34(6) (2005)
7. Jianghong Yao, Boxia Ya, Jingjun Xu, Guangyin Zhang, “Study on the optical and polingcharacteristics of near-stoichiometric Er:LiNbO3 and Er:Mg:LiNbO3 crystals”, OSA Trends in Optics and Photonics (TOPS) Vol.99, 132(2005)
8. 邓浩亮, 贾国治, 姚江宏, 徐章程, “非对称双量子阱中载流子耦合的温度依赖性”, 发光学报, 26, 753-756(2005)
9. 颜博霞, 姚江宏, 陈亚辉, 许京军, 张光寅, “高掺镁铌酸锂晶体周期极化及倍频特性研究”, 红外与毫米波学报 24(6),1-4(2005)

Conference

1. 徐章程, 贾国治, 宁海波, 孙亮, “阳极氧化多孔氧化铝的结构与红外滤光特性”, 第十三届全国电化学会议, 广州(2005.11.24-28)
2. Zhangcheng Xu, “Submonolayer InGaAs/GaAs quantum dot heterostructure and lasers”, 日本崎玉工业大学第 3 届青年学者研讨会, 日本崎玉(2005 年 9 月 10 日) (特邀报告)
3. 徐章程, “Submonolayer InGaAs/GaAs quantum dot heterostructure and lasers”,京津地区激光界青年科学家论坛, 天津(2005 年 12 月 2 日) (特邀报告)
4. Jianghong Yao, Boxia Ya, Jingjun Xu , Guangyin Zhang, “Study on the optical and polingcharacteristics of near-stoichiometric Er:LiNbO3 and Er:Mg:LiNbO3 crystals”, The tenth International Conference on Photorefractive Effects, Materials, and Devices, Sanya, Hainan, China(2005)

2005年获奖情况

序号	项目名称	颁奖部门	等级	获奖人
1	光折变新效应、机理与器件的研究	国务院	国家科学技术奖励(国家自然科学二等奖)	许京军、张光寅、刘思敏、张国权、孔勇发
2	固体激光器及其谐振腔	天津市人民政府	天津市自然科学二等奖	张光寅、宋峰、颜彩繁、焦志勇、张包铮

来访人员名单

序号	姓名	国家或地区	单位	职称或职位	来访时间	来访目的
1	Christian Pruner	奥地利	维也纳大学实验物理所（Institute for Experimental Physics, Vienna University）	博士（Dr.）	2005.03.10-2005.05.30	Visiting
2	施毅 王慧田	中国	南京大学物理系	系主任 长江学者	2005.07.26-2005.07.27	工作访问
3	David D. Nolte	美国	普渡大学（Purdue university）	教授（Prof.）	2005.07.26-2005.07.27	Visiting
4	俞平	美国	密歇根大学（Michigan University）	教授（Prof.）	2005.07.29-2005.08.01	工作访问
5	Romano A. Rupp	奥地利	维也纳大学实验物理所（Institute for Experimental Physics, Vienna University）	主任（Dean）、教授（Prof.）	2005.07.29-2005.08.30	Visiting
6	魏台辉	台湾	中正大学	教授	2005.08.30	访问、讲学
7	李树杰	日本	大阪大学蛋白质研究所	研究员	2005.10.11	访问
8	叶朝晖	中国	武汉光电国家实验室	主任、院士	2005.10.31	访问
9	David Pitt David N. Batchelder	英国	雷尼绍公司（Renishaw plc）	教授（Prof.）	2005.10.31	Visiting Lecture
10	孙甲明	德国	罗森多夫研究中心(Rossendof Center)	教授（Prof.）	2005.11.16	访问

Report on the

Tenth International Conference on Photorefractive Effects, Materials, and Devices

Sanya, Hainan, P. R. China, July 19 to July 23, 2005

http://prc.nankai.edu.cn/

Scientific committee

Gérald Roosen	Institut d'Optique, Orsay, France
Giancarlo Abbate	University of Naples, Italy
Aharon J. Agranat	Hebrew University, Jerusalem, Israel
Dana Anderson	Boulder University, USA
Karsten Buse	Bonn University, Germany
Jean-Pierre Huignard	Thales, Orsay, France
Kazuo Kuroda	University of Tokyo, Japan
Loïc Mager	IPCMS, Strasbourg, France
David Nolte	Purdue University, Purdue, USA
Kehar Singh	Indian Institut of Science and Technology, India
Serguei Odoulov	Institute of Physics, National Academy of Sciences, Ukraine
Paul Michael Petersen	Risoe National Laboratory, Denmark
Serguei Stepanov	INAOE Puebla, Mexico
Jingjun Xu	Nankai University, China
Gilles Pauliat	Institut d'Optique, Orsay, France
Philippe Lemaire	Centre Spatial de Liège, Belgique

Organizing committee

Chairman:	Jingjun Xu, Photonics Center, Nankai University, China
Co-chair:	Eckhard Krätzig, Osnabrück University, Germany
Organizers:	Guangyin Zhang, Photonics Center, Nankai University, China
	Qian Sun, TEDA Applied Physics School, Nankai University, China
	Guoquan Zhang, Photonics Center, Nankai University, China
	Zhigang Chen, Nankai University, China and San Francisco State University, USA
	Lambertus Hesselink, Stanford University, USA
	Qihuang Gong, Peking University, China
	Jun Fu, Hainan Normal University, China
	Hui Huang, Kunming Institute of Physics, China

1. Attendance

The tenth international Conference on Photorefractive Effects, Materials, and Devices was successfully held in Sanya, Hainan, China, from July 19 to July 23, 2005. This conference attracted 125 attendants, including 73 regular attendants, 25 student attendants and 27 companions. They were from 15 countries. The large number of student participants highlights the strong activity of the research in the photorefractive field. The list of participants is attached to this report.

2. Papers, Proceeding and Presentations

This conference received 140 full-length papers and they were published on *Trends in Optics and Photonics Series* (volume 99, editors: Guoquan Zhang, Detlef Kip, David Nolte and Jingjun Xu) by the Optical Society of America. These papers were divided into 10 sections: Mateiral preparation and characterization: Inorganic (47 papers), Material preparation and characterization: organic (18 papers), Wave mixing (8 papers), Modeling (9 papers), Solitons and optical lattices (15 papers), Applications: Storage (11 papers), Applications: Adaptive interferometry (10 papers), Applications: Laser Source (4 papers), Applications: Special filter (10 papers), Applications: Miscellaneous (8 papers). The material preparation and characterization continues to be an important element of the conference. Novel materials are continually being developed and new effects are being investigated intensively to pave the way for applications such as holographic storage, spectral filters, laser source and adaptive interferometric techniques. Sensitive detecting techniques based on adaptive interferometry are well developed and applied to practical problems. New phenomena such as dispersive-phase-coupling-induced superluminal light propagation are reported which use the well-understood mechanism of photorefractive wave mixing. The challenging topic of holographic storage is well represented and new recording techniques are reported with an emphasis on nonvolatile holographic recording. One of the significant advances in recent years is nonlinear light propagation in photo-induced optical lattices, in which nonlinear interaction between the light and the lattice leads to novel control of light propagation. All these developments confirm the vitality and versatility of this research field. Although the volume is divided into ten sections, the border among the different sections is somewhat blurred, as it must be. Additional copies of the Proceeding volume can be ordered directly by contacting the publisher of OSA or Dr. Lin Dorris who are responsible for editing this conference proceeding.

Totally, 3 plenary talks, 11 invited talks, 62 oral talks and 101 posters were arranged in this conference. All the oral presentations were presented in a single conference room, while the posters were posted in an additional hall.

3. Awards

The photorefractive effects and materials offer a broad potential applications and practical devices such as non-destructive vibration sensors in the automotive or aeronautic

fields, holographic mass storage memories, new self-organizing laser sources for telecommunications, and so on. One of the main aims of such a meeting is also to promote the development of photorefractive based commercial systems. Therefore, a best application award was issued in every of this series of meeting. The best application award of this conference, for an amount of 2000 USD provided by Nankai University, OSA and the National Nature Science Foundation of China, was awarded to Marc GEORGES, Cédric THIZY, Philippe LEMAIRE (*Centre Spatial de Liège, Liege Science Park, Angleur, Belgium)* and Guy-Michel HUSTINX (*OPTRION S.A., Avenue des Chasseurs Ardennais, Angleur, Belgium)* for "***Dynamic holographic interferometry with BSO crystals: Industrial system approach, applications and commercialisation***".

Best Application Award

To encourage the participation of students in science, OSA offers two OSA Student Travel Awards for two students attending the conference. These two OSA Student Travel Awards, selected by the conference chair Prof. Dr. Jingjun Xu and the OSA representative Prof. Dr. David Nolte based on the quality of their presentations, were awarded to Mr. Fang Bo from Nankai University of China and Mr. Malte Gather from University of Cologne of Germany. Their detailed contact information are

Mr. Fang Bo, Photonics Center, College of Physics Science, Nankai University, Tianjin 300071, China. Tel/Fax: +86-22-23499944, email: bofang@mail.nankai.edu.cn

Mr. Malte Gather, Room 139, Institut fuer Physikalische Chemie, Universitaet zu Koeln, Luxemburgerstr. 116, 50939 Koeln, Germany. Tel: +49 (0) 221 470 -3055, Fax: +49 (0) 221 470 -7311, email: m.gather@uni-koeln.de

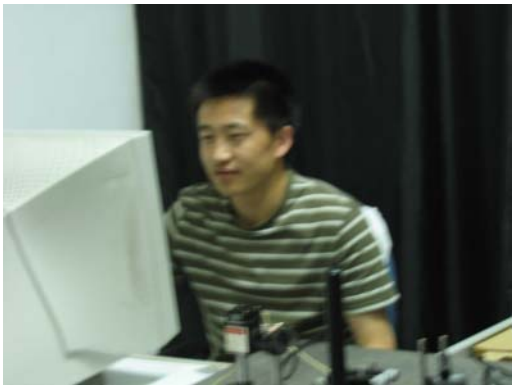

Fang Bo

Malte Gather

4. Registration Fee and Financial Statement

The registration fee for a regular attendant is 300 USD (pre-registration) or 350 USD (on-site registration). For a student, the registration fee is 200 USD (pre-registration) or 250 USD (on-site registration). For a companion, the registration fee is 60 USD. This registration fee includes the meal fee during the conference. We also waive off the registration fee for the following participants in order to support them to attend this conference: Oksana Ostroverkhova (USA), M. P. Petrov (Russia), Mathieu Chauvet (France), Vera Marinova (Bulgaria), Sc. Irina I. Davidenko (UKRAINE), Nicolay A.Davidenko (UKRAINE), Ilya Steinberg (Russia), Roman Romashko (Russia), and Stanislav M. Shandarov (Russia).

The Conference Budget is also attached in this report. The deficit will be covered by Nankai University.

5. Conclusion

This meeting was a full success, both for the large attendance for such a topical meeting, and for the quality of the presented scientific communications. The maturity reached by some of the photorefractive materials has now allowed the development of new industrial applications. Based on some communications presented here, other new applications are expected for the next coming years.

The success of this meeting has convinced the scientific committee and the organizing committee to settle a new meeting on the same topics in 2007. This next meeting will be organized by Prof. Dana Anderson from Boulder University and Prof. Lambertus Hesselink from Stanford University in USA.

6. Acknowledgment

We would like to thank Lin Dorris from the Optical Society of America for her highly professional assistance in the preparation of the conference Proceeding, as well as all the people that have helped us in the review of all submissions. We are also very indebted to all participants for the success of this conference and the quality of the presentations. This conference is supported financially and co-sponsored by Nankai University, the Optical Society of America, the National Natural Science Foundation of China, the Physics Society of China, the Ministry of Education of China, and the Tianjin Municipal Science and Technology Commission.

List of participants

No.	Name	type	Nationality
1	Song Liang	Student	China
2	Huizhen Kang	Student	China
3	Song Liang	Student	China
4	Suhua Luo	Student	China
5	Yuhong Wan	Student	China
6	Dexin Yang	Student	China
7	Peng Zhang	Student	China
8	Yu Zhou	Student	China
9	Fang Bo	Student	China
10	Bo Fu	Student	China
11	Jun Sun	Student	China
12	Zheyu Fang	student	China
13	Dapeng Yang	student	China
14	Mathieu Feuillade	Student	France
15	Naima Khelfaoui	Student	France
16	Andreas Selinger	Student	Germany
17	Christoph Merschjann	Student	Germany
18	Elisabeth Soergel	Student	Germany
19	Evelin Weidner	Student	Germany
20	Gather Malte	Student	Germany
21	Kathrin Bastwoeste	Student	Germany
22	Pismennaya Katsiaryna	Student	Germany
23	Stephan Hausfeld	Student	Germany
24	Ilya Sh. Shteynberg	Student	Russia
25	OLGA CABALLERO	Student	Spain
26	David VERSTRAETEN	Regular	Belgium
27	MARC P. GEORGES	Regular	Belgium
28	Jaime Frejlich	Regular	Brazil
29	Vera M. Gospodinova	Regular	Bulgaria
30	Yunying Bu	Regular	China
31	Shaokui Cao	Regular	China
32	Aqiang Guo	Regular	China
33	Chunfeng Hou	Regular	China
34	Hui Huang	Regular	China
35	Yuanming Huang	Regular	China
36	Zhuqing Jiang	Regular	China
37	Yin Li	Regular	China
38	Liyong Ren	Regular	China
39	Shiquan Tao	Regular	China

40	Dayong Wang	Regular	China
41	Baoli Yao	Regular	China
42	Jianlin Zhao	Regular	China
43	Baiquan Tang	Regular	China
44	Qiang Gao	Regular	China
45	Xuanyi Yu	Regular	China
46	Guoquan Zhang	Regular	China
47	Jingjun Xu	Regular	China
48	Qian Sun	Regular	China
49	Yongfa Kong	Regular	China
50	Cibo Lou	Regular	China
51	Qiang Wu	Regular	China
52	Yudong Li	Regular	China
53	Alexei A. Kamshilin	Regular	Finland
54	Kimmo Paivasaari	Regular	Finland
55	Delphine Wolfersberger	Regular	France
56	Gérald ROOSEN	Regular	France
57	Gilles Pauliat	Regular	France
58	Jean Claude LAUNAY	Regular	France
59	Jean-Pierre HUIGNARD	Regular	France
60	Mathieu Chauvet	Regular	France
61	Robert Frey	Regular	France
62	Cornelia Denz	Regular	Germany
63	Detlef Kip	Regular	Germany
64	Eckhard Kraetzig	Regular	Germany
65	Helge A. Eggert	Regular	Germany
66	Jürgen Petter	Regular	Germany
67	Karsten Buse	Regular	Germany
68	Mirco Imlau	Regular	Germany
69	Vladislav Matusevich	Regular	Germany
70	Hideki Hatano	Regular	Japan
71	Kazuo Kuroda	Regular	Japan
72	LIU Youwen	Regular	Japan
73	Qiao Haijun	Regular	Japan
74	Ryushi Fujimura	Regular	Japan
75	Tsutomu Shimura	Regular	Japan
76	Yasuo Tomita	Regular	Japan
77	Anatoly V. Khomenko	Regular	México
78	Ewa Weinert-Raczka	Regular	Poland
79	Mikhail Petrov	Regular	Russia
80	Roman V. Romashko	Regular	Russia
81	Sergey Sharangovich	Regular	Russia
82	Stanislav M. Shandarov	Regular	Russia
83	Yu. N. Kulchin	Regular	Russia

84	Mercedes Carrascosa	Regular	Spain
85	Gunter Peter	Regular	Switzerland
86	Irina Davidenko	Regular	Ukraine
87	Nicolay Davidenko	Regular	Ukraine
88	Ruslan Lymarenko	Regular	Ukraine
89	Chen Zhigang	Regular	USA
90	Dana Anderson	Regular	USA
91	David D. Nolte	Regular	USA
92	Hans- Peter Wagner	Regular	USA
93	Heidrun Schmitzer	Regular	USA
94	Hesselink Lambertus	Regular	USA
95	Mohammad Sayeh	Regular	USA
96	Oksana Ostroverkhova	Regular	USA
97	Yang Jianke	Regular	USA
98	Yu Ping	Regular	USA